Journal of Geodynamics 77 (2014) 89–109

Contents lists available at ScienceDirect

Journal of Geodynamics

journal homepage: http://www.elsevier.com/locate/jog

The Al Hoceima Mw 6.4 earthquake of 24 February 2004 and its aftershocks sequence

Jérôme van der Woerd[a,*], Catherine Dorbath[a,b], Farida Ousadou[c], Louis Dorbath[a], Bertrand Delouis[d], Eric Jacques[e], Paul Tapponnier[e,f], Youssef Hahou[g], Mohammed Menzhi[h], Michel Frogneux[a], Henri Haessler[a]

[a] Institut de Physique du Globe de Strasbourg, UMR 7516, CNRS – Université de Strasbourg, 5, rue Descartes, 67084 Strasbourg Cedex, France
[b] Institut de Recherches pour le Développement, Unité de Recherches 154, France
[c] Centre de Recherche en Astronomie Astrophysique et Géophysique (CRAAG), Bouzareah, 16340 Alger, Algeria
[d] GeoAzur, Observatoire de la Côte d'Azur, CNRS, Université de Nice Sophia Antipolis, 250 Rue Albert Einstein, Sophia Antipolis, 06560 Valbonne, France
[e] Institut de Physique du Globe de Paris, UMR7154, 1 rue Jussieu, 75238 Paris Cedex 05, France
[f] Earth Observatory of Singapore, Nanyang Technological Universit N2-01A-09, 50 Nanyang Avenue, 639798, Singapore
[g] Department of Geology, University Mohammed V, Faculty of Sciences, Rabat, Morocco
[h] Geophysics Laboratory, CNRST, Rabat, Morocco

ARTICLE INFO

Article history:
Received 28 May 2013
Received in revised form
14 December 2013
Accepted 22 December 2013
Available online 5 January 2014

Keywords:
Al Hoceima
Seismicity
Aftershocks sequence
Focal mechanisms
Tomography
Teleseismic inversion

ABSTRACT

The Al Hoceima Mw 6.4 earthquake of 24 February 2004 that occurred in the eastern Rif region of Morocco already hit by a large event in May 1994 (Mw 5.9) has been followed by numerous aftershocks in the months following the event. The aftershock sequence has been monitored by a temporary network of 17 autonomous seismic stations during 15 days (28 March–10 April) in addition to 5 permanent stations of the Moroccan seismic network (CNRST, SPG, Rabat). This network allowed locating accurately about 650 aftershocks that are aligned in two directions, about N10-20E and N110-120E, in rough agreement with the two nodal planes of the focal mechanism (Harvard). The aftershock alignments are long enough, about 20 km or more, to correspond both to the main rupture plane. To further constrain the source of the earthquake main shock and aftershocks (mb > 3.5) have been relocated thanks to regional seismic data from Morocco and Spain. While the main shock is located at the intersection of the aftershock clouds, most of the aftershocks are aligned along the N10-20E direction. This direction together with normal sinistral slip implied by the focal mechanism is similar with the direction and mechanisms of active faults in the region, particularly the N10E Trougout oblique normal fault. Indeed, the Al Hoceima region is dominated by an approximate ENE-SSW direction of extension, with oblique normal faults. Three major 10–30 km-long faults, oriented NNE-SSW to NW-SE are particularly clear in the morphology, the Ajdir and Trougout faults, west and east of the Al Hoceima basin, respectively, and the NS Rouadi fault 20 km to the west. These faults show clear evidence of recent vertical displacements during the late Quaternary such as uplifted alluvial terraces along Oued Rihs, offset fan surfaces by the Rouadi fault and also uplifted and tilted abandoned marine terraces on both sides of the Al Hoceima bay.

However, the N20E direction is in contrast with seismic sources identified from geodetic inversions, which favour but not exclusively the N110-120E rupture directions, suggesting that the 1994 and 2004 events occurred on conjugate faults. In any event, the recent seismicity is thus concentrated on sinistral N10-20E or N110-120E dextral strike-slip faults, which surface expressions remain hidden below the 3–5 km-thick Rif nappes, as shown by the tomographic images build from the aftershock sequence and the concentration of the seismicity below 3 km. These observations may suggest that strain decoupling between the thrusted cover and the underlying bedrock and highlights the difficulty to determine the source properties of moderate events with blind faults even in the case of good quality recorded data.

1. Introduction

The region of Al Hoceima, Morocco, was shaken by a strong Mw 6.4 earthquake (CSEM, USGS, Harvard) on February 24th, 2004 at 2h27mn (UTC) (Jabour et al., 2004). It is the largest earthquake

* Corresponding author. Tel.: +33 368850349.
E-mail address: jeromev@unistra.fr (J. van der Woerd).

0264-3707/$ – see front matter © 2013 Elsevier Ltd. All rights reserved.
http://dx.doi.org/10.1016/j.jog.2013.12.004

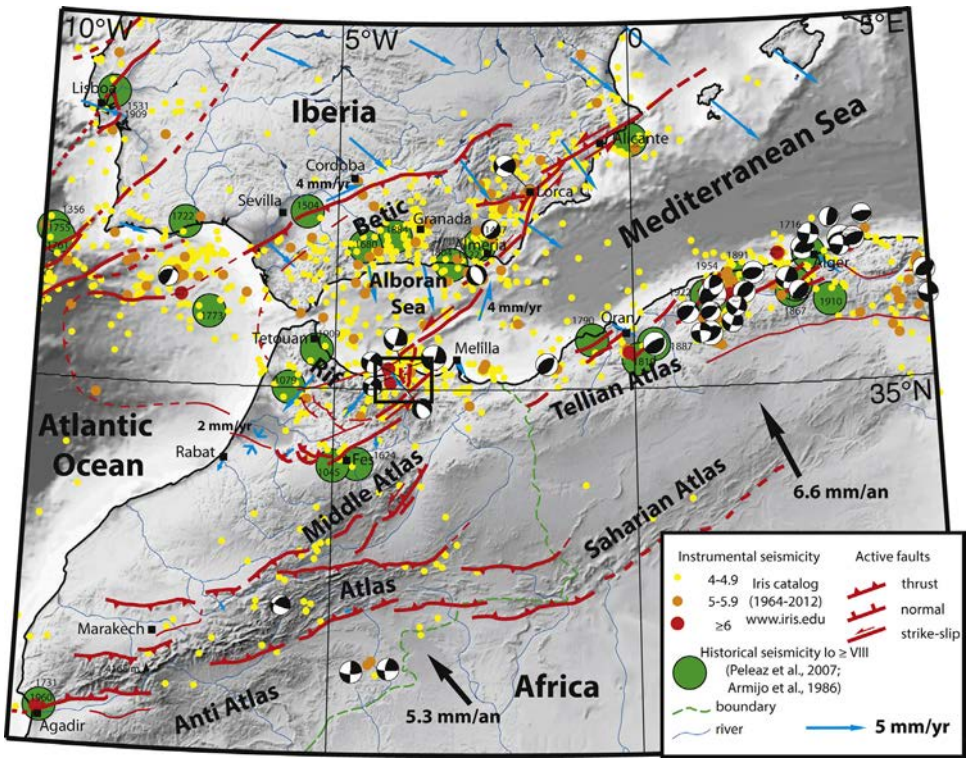

Fig. 1. Seismotectonic map of western Mediterranean showing active structures of Africa–Iberia collision zone. Instrumental seismicity (1964–2012) from Iris catalogue. Historical seismicity from Armijo et al. (1986) and Pelaez et al. (2007). Focal mechanisms from Harvard catalogue. Active faults are summarized from various publications and modified following SRTM DEM and satellite image interpretations. Nubia-Europe velocities (black arrows) are from Nuvel-1A model (DeMets et al., 1990). GPS velocity field from Nocquet (2012). Black rectangle is Fig. 2.

since at least two centuries (Fig. 1; El Mrabet, 2005a,b; Pelaez et al., 2007) in the Al Hoceima region considered as the most seismically active of Morocco (Cherkaoui et al., 1990; El Alami et al., 1998; Bezzeghoud and Buforn, 1999). An earthquake of magnitude Mw 6.0 occurred on 2nd May 1994 in the same area about 10 km to the west-northwest of the 2004 event in the morning of a spring day, when most of the local people were in the fields and only few casualties were to deplore. The 2004 earthquake occurred in the night, in the winter season, and caused more than 800 fatalities. While the magnitude of the 2004 earthquake was larger, this difference alone does not explain the difference in human loss. Traditional houses made of stones and adobe and heavy roofs suffered considerable destructions while the modern building in Al Hoceima experienced weak damages. However, recent buildings suffered heavy damages, as far as complete collapse in Imzouren, some 12 km south-east of Al Hoceima (Fig. 2) resulting mainly from bad design (Murphy Corella, 2005) though without significant site effect (Goula et al., 2005). An accelerometer installed close to a dam on the Nekor river, about 10 km southeast from the epicentre recorded a maximum horizontal acceleration of 0.24 *g*, a relatively high value (CNRST, 2004).

Despite several geophysical studies since the earthquake (Stich et al., 2005; Cakir et al., 2006; Akoglu et al., 2006; Biggs et al., 2006; Tahayt et al., 2009), the source of the 2004 event remains debated and puzzling (Galindo-Zaldivar et al., 2009). Indeed, similarly to the 1994 event, the 2004 event did not rupture to the surface and occurred along a fault that has no cumulative surface expression, to the contrary of well expressed normal faults in the Nekor basin (Trougout and Ajdir faults) and to the west (Rouadi fault), or such as the Nekor strike-slip fault (Morel, 1988; Van der Woerd et al., 2005) (Figs. 2 and 3). Surface deformations (open cracks, ground ruptures, landslides) were observed mainly along a 10 km-wide strip running from Ajdir to Beni Abdellah, in a roughly NNE-SSW direction (Figs. 2b and 4; Ait Brahim et al., 2004), but modelling of radar interferograms (InSAR) suggest a WNW-ESE fault plane (Cakir et al., 2006; Akoglu et al., 2006; Tahayt et al., 2009; Biggs et al., 2006). In addition, the aftershock clouds extend along two almost perpendicular directions similarly to the directions of the nodal planes of the main shock focal mechanism (this study; Harvard catalogue; USGS) with the main shock at the intersection of the two clouds (Fig. 2b) making any attempt to link the seismicity to a preferential fault plane difficult.

The Rif region of northern Morocco belongs to the complex plate boundary between western Africa and western Europe, which extends for more than 1500 km E-W from Portugal to Tunisia and 1000 km N-S from France to south Morocco, and comprises several collisional belts, the Pyrenees, the Betics, the Rif, the Middle Atlas, the Atlas, and the Tellian Atlas (Fig. 1). North of the Rif, the Alboran Sea, characterized by a thinned continental crust, resulted from extension in a back arc setting during the Oligo-Miocene (Watts et al., 1993; Seber et al., 1996). The knowledge of the present day tectonics in the Rif has strong implications in the understanding of strain pattern in the western Mediterranean region (Ait Brahim and Chotin, 1984; Ait Brahim et al., 1990; Morel and Meghraoui, 1996; Lopez Casado et al., 2001). While the convergence between western Africa and western Europe can be assessed by plate tectonic models or GPS velocity fields (DeMets et al., 1990, 1994; Nocquet and Calais, 2003; Nocquet, 2012), the manner and where the strain is taken into account remains debated, mostly because the rates of deformation are slow and need to be averaged over long time intervals.

Both earthquakes of 1994 and 2004 are characterized by blind ruptures that have not propagated to the surface making their seismotectonic characterizations challenging. The challenge is reenforced as these two earthquakes are the largest known in this part of the Rif since several centuries (El Mrabet, 2005a; Pelaez et al., 2007). It has been proposed that the ruptures remained located

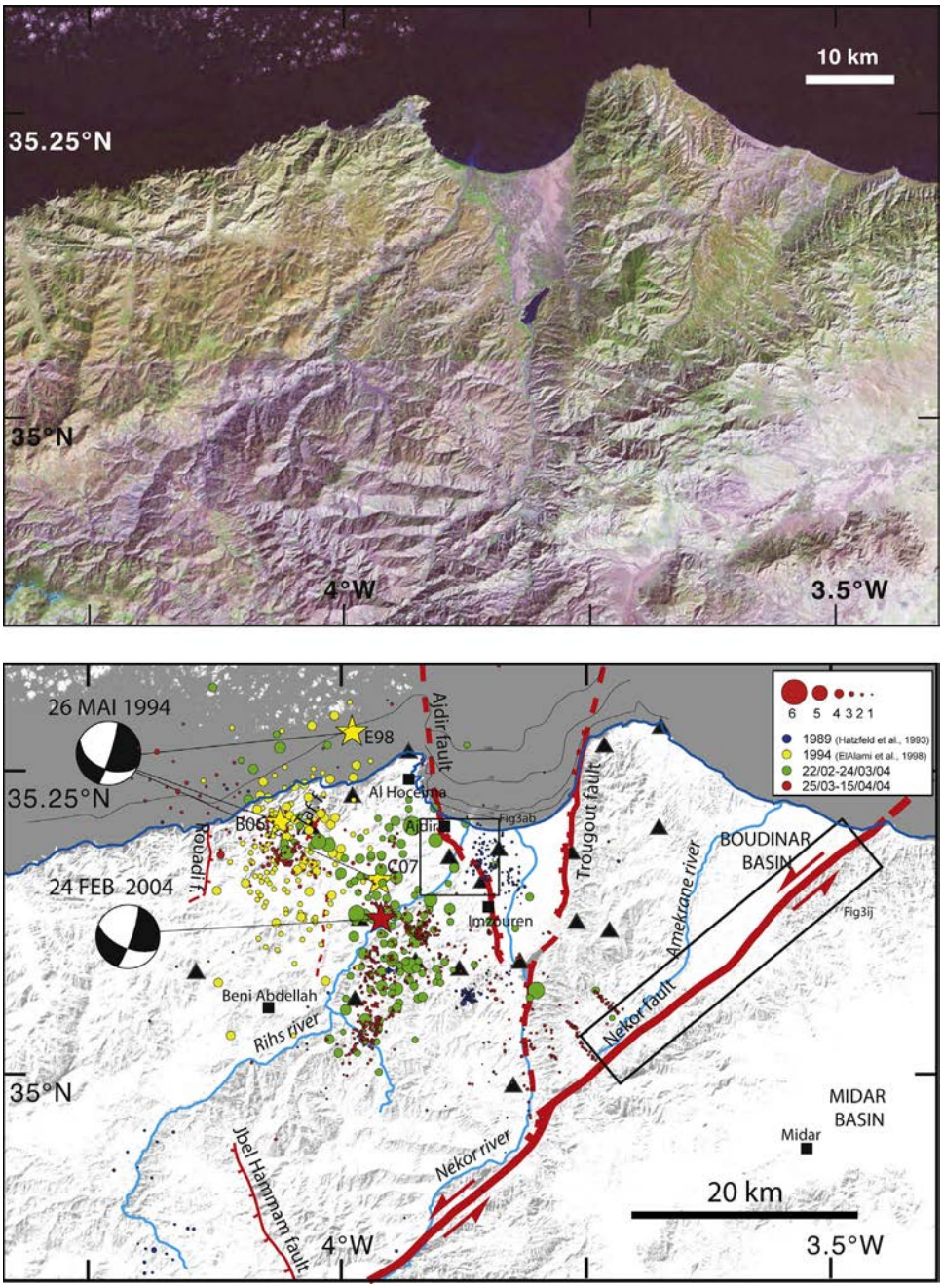

Fig. 2. (a) Landsat satellite image of Rif region around Al Hoceima. (b) Seismotectonic map of epicentral region of Al Hoceima Mw 6.4 earthquake on 24 February 2004. Active faults mapping from interpretation of high resolution SPOT images (pixel size: 2.5 m) and field observations. C97, A98 and B06 are epicenters for magnitude Mw 6.0 event of 26 May 1994 from Calvert et al. (1997), El Alami et al. (1998) and Biggs et al. (2006), respectively. Red star is epicentre of 2004 event relocated (this study). In red, aftershocks recorded by local network (black triangles) from March 25 to April 10, 2004. In blue, background seismicity recorded during a 5-week-long local survey in 1989 (Hatzfeld et al., 1993; Cherkaoui et al., 1990); in yellow, epicentres recorded during a local survey following the 1994 event (El Alami et al., 1998); in green, relocated aftershocks recorded regionally of the 2004 event (this study). (For interpretation of the references to color in this figure legend, the reader is referred to the web version of the article.)

below a structural level made of shallow dipping décollement, remnants of the Miocene Rif nappes (Galindo-Zaldivar et al., 2009; Negro et al., 2007; Mattauer, 1964). However, the nearby occurrence of active faults shaping the landscape of the lower Nekor basin as well as the well-known Nekor and Jebbha strike-slip-faults remains to be explained (Leblanc and Olivier, 1984).

To better document the deformation of the Al Hoceima region, we present here an aftershocks study of the 2004 event together with a review of recent seismological and geological data.

The main shock of February 24, 2004 was followed by a large number of aftershocks, some of them with magnitude greater than 5 between February 25th and 28th, and on March 20th (Table S3). The main shock and the aftershocks were located independently by the national seismological network of Spain and Morocco and by the European-Mediterranean Seismological Center. The analysis of the aftershocks we present here results from 15 days of recording with a temporary network installed in the epicentral area from March 29 to April 11 2004 (Dorbath et al., 2005; Table 1). The main shock and the largest aftershocks were relocated. The P and SH waveforms recorded at teleseismic distances were then inverted. We then compare these results with the main tectonic features of the region.

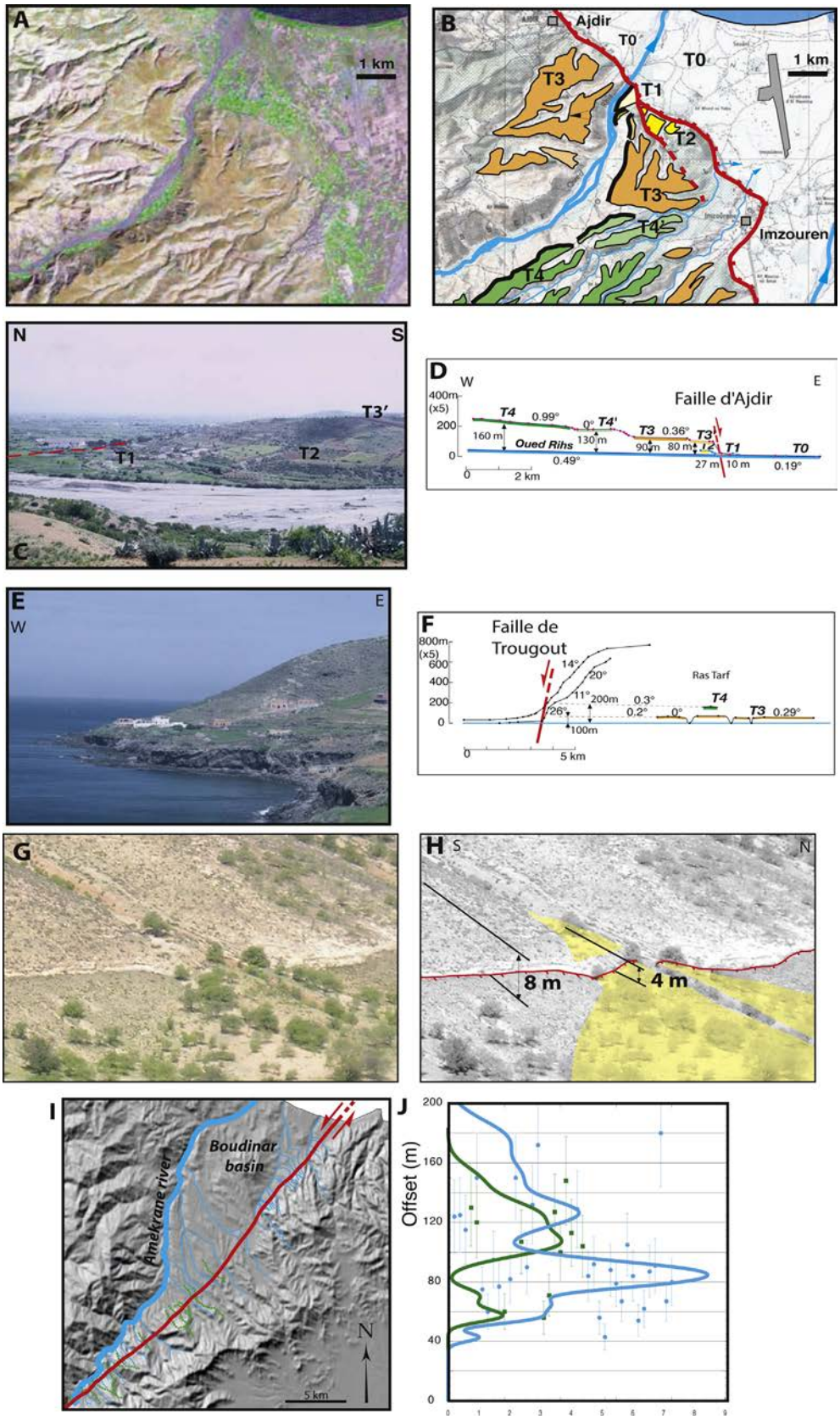

Fig. 3. (a–d) Details of Ajdir normal fault in northwestern Al Hoceima bay. (a) Landsat image enhancement of Ajdir normal fault from Ajdir to Imzouren. (b) Ajdir normal fault map from image interpretation and field observations. Typical embedded fan-shaped terraces abandoned by the northeast flowing Rihs river indicate that they result from uplift along the Ajdir normal fault. (c) View to east of abandoned terraces of the Rihs river uplifted in front of the Nekor basin. (d) projection of terrace heights along Rihs river from 1:50,000 scale topographic map. The several kilometre-long swath of terraces indicate uplift of 10–160 m. (e and f) Details of Trougout normal fault along northeastern Al Hoceima bay. (e) View to north along northeast shore of Al Hoceima bay. Recent uplift is marked by uplifted sea benches. (f) W-E projected topographic profiles indicating possible vertical uplift of 2 marine terraces of about 100 and 200 m. (g and h) Details of Rouadi normal fault 15 km west of Al Hoceima.

Fig. 4. (a–d) Details of ground ruptures visible in the field about 1 month after the 2004 event. (a) En échelon ground fissures with about 10 cm of vertical displacement near slope top along Rihs river bed interpreted to result from ground subsidence near instable steep slope of river incision. (b) Large blocks chaos resulting from local landsliding in slope along Rihs river. (c) Open NE oriented crack with a few centimetres of vertical offset along Tafensa normal fault indicating uplift of upper side, i.e., northwest. (d) Same location as (c), en échelon open cracks across colluvium indicating uplift of right side, i.e., northwest.

Table 1
Seismic station name, location and recording period.

Name	Latitude	Longitude	Elevation	Installation period
ABIM	35.2615	−3.9293	139	2004/03/29–2004/04/11
AERM	35.1812	−3.8442	10	2004/03/31–2004/04/11
AGHM	35.0440	−3.9862	433	2004/04/01–2004/04/10
AITM	35.1375	−3.9687	355	2004/03/31–2004/04/11
BARM	35.0900	−3.8190	146	2004/03/31–2004/04/11
CIMM	35.1772	−3.8907	119	2004/03/29–2004/04/11
ICHM	35.0782	−4.1448	615	2004/04/08–2004/04/11
IGHM	35.1960	−3.6843	406	2004/03/29–2004/04/02
IJLM	35.1340	−4.1057	298	2004/04/04–2004/04/11
IHNM	35.0807	−3.9267	360	2004/04/06–2004/04/11
IMZM	35.1608	−3.8575	43	2004/03/29–2004/04/11
KARM	35.1077	−3.7262	837	2004/03/30–2004/04/11
LAZM	35.2638	−3.7297	66	2004/03/29–2004/04/03
NEKM	34.9892	−3.8223	386	2004/03/29–2004/04/10
RASM	35.2827	−3.6802	66	2004/03/30–2004/04/03
TAFM	35.1952	−4.0318	344	2004/03/29–2004/04/11
TIFM	35.0900	−3.8822	279	2004/03/29–2004/04/11
TIRM	35.1188	−3.7700	245	2004/03/29–2004/04/11
TROM	35.1770	−3.7715	99	2004/03/29–2004/04/11
YOUM	35.2205	−3.9855	316	2004/03/31–2004/04/11

2. Tectonic summary

The Al Hoceima region is part of the Rif mountain belt, which, with the Betics, form the west vergent Gibraltar arc of lower Miocene age (Andrieux et al., 1971; Tapponnier, 1977; Gutscher et al., 2002; Frizon de Lamotte et al., 1991; Fig. 1). Several models have been proposed to explain the simultaneous uplift of the Betics and Rif ranges and the subsidence of the Alboran Sea in between during the Miocene implying various subduction geometries and roll-back mechanisms (Platt and Vissers, 1989; Watts et al., 1993; Seber et al., 1996). The Alboran Sea is floored by a less than 20 km-thickcontinental crust, underlain by an abnormally high velocity upper mantle in the vicinity of the Gibraltar strait, which becomes abnormally low to the east (Payo and Ruiz de la Parte, 1974; WGDSSAS, 1978). The western part of the Alboran Sea experienced an important subsidence with an accumulation of 7 km of Neogene sediments and is not disturbed by faulting, while east of 4° W, the topography of the seafloor is strongly perturbed by volcanic ridges and faulting. The most prominent feature within the Alboran Sea is the so-called Alboran ridge, a 150 km-long anticlinorium bordered on its southeastern flank by a reverse fault dipping to the northwest (Morley, 1992; Woodside and Maldonado, 1992; Bourgois et al., 1992; Martinez-Garcia et al., 2011; Fig. 1). The

(g) View to NNE of Rouadi normal fault marked by an east facing cumulative scarp across colluvial slope and debris fan. (h) Interpretation of photo in (g). Yellow colour underlines fan shape deposit crosscut by normal fault and offset about 4 m. Vertical offset of colluvial slope may reach 8 m. (i and j) Evidence of sinistral geomorphic offset along Nekor fault southeast of Boudinar basin. (i) High resolution SPOT image with mapped fault and highlighted stream-bed and ridge-crest cumulative offsets. (j) Plot and distribution of measured offsets, in blue, stream-bed offsets, in green, ridge-crest offsets. (For interpretation of the references to color in this figure legend, the reader is referred to the web version of the article.)

southwestern prolongation of this fault coincides with the Jebha strike-slip fault, although such a connexion has not been identified on seismic reflection profiles (Bourgois et al., 1992).

Recent GPS displacement fields have been interpreted with a distinct western Alboran micro-plate or block separated from the Mediterranean to the east by a roughly NNE-SSW line joining the Al Hoceima region to the eastern Betics, namely the Carboneras and Palomares fault zones (Koulali et al., 2011; Martinez-Garcia et al., 2011). This structure has long been identified as a region of intense seismicity across the eastern Alboran sea (Andeweg and Cloetingh, 2001; Buforn et al., 1995; Calvert et al., 1997) and is inheritedfrom the Miocene westward expulsion of the Alboran block (Andrieux and Mattauer, 1973; Tapponnier, 1977). Based on GPS data, about 4.5 mm/yr of left-lateral shear may be accommodated along this active seismic and tectonic boundary (Koulali et al., 2011; Fadil et al., 2006) (Fig. 1). How exactly, and along which faults, such displacement is accommodated and absorbed remains to be determined. The geometry of the Jebha and Nekor left-lateral strike-slip faults as well as the north-south normal faults in between and the recent 1994 and 2004earthquakes of magnitude ≥6 may accommodate part or totally this left-lateral shear across the western Mediterranean (e.g., Morel and Meghraoui, 1996).

The presence of the western Alboran block may explain the complex geometry of the northern boundary of the African plate in the western Mediterranean, in contrast with the tectonic strain in the Tell towards east, and also, with the more narrow plate boundary west of Gibraltar, namely the Gloria fault zone. It marks the westernmost limit of NW-SE right lateral shear along the northern African plate, with the Yusuf fault zone being the last NW-SE right-lateral fault as opposed to a through going E-W right-lateral shear zone across the Alboran sea (Martinez-Garcia et al., 2011). It probably explains that part of the deformation at the northwestern tip of the African plate is taken into account across the Middle Atlas and Atlas to the south, up to the Betics towards north. Determining the slip-rates of known active faults, the location of past large earthquakes as well as the best determination of earthquake source mechanisms, in particular for moderate to large earthquake of magnitude 6–6.5 is thus an important step towards a better knowledge of seismic hazard in the western Mediterranean region.

3. Seismological observations from the temporary network

3.1. Data and processing

The post-seismic field study resulted from a common initiative between Centre National de la Recherche Scientifique et Technique (CNRST, Rabat), Ecole et Observatoire des Sciences de la Terre (EOST, Strasbourg) and Institut de Physique du Globe de Paris (IPG, Paris). Unfortunately, the fieldwork began quite late, more than 4 weeks after the occurrence of the main shock. In a first step, 17 stations were installed. After few days, 3 of them were moved to improve the coverage of the aftershocks on the base of the first locations (Table 1 and Fig. 5).

3.1.1. Instrumentation

All sites were equipped with TAD station and the sensors were 2 Hz vertical Mark Product L22. The conception and the design of these stations are rather old but they are robust and easy to maintain. The time is given by an internal clock and periodical GPS recordings control their very low drift (few thousandths of second per day). Two major drawbacks of the stations are their low dynamic (10 db) and their low capacity of storage on a flash card (4 Mo). The first one is not crucial since we are mainly interested by arrival times and not by amplitudes and waveforms. The second one is solved by frequent visits, about every 48 h. But the most awkward problem with this kind of station consists in the triggering system.

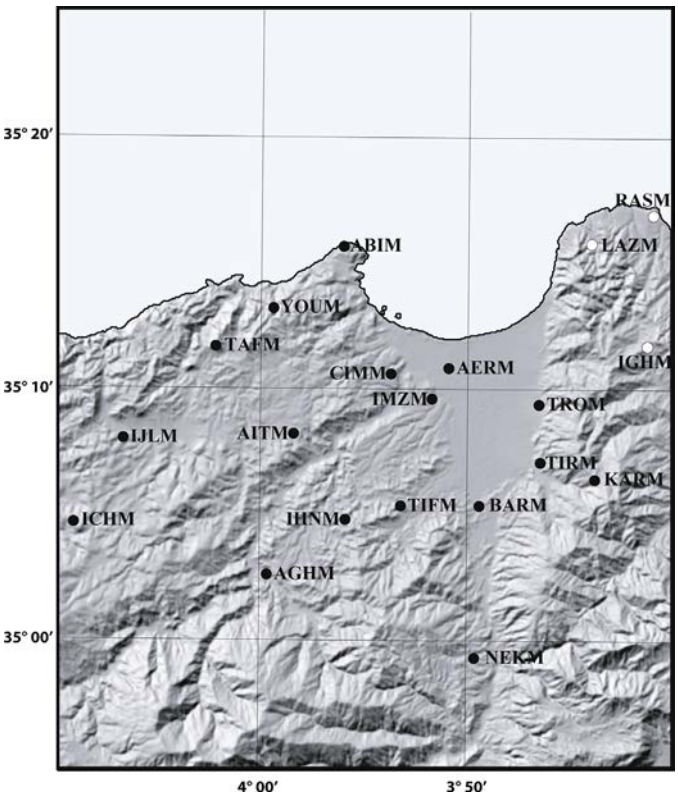

Fig. 5. Location map of seismological stations installed in epicentral area during aftershock survey following the February 24, 2004 event. Stations RASM, LAZM and IGHM (white circles) were moved to IJLM, ICHM and AGHM after few days of survey. The network recorded during 14 days, from 28 March 2004 to 10 April 2004.

It needs a careful choice of the STA/LTA ratio to avoid the triggering by the S-Waves rather than by the P-Waves and a rapid filling of the memory, and to record the largest number as possible of events by the largest number of stations as possible to insure good quality locations. Recording was done at a rate of 100 samples per second. Each record has a length of 4098 samples, that is about 40 s.

3.1.2. Network

In the lack of primary surface faulting, the geometry of the network has been guided by the locations of the main shock and largest aftershocks by national and international agencies (CSEM, USGS, IGN). The distribution of damage has also been taken into account, although at a lower degree since local site effects may be misleading. After few days, the geometry was modified, the 3 easternmost stations RASM, LAZM and IGHM were moved to IJLM, ICHM and AGHM to reinforce the western part of the network where intense seismic activity had been detected (Fig. 5 and Table 1). This geometry was quite convenient with regard to the seismicity, even if one more station should have been welcomed midway between AGHM and NEKM in the south and another farther south of the southernmost station NEKM (Fig. 5). Unfortunately, the access to this region was difficult due to the lack of roads.

3.1.3. Data analysis

As we used only one component vertical sensor, the identification and, consequently, the reading of S-arrival times are a little bit puzzling. Hypothetic S-arrival times have been read systematically. The Wadati method applied to these readings gives a rather low V_p/V_s ratio of 1.67, a little bit larger than the value of 1.64 found by Hatzfeld et al. (1993) in the same region with vertical sensors during a 5 weeks survey. A first location has been performed using a slightly modified version of Hypoinverse (Klein, 1978). The events

Table 2
Crustal velocity model.

H_{top} (km)	V_p (km/s)
0	5.5
6	5.9
48	7.9

with less than 8 P and 2 S-arrival times contributing to the final solution have been discarded. On average, each event is located using more than 10 P and nearly 6 S-arrival times. The velocity model was taken from Hatzfeld et al. (1993) with the V_p/V_s ratio we found (Table 2). We eliminated the events with rms greater than 0.2 s and large horizontal errors, greater than 2 km, but we kept the events with large vertical errors when they are close to the surface and at a distance to the nearest station larger than the depth. The mean rms is 0.06 s, the mean horizontal error 0.8 km and the mean vertical error 1.7 km (including the few events with large vertical errors). The output of the programme is then used as input data (travel times) in the tomoDD scheme (Zhang and Thurber, 2003). This procedure allows computing simultaneously the location of the events and the 3-D velocity structure. It is an improvement of the classical Simulps method (Thurber, 1983) that uses the hypoDD location process (Waldhauser and Ellsworth, 2000). The figures of this paper only present the final relocation from this code. The comparison between the overall distribution of the seismicity using Hypoinverse and tomoDD shows no significant changes, only at small scales are changes noticed. The magnitudes have been determined from the coda length using the common relation $Md = 2 \times \log(t) - 0.87$, where t is the coda length in seconds.

3.1.4. Event catalogue

More than 650 events have been located between March 29 and April 11, 2004 with magnitudes from 0.9 to 3.5 (Fig. 6 and Table S1). The catalogue appears to be complete for magnitudes greater than 1.7. The b value in the Gutenberg–Richter law is quite high, 1.4, probably resulting from an overestimation of the low magnitudes.

3.1.5. Focal mechanisms

Aftershock focal mechanisms have been manually constructed from the first arrival P-waves polarities. We have only considered relocated events that have at least nine polarities and covering at least 3 quadrants. Among 676 relocated aftershock, 164 focal mechanisms have been determined without any erroneous polarity (Table S2 and Fig. S1).

3.1.6. Global stress tensor

The stress tensor at the depth of the aftershocks can be obtained from the inversion of focal mechanisms. Several inversion schemes are available. We used the method of Michael (1984, 1987) with the soft modification introduced by Dorbath et al. (2010), which allows to eliminate from the process the focal mechanisms presenting a "large" misfit between the observed and calculated slip angles for both planes. Instead of a single operation, the inversion follows an iterative process. Due to the high quality of the focal mechanisms, the threshold to define 'large' was fixed to 15°. Hereafter, the values given for the directions of σ_1, σ_2, σ_3 and R are those obtained through the inversion. We present also 100 tensors obtained through a bootstrap method for each inversion, so that one can estimate the uncertainties on the principal directions of the tensors.

The inversion was performed for a set of 169 focal mechanisms (164 from the aftershock sequence plus the main shock and 4 large aftershocks that occurred before the deployment of our local network). The inversion leads to a well-constrained solution with σ_1 and σ_3 trending N337E and N246E, respectively. The shape factor R defined as $R = (\sigma_1 - \sigma_2)/(\sigma_1 - \sigma_3)$ is 0.7. The mean misfit between observed and calculated direction of slip is $8° \pm 4°$ (Table 3).

In order to assess the possible change of stress regime at a more local scale, we have also calculated the stress field for aftershock areas corresponding to the different clusters.

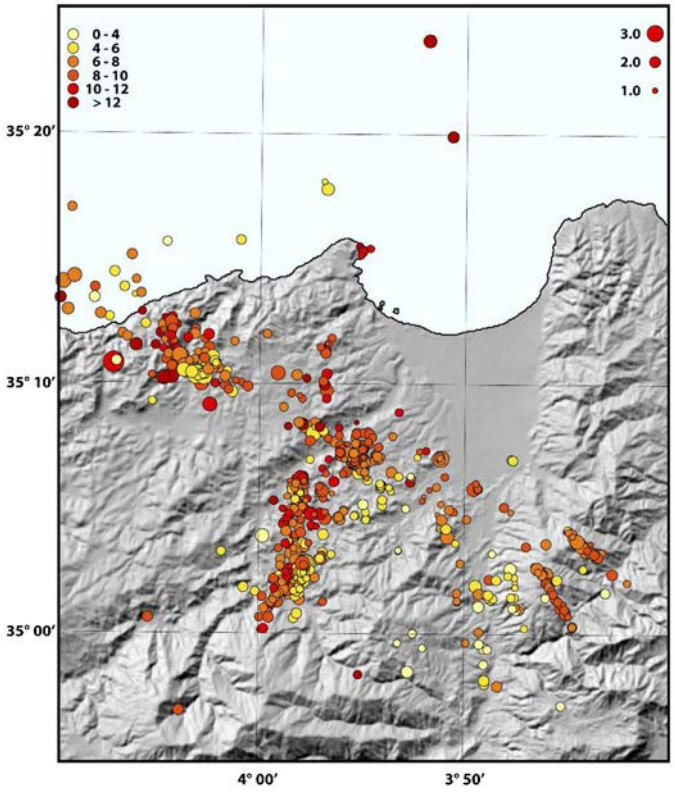

Fig. 6. Distribution of aftershocks recorded during temporary field survey from 28 March to 10 April 2004.

3.2. Results

The aftershocks depict roughly a T shape distribution with a long, discontinuous N110-120E branch and a dense N10-20E branch to the south (Fig. 6).

Table 3
Stress tensor characteristics of the Al Hoceima earthquake sequence.

Events subset	Maximum stress σ_1 azimuth/plunge (°)	Minimum stress σ_3 azimuth/plunge (°)	Misfit $\Delta\sigma$ (°)	$R\,(\sigma_2-\sigma_3)/(\sigma_1-\sigma_3)$	Retained/total subset
Al Hoceima 2004, this study	N337/23	N246/03	8 ± 4	0.7	131/169
Western cluster (see Fig. 8)	N341/17	N251/02	7 ± 4	0.5	11/13
Northern cluster (see Fig. 9)	N341/19	N250/03	6 ± 4	0.8	59/77
Eastern cluster (see Fig. 11)	N370/81	N240/06	6 ± 4	0.8	34/37
Southern cluster (see Fig. 12)	N337/15	N247/00	7 ± 4	0.6	38/42
Temporary network 1989 (Hatzfeld et al., 1993)	N334/44	N246/02	9 ± 4	0.9	37/42

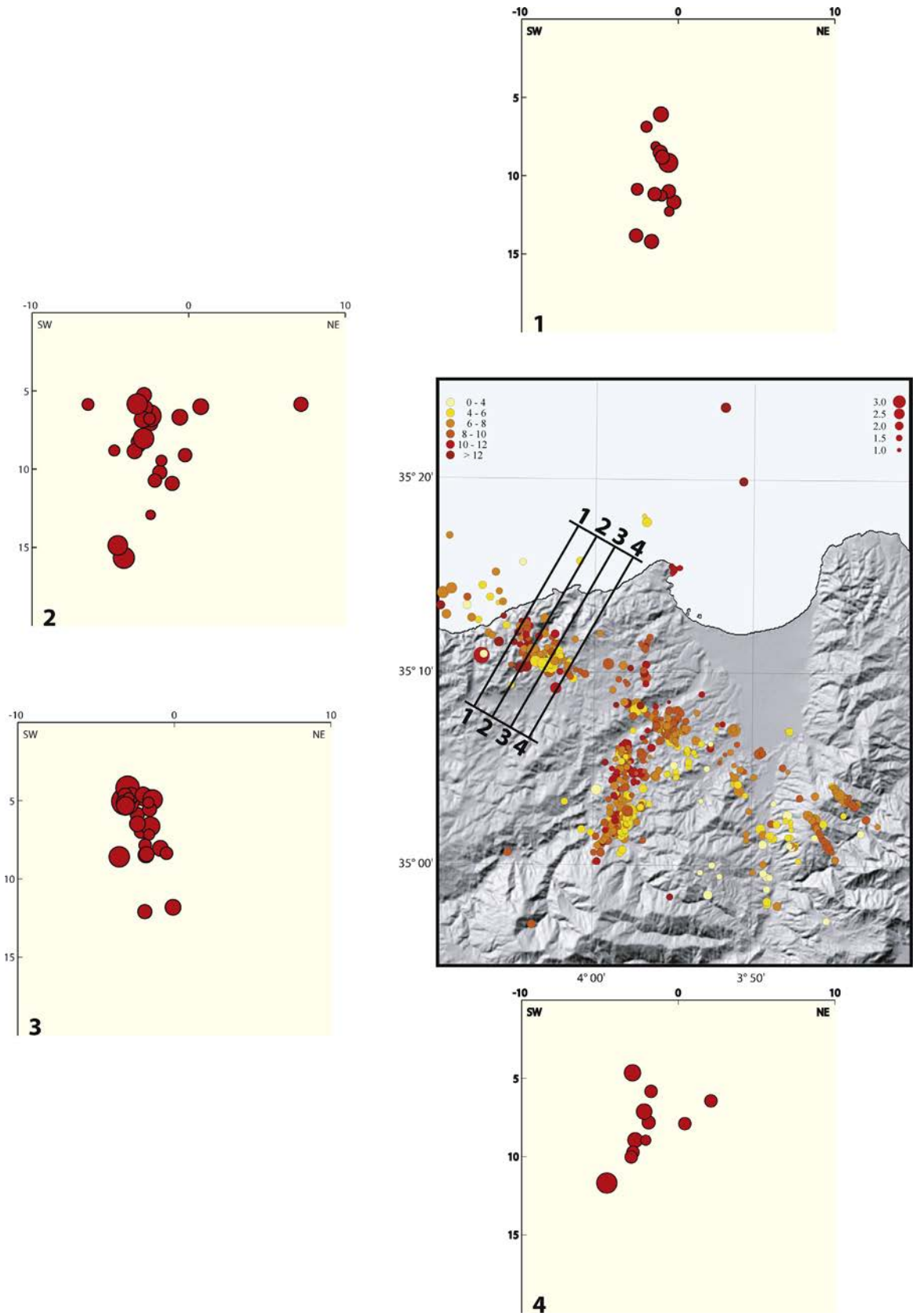

Fig. 7. Vertical sections across western cluster of N115E branch.

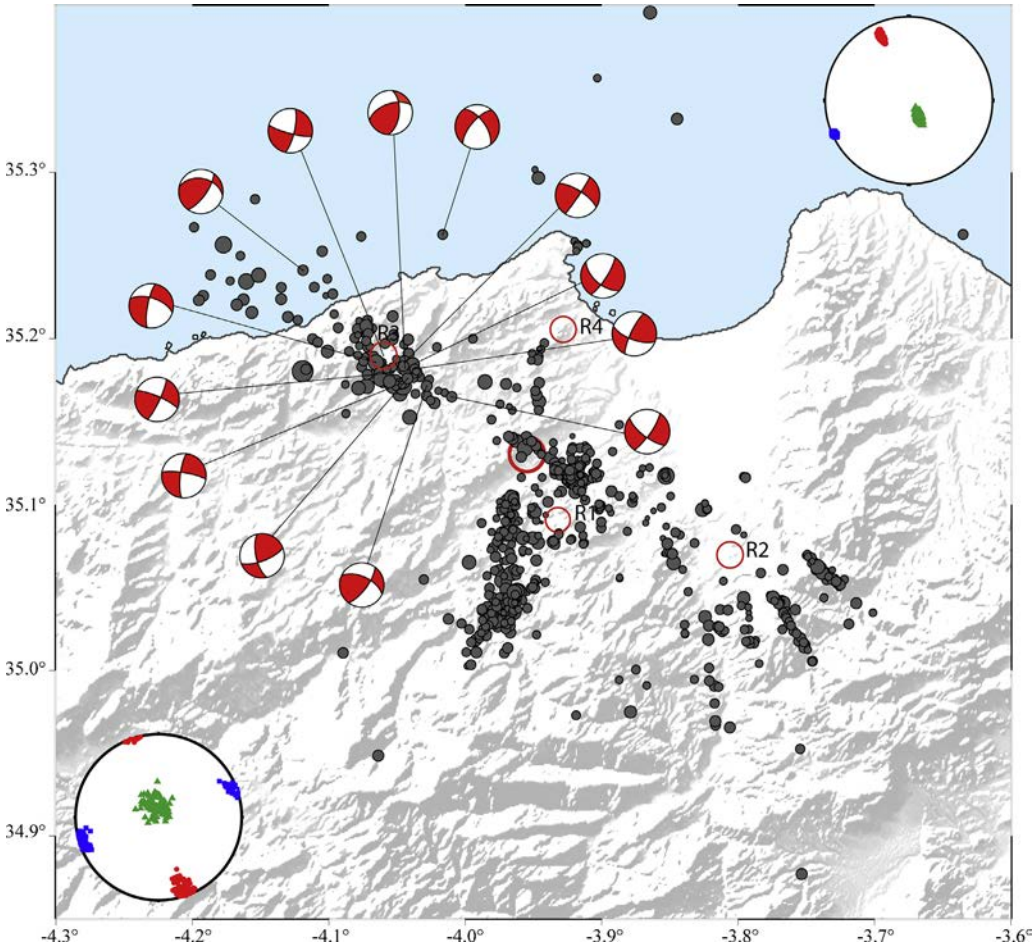

Fig. 8. Focal mechanisms in western cluster. Bottom: corresponding local stress tensor. Top: global stress tensor. σ_1 in red, σ_2 in green and σ_3 in blue. R1–R4 are master events used for relocalization with focal mechanisms from http://www.globalcmt.org/. (For interpretation of the references to color in this figure legend, the reader is referred to the web version of the article.)

The long N110E branch runs from the coast, and even offshore, to the Nekor fault (Figs. 2 and 6) discontinuously over 35 km. To the west (near Tafensa), the seismic activity is denser where some of the largest aftershocks occurred. Our coverage to the west is not sufficient to give a precise picture of the termination of this cloud, which is partly under sea. Vertical NE-SW sections across this cluster (Fig. 7) show a mostly vertical (or slightly south dipping) distribution between 5 and 15 km. The focal mechanisms are mainly strike slip (Fig. 8) with nodal planes grossly WNW-ESE and SSW-NNE. Most of the mechanisms present a normal component and, occasionally an inverse one, like the westernmost determined mechanism. The normal component is dominant when the fault plane is N150-160E. Only 13 solutions are built in this area, consequently, the local tensor is not well defined (Fig. 8). The inversion leads to a tensor with σ_1 and σ_3 striking N341E and N251E, respectively, both almost horizontal, with directions very close to those of the "global" tensor, and a 0.5 shape factor (Table 3).

In the area at the intersection of the two branches, the largest number of focal mechanisms is determined due to the important activity and to the central situation of that zone in our network (Fig. 9). They are principally strike-slip like along the western segment. Nearly pure strike-slip occurs on fault oriented N20E (respectively N200E) and a normal component appears when the fault plane moves off. The normal component then becomes preponderant and pure normal faulting occurs on fault planes striking about N160E. In this area, the local stress tensor principal directions are N341E and N250E for σ_1 and σ_3, respectively, very similar to the global tensor, and the shape factor is equal to 0.8 (Table 3).

East of the intersection with the N20E branch, the seismicity along the N115E branch decreases together with the magnitudes. Clear dense aftershock alignments display a kind of "horse tail" shape that abuts on the Nekor fault (Figs. 2 and 6) with mostly normal focal mechanisms (Fig. 10). There, the local stress tensor changes clearly, σ_1 is vertical so that the tensor is extensive. However, the direction of σ_3 is N240E close to the direction of σ_3 in the two previous studied areas. Note that although the *R* factor is 0.8, there is a clear symmetry of rotation of σ_1 and σ_2 around the σ_3 direction (Table 3).

The N20E branch extends from the northern bank of the Oued Rhis about 10 km south of Al Hoceima to the northern flank of the Jbel Hamman for about 20 km southwards (Figs. 2 and 6). North of the Oued Rhis the activity is sparse and deep. From the intersection with the N115E branch to the south a compact cluster of events are distributed vertically (or slightly dipping west) between about 4 and 12 km (Fig. 11). The focal mechanisms built along the southern cluster (Fig. 12) show mostly left-lateral strike-slip faulting when the general direction of the branch is considered. When the fault plane is nearly vertical with an azimuth close to N20E, then the mechanism is almost purely left-lateral. Otherwise, a normal component is present similarly to the cluster near Tafensa. When the dipping plane strikes about N160E, the corresponding mechanism is almost purely normal. A few reverse mechanisms are present when the fault planes strike N60-70E. Along this segment σ_1 and

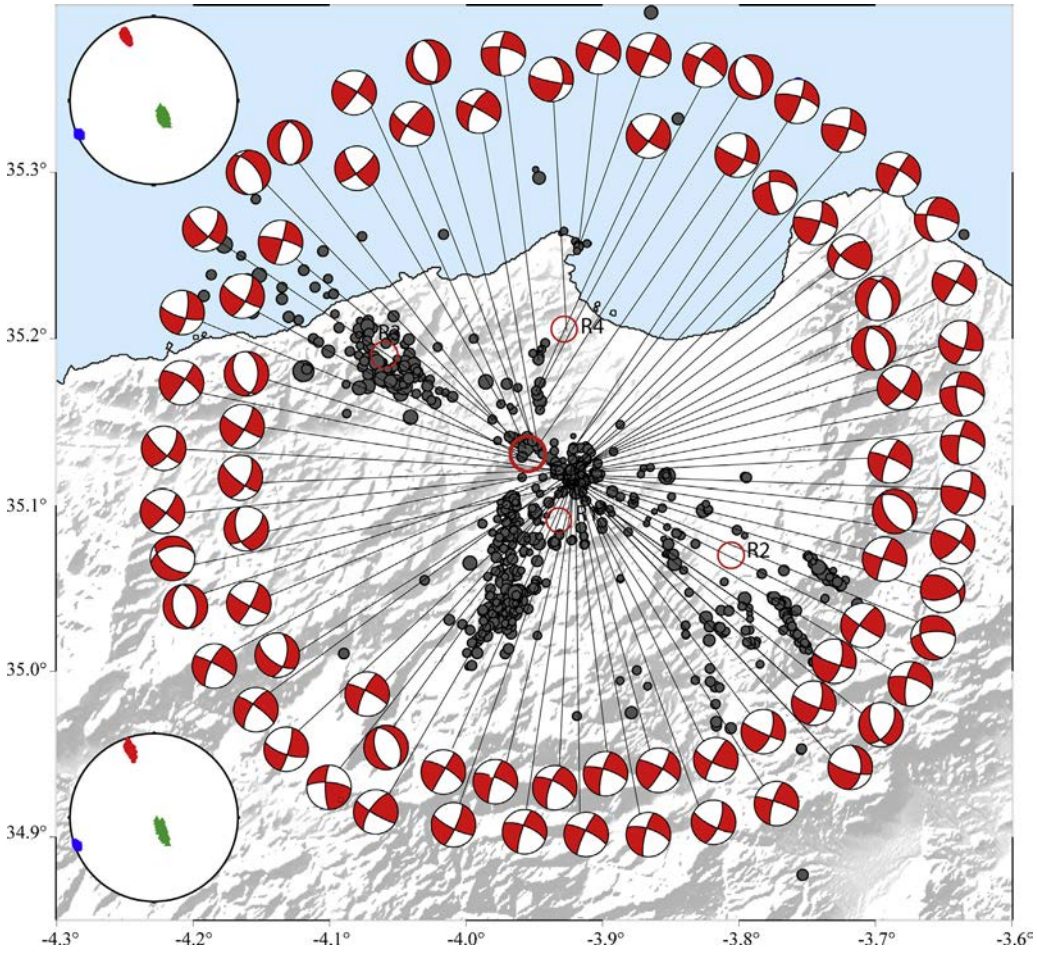

Fig. 9. Focal mechanisms in epicentral area. Stress tensors, and R1–T4, same as Fig. 8.

σ_3 strike N337E and N247E, values very near those of the global tensor (Table 3).

4. Relocation of the main shock and early aftershocks

To gain more precision on the aftershock sequence we relocated the main shock and aftershocks that occurred before the installation of our temporary network through a master event technique. We used stations of the Spanish national network (IGN) and the national network of Morocco (CNRST). The arrival times of P and S waves were taken from the respective bulletins. We selected a dozen of Spanish stations to have the best azimuthal coverage as possible to the north and to the east, where the station of Mellila (Fig. 1) was particularly welcome. The arrival times at the Spanish stations are read with a high precision, better than a tenth of a second. The stations from Morocco do not offer such a high quality and the arrival times are usually read with a precision of half of a second. We took this difference into account by affecting a lower weight to the data from Morocco. Nevertheless, the presence of such data to the south and to the west complements the azimuthal coverage and is of a crucial importance. During our fieldwork some aftershocks occurred with magnitudes large enough to have been also recorded by both permanent networks. We selected 5 of these events as master events. The epicentres of the selected events cover the whole aftershocks cloud, so that one of them, at least, is close enough to a particular relocated aftershock. In such manner, we always satisfy the conditions required to run properly the routine of the master event technique (Besse, 1986). In this process, the depth of the event is kept fixed and equal to the depth of the master event selected that is, in our case, between 6 and 10 km.

The main shock and 150 aftershocks were relocated (Table S3 and Fig. 13). The relocated aftershocks were selected on the base of their magnitude given by the Spanish network (IGN). We kept only the events with a magnitude 3.5 or greater and with rms of the differences between observed and calculated travel times less than 1 s. To evaluate the errors only two events recorded during the temporary campaign satisfy the criteria of magnitude, out of the master events. The differences between the locations obtained directly from our network and through the relocation scheme are, respectively, about 2 km and 2.5 km, however errors double of these values cannot be discarded in some unfavourable cases. The main shock epicentre position is 35°07.72′ N, 3°57.31′ W to be compared to the position found by the Spanish network, 35°08.54′ N, 3°59.81′ W (IGN) and the national network of Morocco, 35°12.00′ N, 3°53.40′ W (CNRST). Our location is in between the two others, but closer to the Spanish epicentre (about 4 km) than to the other one (almost10 km), which reflects, for a part, the highest weight attributed to the Spanish data. The main shock struck almost exactly at the intersection of the two main aftershock branches (Fig. 13).

The distribution of the early aftershocks is globally the same as the distribution of the late aftershocks, with, however, more events along the N20 branch (Fig. 13). There are more large events at the northern extremity of the N20E branch and lower magnitude events along the main segment of the N20E branch and at the western extremity of the N110E branch. Only very few events are

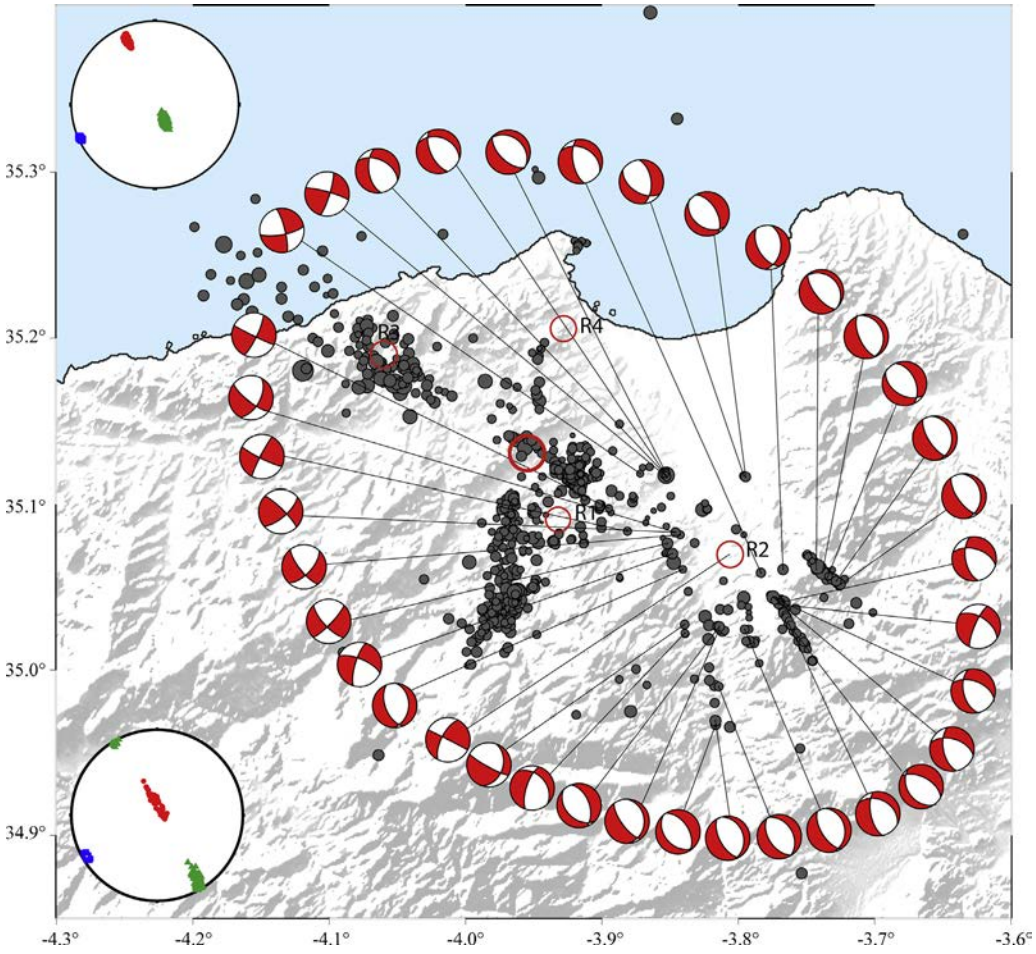

Fig. 10. Focal mechanisms in eastern part of N115E branch. Stress tensors, and R1–T4, same as Fig. 8.

relocated along the eastern extremity of the N110E branch (note that only events of magnitude greater than 3.5 are considered). Considering the temporal evolution of the activity, the important fact to mention is that the first event that was located at the western extremity of the N110E branch (35°11.36 N, 4°03.40 W) occurred almost 5 h after the main shock while 30 events already occurred on the N20E branch and in the zone of intersection of the two branches.

5. Modelling of the main shock from P and SH waves, teleseismic inversion

Teleseismic P and SH waveforms were inverted to obtain an independent determination of the main shock focal mechanism, seismic moment, source depth, as well as an estimation of source dimension. Broadband seismograms used here were recorded by the IRIS and GEOSCOPE networks and data processing includes deconvolution from the instrument response, integration to obtain displacement, equalization to a common magnification and epicentral distance, and bandpass filtering from 0.01 Hz to 0.8 Hz (P waves) or to 0.4 Hz (SH waves). Synthetic seismograms were computed using the Nabelek (1984) procedure, with a simple half-space crustal velocity model at the source and stations. We increased the number of point sources according to two criteria: (i) an additional point source should improve significantly the waveform fit, and (ii) a point source should amount for a minimum of 10% of the total seismic moment. In such a way we introduce some degree of complexity in the model as required by the data, avoiding the incorporation of unconstrained features. The Nabelek's method allows simulating an extended source using a series of point sources, one at the hypocenter and the others at specified distances and azimuths with respect to the first one. With the models constituted by three point sources a crude estimation of the source dimension can be obtained, corresponding to the distance between the point sources located on both sides of the hypocenter.

P and SH waveforms could be reproduced by a series of three point sources (subevents) aligned either along the N110E branch of the aftershock distribution, or along the N20E branch (Figs. 14 and 15). In both cases, the dominant part of the source is represented by a strike-slip focal mechanism corresponding to a point source located at the hypocenter (strike, dip, rake) = (295, 89, 170) or (25, 80, 001). Two secondary point sources displaying larger normal faulting components are required to explain the complex behaviour of the P waveforms. Those two additional sub-events are delayed 1 and 3.5 s with respect to rupture nucleation time. Overall, the two models indicate a rupture dimension of the order of 15 km with most seismic moment concentrated around the hypocenter. In the N110E case (Fig. 15), rupture propagated more extensively towards the east, whereas in the N20E case (Fig. 14) it propagated more extensively towards the south. The rupture developed at shallow depth, around 7 km or less. The two solutions (N110E or N20E) are undistinguishable from the RMS waveform misfit error point of view. They can be considered to be equally likely and teleseismic data do not allow us to discriminate between the two trends. The seismic moment resulting from the inversion is 4.0E + 25 dyne cm, corresponding to Mw = 6.4.

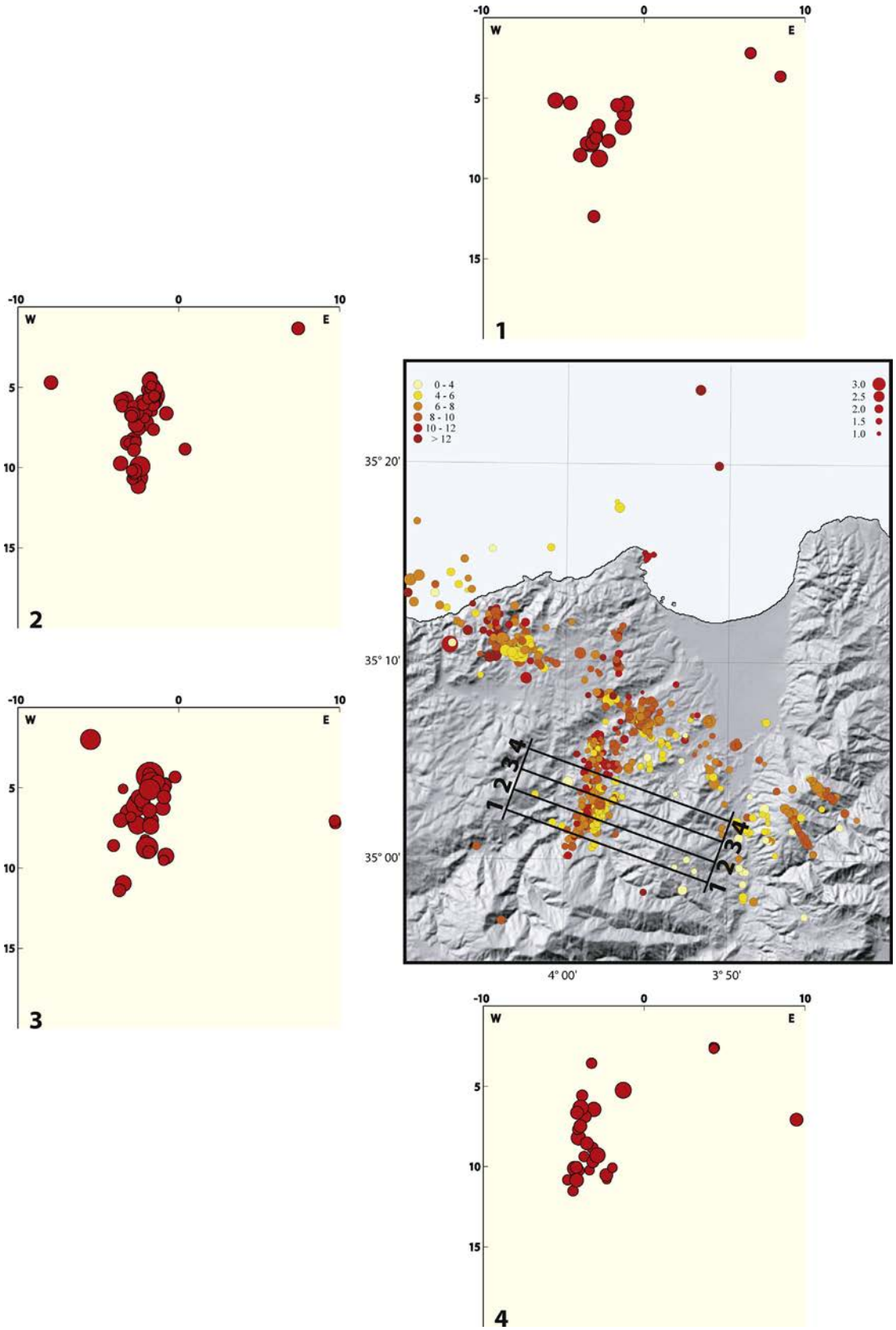

Fig. 11. Vertical sections across southern part of N20E aftershock branch.

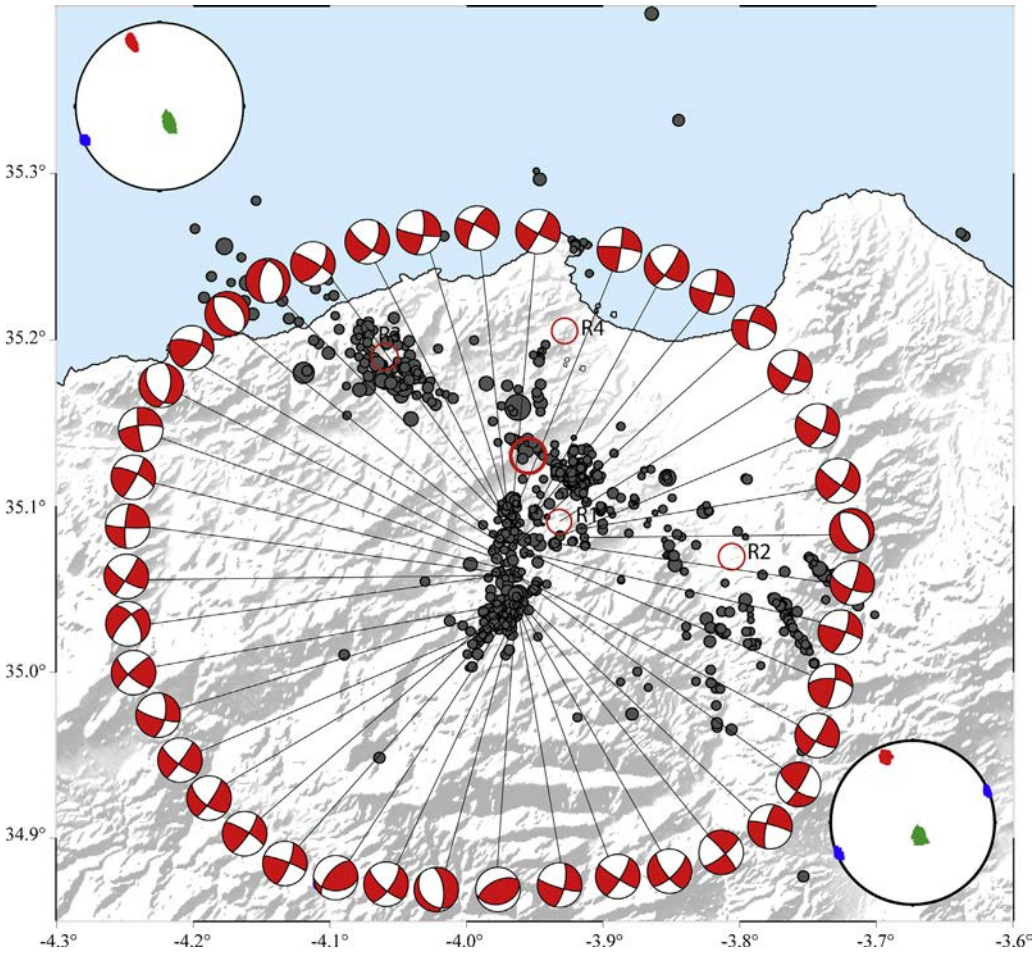

Fig. 12. Focal mechanisms in southern cluster. Stress tensors, and R1–T4, same as Fig. 8.

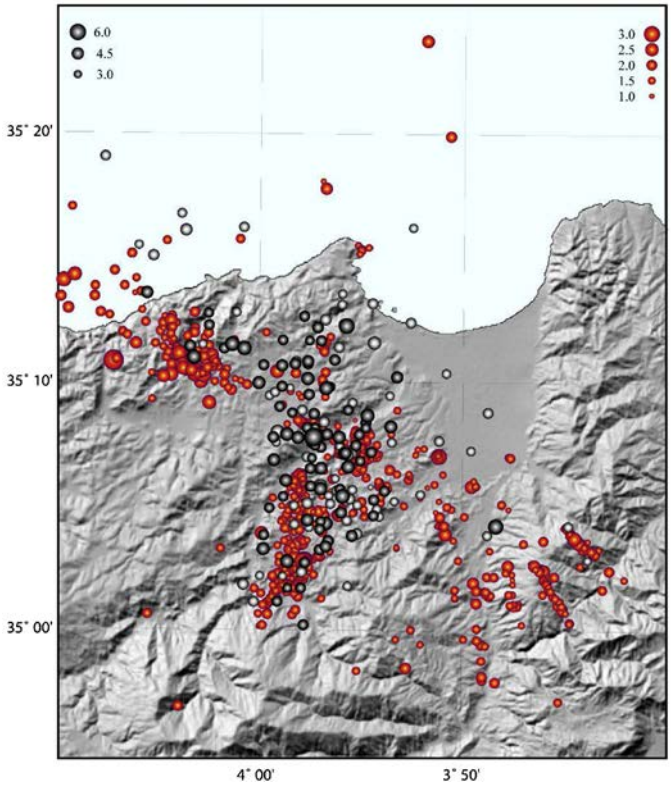

6. Seismic tomography

The travel-times of the best-located aftershocks have been used for a tomographic inversion using tomoDD code (Zhang and Thurber, 2003). From the 676 selected events, we obtained about 11,400 absolute travel-times (~38% being S waves), and constructed more than 50,100 differential travel-times with inter event distances of less than 10 km.

We tested several inversion grids and found stable results, i.e., a velocity model independent of the sampling of the volume, with a grid spacing of 4 km horizontally and 3 km vertically from the surface down to 15 km, the maximal depth of the hypocenters. The rotation of the grid does not change the results of the inversion, and hereafter we present the results on a grid rotated 40° anti-clockwise, allowing the Y nodes to be about parallel to the major tectonic directions (i.e., the Nekor fault) (Fig. 16). After 15 iterations, the weighted rms travel time residual was reduced to 0.03 s.

The starting 1D velocity model was constructed with the VELEST (Kissling et al., 1994), and tomoDD methods. Both methods resulted in a simple model with a quasi-uniform P-wave velocity structure at about 5.72 km/s down to the maximum depth of resolution. V_p/V_s ratio did not change compared to the value given by the Wadati method (see Section 3.1) and then 1.67 was taken in the inversion. The robustness of the solution has been tested through numerous

Fig. 13. Main shock and large early aftershocks relocated (black) (Table S3). Aftershocks recorded by local network (this study) in red (Table S1). Note difference in symbol size for magnitudes.

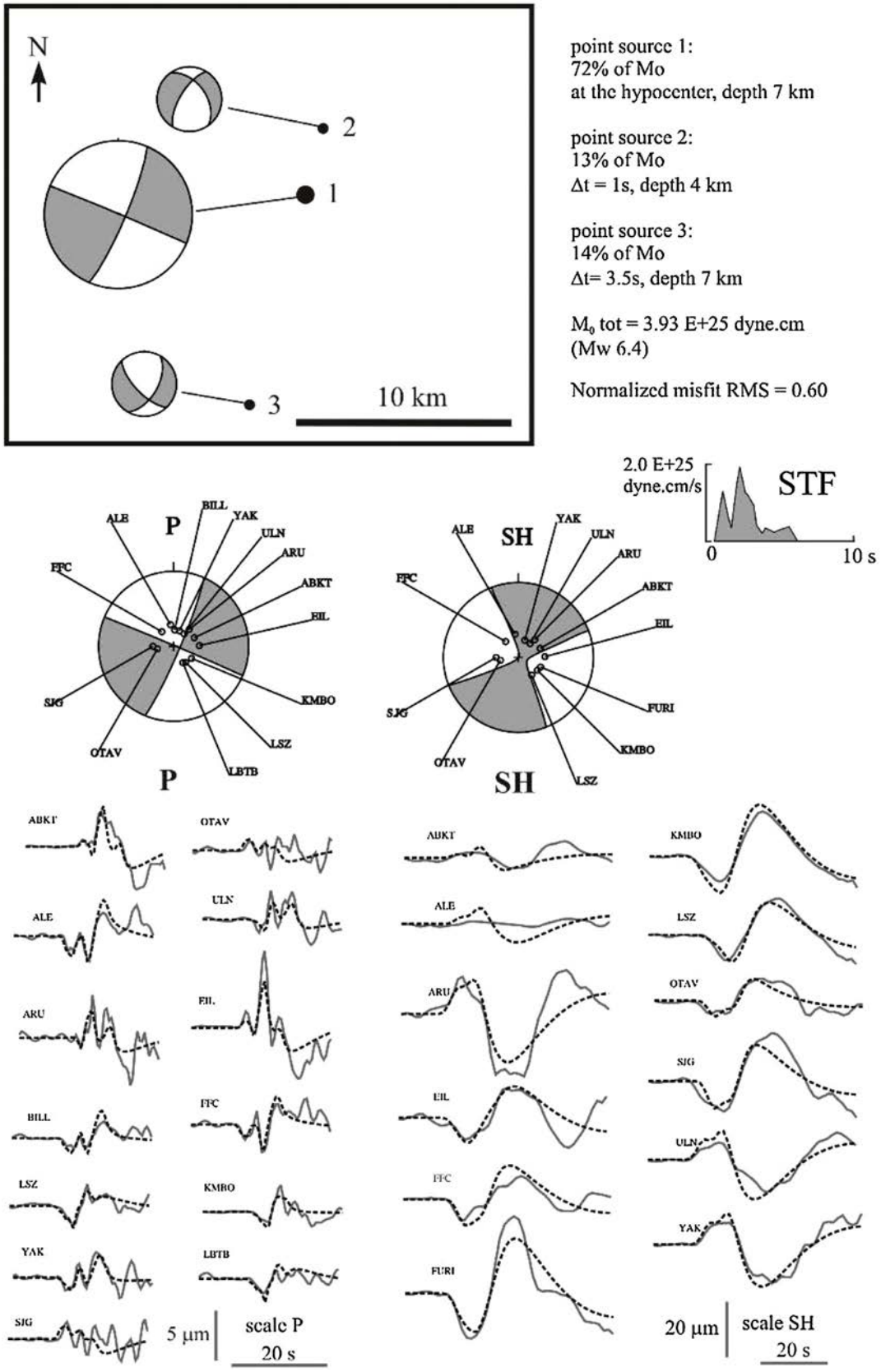

Fig. 14. Result of teleseismic modelling with three subevents aligned along N20E direction. Frame at top shows relative location of three subevents (point sources) with their corresponding focal mechanisms. Predominant subevent number 1 is located at hypocenter. Focal mechanisms for P and SH waves (compression shaded) with station distribution are drawn at centre of figure. Beside, STF (global source time function), displays evolution of seismic moment rate with time. At bottom, waveform fit with observed and computed signals drawn in continuous and dashed lines, respectively (P waves on left, SH waves on right).

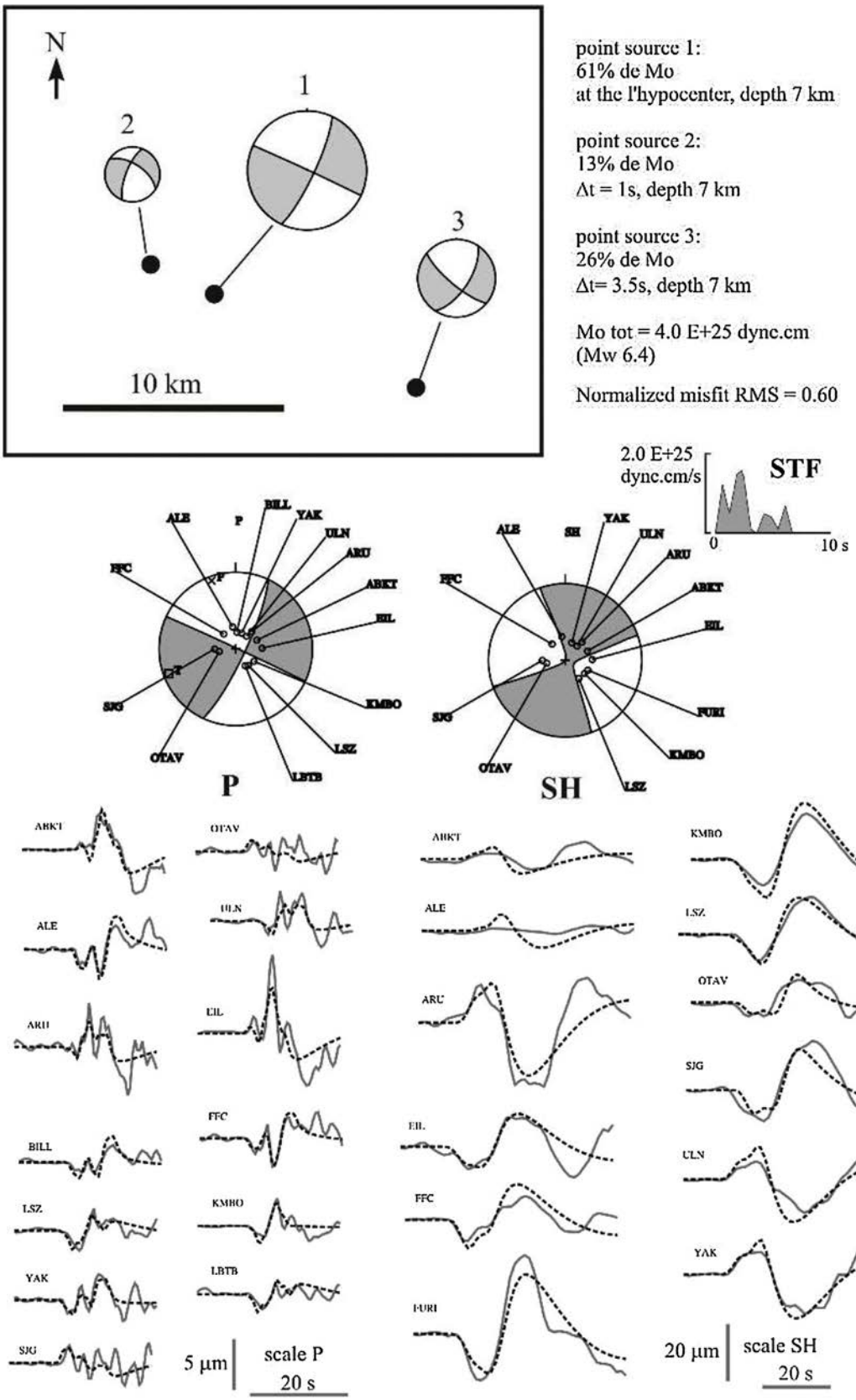

Fig. 15. Same as Fig. 14 but for three subevents aligned along the N110E direction.

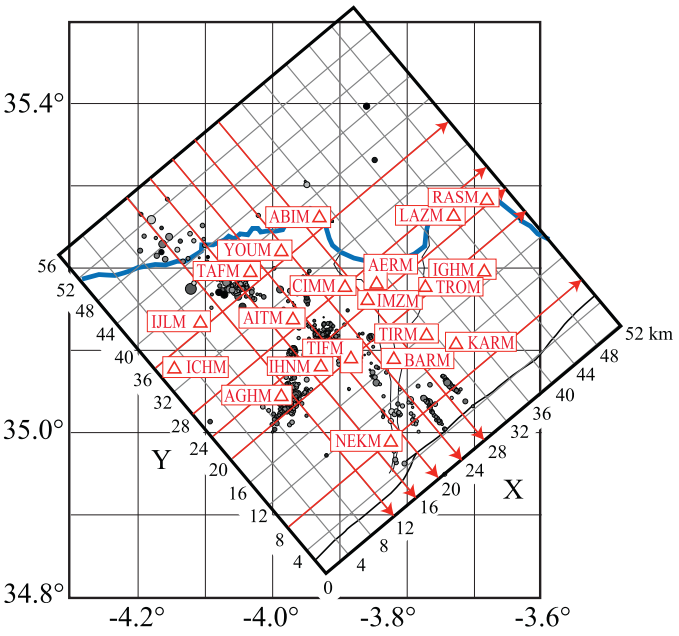

Fig. 16. Location of grid of tomographic model. Blue line is coastline for reference. Black lines are faults, bold is Nekor fault. Positions and names of seismological stations of temporary network are indicated. (For interpretation of the references to color in this figure legend, the reader is referred to the web version of the article.)

usual tests. In particular, the results of checkerboard tests led us to choose the value 50 of the derivative weight sum (DWS) as the limit of the best resolved part of the model. Thereafter, the parts of the velocity model where the DWS is lower than 50 is made opaque on the figures (Figs. 17–19).

We present here only the P-wave velocity model on three figures as map views of the 4 upper layers (Fig. 17) and cross sections along *X* (Fig. 18) and *Y* (Fig. 19) directions.

7. Discussion

7.1. Complexity of the seismicity

The source fault of the 2004 Al Hoceima earthquake remains uncertain despite many efforts in seismological, geodetic and geologic data analysis. We present the first results from a local seismological aftershock survey (Dorbath et al., 2005). From March 29 to April 11, 2004, our seismological field survey, about 1 month after the event, recorded a set of more than 600 aftershocks in the epicentral area (Figs. 2 and 6). At first order, the aftershocks are distributed along two directions with the main shock located right at the intersection of the two linear clouds (Figs. 2, 6 and 13).

In the NW-SE direction the seismicity is discontinuous, with a main cluster to the northwest, another cluster in the centre near the epicentre of the main shock, and to the southeast the seismicity becomes less dense with clear distinct linear clusters that veer to the S-SE. In particular, two of these linear clusters that strike about N135E and N145E, mark the easternmost extension of the seismicity during our survey (Fig. 6). These alignments are largely dominated by normal faulting (Fig. 10). The geometry and the types of faulting of the easternmost clusters suggest a 'horse-tail' termination of a right-lateral, N110-120E, sub-vertical strike-slip fault. This 'horse-tail' terminates sharply on the Nekor fault, no aftershock is located south of the surface trace of the Nekor fault (Fig. 2b). From NW to SE, the three clusters, although discontinuous and distant about 40 km, are aligned in a N120-130E direction.

In the N-S direction, the seismicity is more continuous and dense, in particular southward from the main shock epicentre. To the north of the main shock epicentre, very few aftershocks are present and they are aligned with those to the south. The average direction of the N-S seismicity is about N10-15E and extends for 15 km southward from the main shock epicentre, or about 20 km if the aftershocks to the north are considered.

Because our survey only started 1 month after the main shock occurrence, we also relocated the main aftershocks that occurred between February 24 and March 22 (Fig. 13). Although the range of magnitudes is not the same, the overall picture is not very different. The N10-15E branch is more pronounced to the north of the epicentre, and the majority of large aftershocks occurred near or southward from the main shock epicentre. The NW-SE direction is still less marked with almost no events to the southeast of the main shock, and only a few in the area of the northwestern cluster (Fig. 13).

Vertical sections across the main clusters, to the northwest (Fig. 7) and to the southwest (Fig. 11), show that the seismicity extends from 3 to 12 km depth along subvertical planes. In fact, to the northwest, the seismicity is more scattered and it is difficult to highlight a preferential planar distribution.

The focal mechanism of the main Mw 6.4 event is almost pure strike-slip with average direction of the focal planes about N10-20E and N110-115E as determined from various institutes (USGS, Harvard) and by this study (Figs. 14 and 15). The directions of the aftershock clouds are thus very similar to the two directions of the strike-slip focal planes, although the N10-20E plane seems in better agreement with the distribution of seismicity. Thus at first glance, it is not possible from the aftershock distributions only, to decide which of the two planes of the almost pure strike-slip focal mechanism was the source of the earthquake or whether both planes were activated during the seismic sequence.

Previous to the 2004 event, the background seismicity was distributed quite differently (Fig. 2). A local microseismological survey in 1989 (Hatzfeld et al., 1993; Cherkaoui et al., 1990) recorded a set of about 300 small magnitude events during 5 weeks that are mostly distributed under the lower Nekor basin and southwest of the Jbel Hammam fault (Fig. 2). Despite the small magnitudes of this background seismicity, it is important to note that it occurred at depths of 5–13 km, comparable to the depths of the earthquake sequences of 1994 and 2004. The presence of such seismicity, west and aligned with the Trougout fault is probably linked to the fault activity at depth.

The 1994 event of Mw 6.0 was located at or near the northwestern cluster, as determined from the 1994 aftershock distributions and the main shock location (El Alami et al., 1998; Bezzeghoud and Buforn, 1999) (Fig. 2). Analysis of InSAR interferrograms spanning the years 1993–1996 confirm the interpretation of the seismological data as a rupture along a NNE-SSW left-lateral fault (about N20E), located about 10 km NW of the 2004 epicentre (Akoglu et al., 2006; Biggs et al., 2006), in contrast with the relocation attempt of Calvert et al. (1997) (Fig. 2b).

It is remarkable that the normal faults that characterize the surface morphology east, south and west of Al Hoceima, that probably root at mid-crustal levels as revealed by the seismicity, were not at all activated during the 1994 or 2004 events. No earthquakes were recorded along the Trougout fault during our survey, and no events recorded in 2004 seem to be related to the background seismicity recorded by the local network in 1989 (Hatzfeld et al., 1993). Another remarkable feature of the local seismicity is the absence of events southeast of the Nekor fault zone, a pattern already recognized by Hatzfeld et al. (1993). In particular, in 2004, the easternmost aftershocks clusters are not crossing the fault.

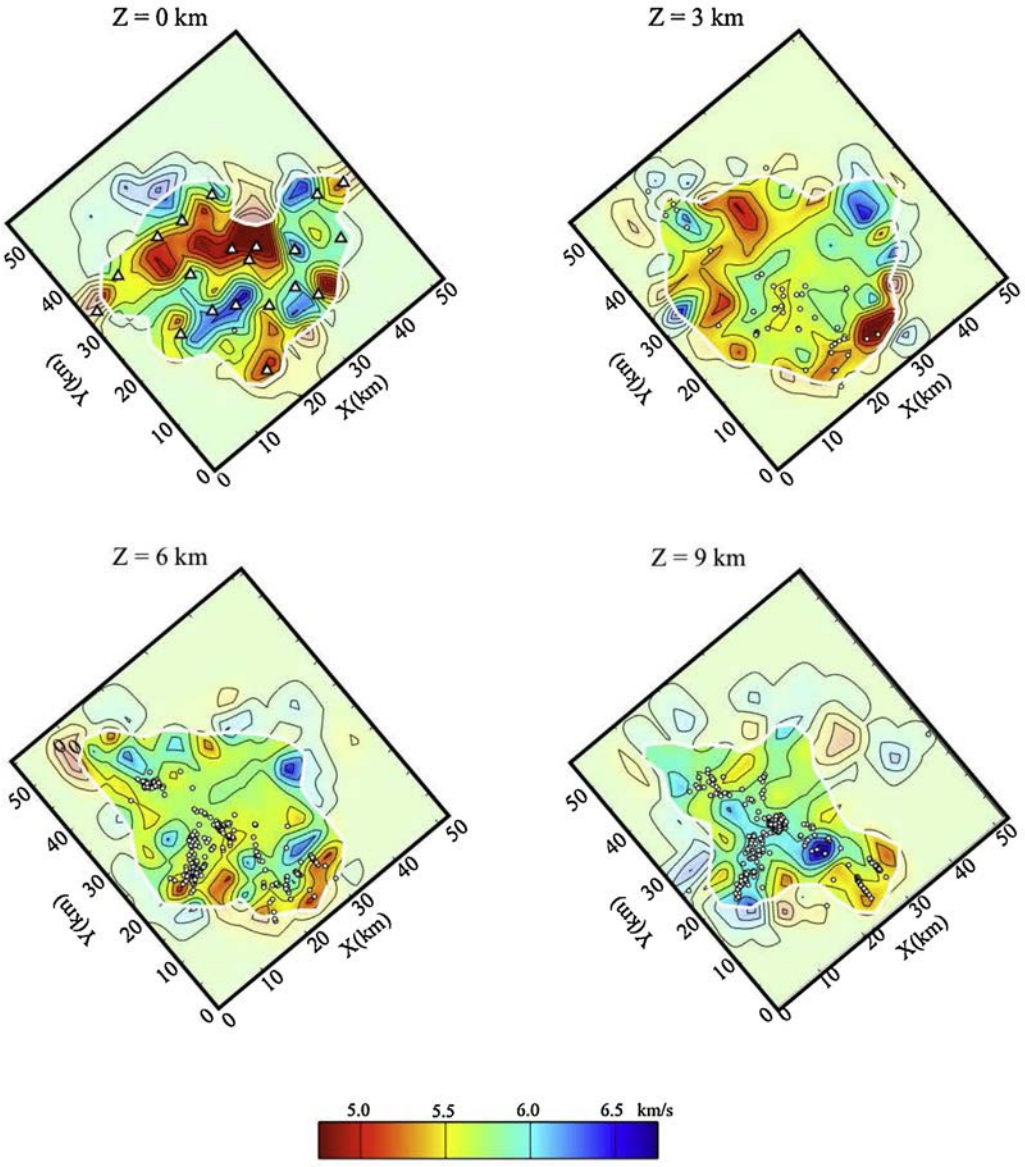

Fig. 17. Map view of the P-wave velocity model at 4 different depth levels. Unresolved parts (DWS lower than 50) are damped.

7.2. *Crustal structure and geometry of active faults*

The depths of the aftershocks are generally comprised between about 3 km and 12 km (Fig. 6, see also Figs. 18 and 19). Very few events are deeper or shallower. Only at the eastern termination of the N110E branch, some events are shallower and reach almost the surface. The main part of the seismic activity occurred in zones covered by south-verging thrust sheets whose thickness is about 3 km in the area (Negro et al., 2007). So that the seismic activity appears to remain bellow shallow nappes that act as barriers to the propagation of the slip or, on the contrary, are incompetent. However that last hypothesis is not supported by the type and quality of the rocks, which form the nappes (Choubert et al., 1984, 1987).

The main structures of the upper crust in the Al Hoceima region show up remarkably well in the tomographic inversion (Figs. 16–19). Sections across the model, perpendicular or parallel to the main structural direction, characterized by the strike of the Nekor fault or of the nappes thrust front (about N50; Choubert et al., 1984, 1987) show clearly a rather vertical low velocity zone aligned with the Nekor fault from surface to depth of about 9 km (Fig. 18). In a previous tomography study, Serrano et al. (2003) observed the coincidence of a pronounced low velocity zone at 5 km depth, parallel to and southeast of the Nekor fault, with a high electric and a low magnetic anomaly. They interpret it as "a fault gouge zone and/or a fluid filled sub-surface rock matrix in the upper crust". Even if the resolution of their velocity model is much lower than ours, due to the smaller number of events and stations in the zone, and to a much larger grid spacing, it is clear that we observe the same structure, with more lateral resolution especially above 6 km. Another feature is the low velocities between the surface and about 5 km that seem to dip slightly towards northwest (section $X = 24$, Fig. 18). The other feature that shows up clearly is a fast velocity zone to the northeast of the surveyed zone (Fig. 17), also visible in sections (sections $Y = 20$–28, Fig. 19). This zone is located underneath the Ras Tarf andesitic massif (12–15 Ma, Choubert et al., 1984; Chotin and Ait Brahim, 1988) and may correspond to the extension of the magmatic body in the crust, in contrast with more deformed part of the crust around it. Note that this zone extends largely under

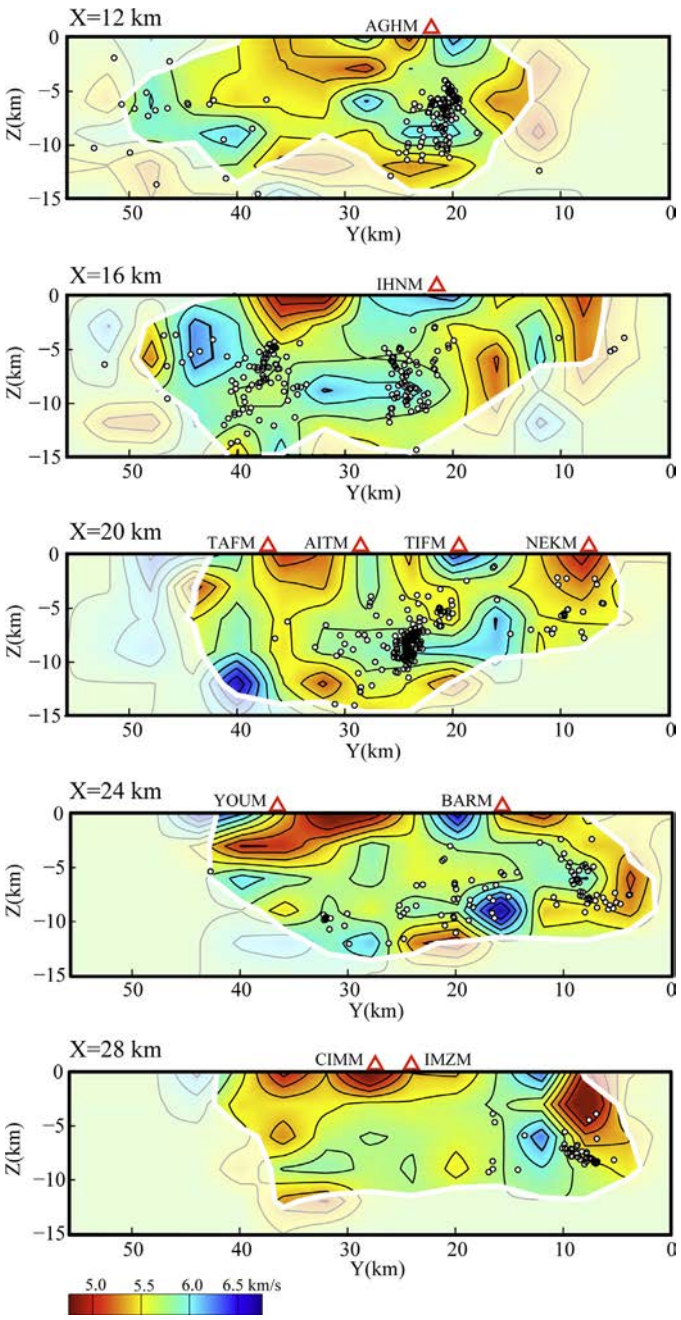

Fig. 18. Vertical cross sections through the 3D P-wave velocity model along the *X* lines (azimuth N40W).

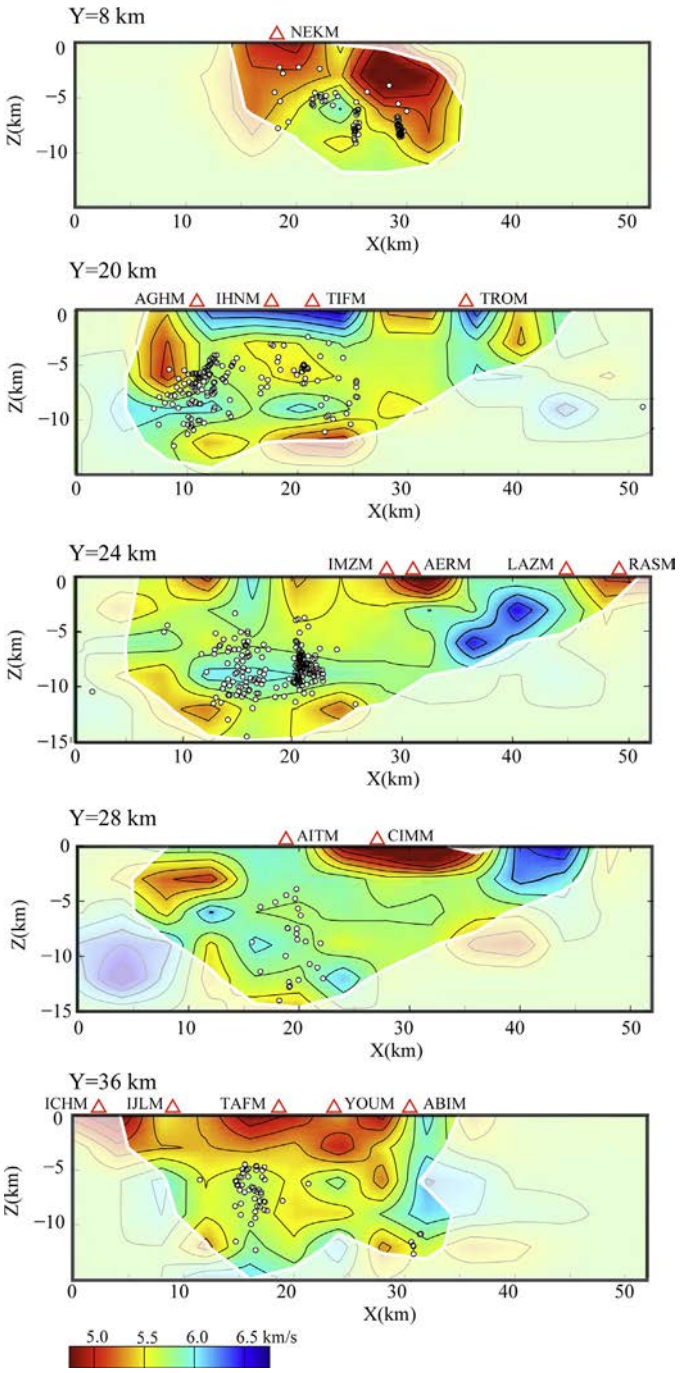

Fig. 19. Vertical cross sections through the 3D P-wave velocity model along the *Y* lines (azimuth N50E).

the lower Nekor basin. In contrast, the lower Nekor basin sediments may show up as a sharp, but relatively thick, slow anomaly near the surface (see section Y28 and Y24, Fig. 19), probably owing to smearing of the surface anomaly into the model as the shallow sediment thickness is less than 400 m (Galindo-Zaldivar et al., 2009).

The absence of surface faulting associated to the 1994 or even with the 2004 events, as well as, the absence of seismicity between the surface and about 5 km, probably indicates a possible decoupling between the overthrusted nappes and the crust underneath (Galindo-Zaldivar et al., 2009). However, as can be inferred from the seismicity recorded in 1989 (Hatzfeld et al., 1993) and the local tomography (Figs. 18 and 19), the graben structure of the lower Nekor basin is clearly a crustal structure that roots at depth of 9–12 km, also in good agreement with the 10–15 km width of the basin east of Al Hoceima.

7.3. Stress tensor

We looked for a possible change of stress regime at a local scale, by calculating the stress field along the aftershocks segments described previously. It was predictable that these changes should not be very large since, when performing the global inversion, 22% of the total amount of focal mechanisms was rejected (remember that the threshold between the observed and calculates slip angles is only 15°). So, the underlying hypothesis of a homogeneous stress field over the whole area is globally justified. However, it is also clear that small heterogeneities exist. When we performed smaller scale inversions, only 12% of the total amount of focal mechanisms

was rejected. So, even more small-scale heterogeneities could exist. The direction of σ_3 (N246E), which is the best-constrained direction in all cases, remains constant within uncertainties (Table 3; see also Figs. 8, 9, 11 and 12).

In order to check if the global tensor is actually representative of the regional stress tensor despite the perturbation due to the occurrence of the 2004 earthquake, we processed in the same way the 42 focal mechanisms constructed in the same area by Hatzfeld et al. (1993) after the 1989 field survey. We obtain a stress tensor with σ_1 and σ_3 trending N334E and N246E, respectively, and $R = 0.9$, very close to that obtained from the 2004 aftershock sequence (Table 3). The R values indicate that the stress field is not so far from a normal regime. As most of our data were collected several weeks after the main 2004 shock, we may conclude that, at that time, the perturbation of the stress field due to the main shock had almost completely vanished.

7.4. Regional deformation of the western Mediterranean

Geophysical source inversions made after the 2004 event have led to contrasting results, whether from seismic (this study; Biggs et al., 2006; Stich et al., 2005) or geodetic (Akoglu et al., 2006; Cakir et al., 2006; Tahayt et al., 2008, 2009) data. Either the fault plane is fixed arbitrarily (Stich et al., 2005; Biggs et al., 2006) or models are discussed and dismissed based on an arbitrary statistical criterion (Cakir et al., 2006; Akoglu et al., 2006) leading to solutions that favour either a N20 or a N110E rupture plane, or rupture on both planes (Tahayt et al., 2008) (Fig. 20). The detailed seismic analysis presented above does not lead to an independent rupture plane determination, although the N20E plane may be favoured because it concentrates the densest and largest concentration of aftershocks.

In any case, both 1994 and 2004 events, whether considered as a system of conjugate strike-slip faults or sub-parallel left-stepping left-lateral faults (Fig. 20), define the southern boundary of the eastern Alboran Sea seismicity that extends from the eastern Betics to the Nekor fault over a length of 500 km (Fig. 1). Recent GPS data in the western Mediterranean have been interpreted to delineate a western Alboran block that moves southward with respect to the eastern Rif at a rate of 4–5 mm/yr (Nocquet, 2012; Vernant et al., 2010; Koulali et al., 2011). The knowledge of the historical seismicity (El Mrabet, 2005a; Pelaez et al., 2007) as well as the magnitudes of these recent strike-slip events are insufficient to account for the totality of the strain accumulated across the complex eastern Alboran block boundary.

In contrast, other faults, which seismic activity is disputed, have clear geomorphic expression, whether offshore across the bottom of the Alboran Sea or onshore, such as the Jebbha and Nekor faults (Fig. 1) or the Ajdir, Trougout and Rouadi normal faults (Van der Woerd et al., 2005) (Figs. 2–4). Even considering a complex strike-slip boundary with stepping faults (Jebbha and Nekor) with intervening extensional basins bounded by normal faults (Trougout) (Fig. 20), the lengths of these individual faults (several tens of km) as well as the expected several mm/yr rate of strain across the faulted zone point to the possibility of large magnitude earthquakes in this part of the Mediterranean.

Our field observations and earthquake sequence analysis is in support of model of deformations that involve a western Alboran block and a trans-Alboran shear zone (e.g., Tapponnier, 1977) as depicted by recent geodetic results (Nocquet, 2012; Koulali et al., 2011; Figs. 1 and 20). The southwestern extension of this block may be roughly located at the southern active thrusting boundary of the Rif. However, active oblique thrusting across the Middle Atlas as well as south vergent thrusting in the Atlas (Sébrier et al., 2006) and seismicity (Agadir Mw 5.9; Duffaud et al., 1962) attest of the propagation of the deformation even farther south, despite low or no geodetic signal (Nocquet, 2012). How this continental deformation of the northwestern African plate extends towards west in the Atlantic remains to be determined. In any event, a localized Iberian–Africa plate boundary from the Gorda ridge to the west towards the Tellian Atlas to the east appears too simplistic and is not reflecting the complex structures that characterize the western Mediterranean.

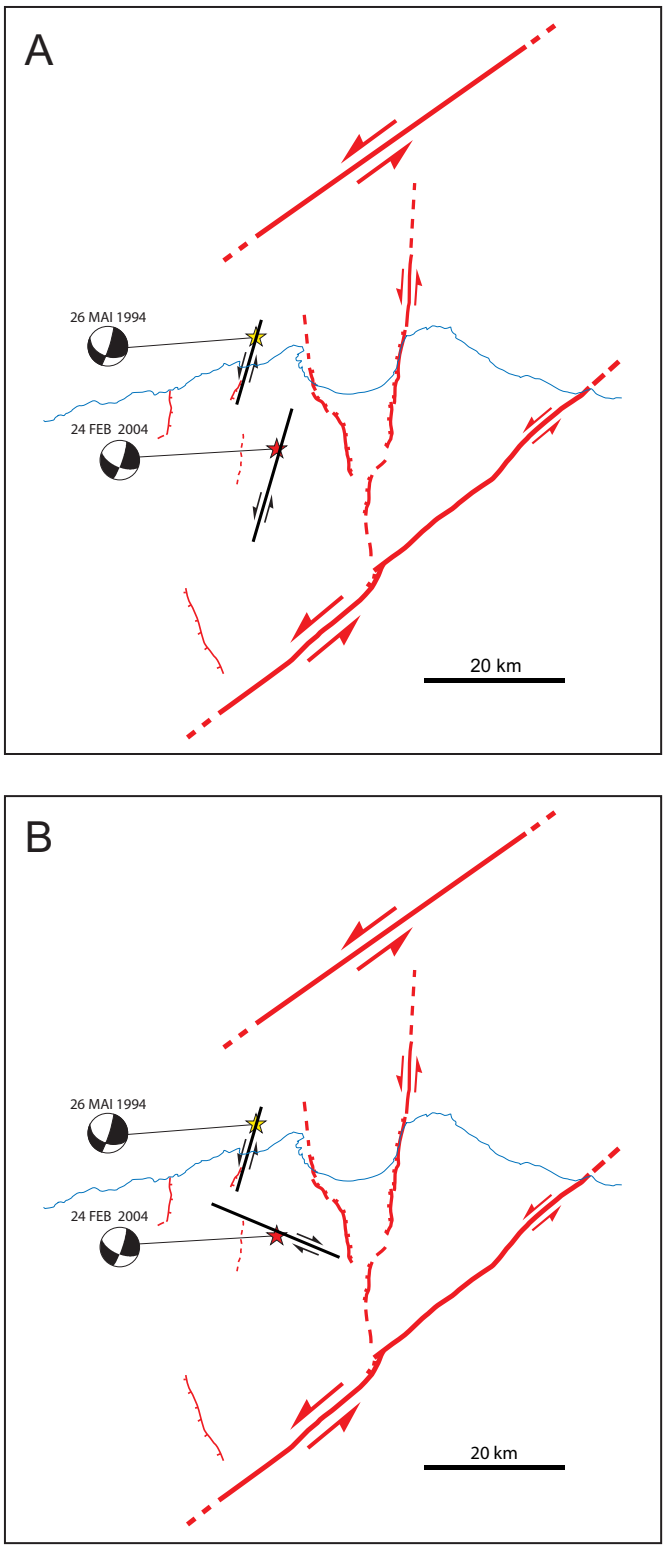

Fig. 20. Simplified map view of active faults in the Al Hoceima region. (a) 2004 event occurred on a NNE striking fault. (B) 2004 event occurred on a ESE striking fault.

8. Conclusions

The studies on the late aftershocks recorded by the temporary seismological network should be summarized in the following points:

(1) The distribution of the aftershocks does not allow deciphering which of the two branches displayed is the actual fault where the main shock occurred. Some observations favour the N20E direction: (a) The aftershock cluster is densest in the N10-15E direction and is about 20 km-long. (b) This direction is in agreement with the left-lateral slipping plane from the main shock focal mechanism. (c) The aftershock clusters along the N120-130E direction is sparse and discontinuous and is slightly oblique to the N110E right-lateral slipping plane of the main shock focal mechanism. (d) The N20E cluster is striking similarly to the 2004 isoseists (Ait Brahim et al., 2004) and is situated in the central part of the maximum intensity lobe, if the lower basin of the Nekor is disregarded, where the soft sediments coverage is responsible of the high intensities observed there. (e) The N20E direction is a major structural direction as outlined by the Trougout oblique normal fault and other NS normal fault in the region, and it is sub-parallel to the rupture direction of the 1994 Mw 6 event. Other results favour slip in the N110E direction: (a) inversion of InSAR interferrograms are best modelled with a steep N110E north-dipping plane (Cakir et al., 2006; Akoglu et al., 2006); (b) the sparse aftershock distribution along the N110E direction may be interpreted as a stress released fault plane; (c) seismicity along the N20E direction may be triggered by conjugate faulting as sometimes observed (Das and Henry, 2003; Hudnut et al., 1989) or due to faulting on both directions (e.g., Meng et al., 2012; Duputel et al., 2012).

(2) The earthquake took place on a fault NNW-SSE or NNE-SSW with no signature at the surface. The aftershocks activity is located below 3 km, probably underneath the upper crustal nappes. The tectonic activity within the basement may be uncoupled with the surface formations following a way to be elucidated.

(3) The aftershocks focal mechanisms show a large amount of strike-slip faulting on nearly vertical faults striking either N20E (left-lateral) or N110E (right-lateral). A component of normal faulting is frequent and is largely dominant when the faults are striking N160E. This indicates that the principal horizontal stress direction is about N160E, while the minimal one is N70E. A careful examination of all the mechanisms shows that these principal stresses are, respectively, $\sigma 1$ and $\sigma 3$ a result confirmed by the inversion of the polarities following Michael (1984).

(4) The main Quaternary active structures mapped in the region were not activated.

(5) The Nekor fault characterized by the absence of seismicity along it and depicted as a sub-vertical low velocity zone in tomography, seems to separate a seismic northwestern block from a southeastern seismically quiescent block.

Acknowledgements

We are grateful for support from Ministère de l'Intérieur, France, via the "Service des Missions et Conférences à l'étranger" EGIDE for travel and field expenses during the field survey in 2004. The field survey has been made possible thanks to the support and welcome of the Wilaya of Al Hoceima, the Wali and Gouverneur of Al Hoceima, M. Mohamed Afoud, the Wali of Taza, M. El Hassan Benameur and the Wali of Taounate, M. Mohamed Amghouz. We thank the Général de Brigade Abdelkrim El Yakoubi, de la Direction Générale de la Protection Civile de Rabat and particularly the driver El Mostafa Kirbi from the fire station Agdal in Rabat, for support and assistance in the field, as well as Centre National de la Recherche Scientifique et Technique and Service de Physique du Globe (Rabat, Morocco). Denis Hatzfeld is thanked for sharing the data of the 1989 microseismicity survey in the Al Hoceima region. The Institut des Sciences de la Terre (Isterre) in Grenoble (CNRS UMR5275 and Université Joseph Fourier) and Denis Hatzfeld are thanked for providing the seismometers. We acknowledge support from Institut National des Sciences de la Terre (INSU CNRS France) to Institut de Physique du Globe de Paris (CNRS UMR7154) and to Institut de Physique du Globe de Strasbourg (CNRS UMR7516). We thank also the French embassy in Rabat, in particular M. Alain Lhéritier from the Service de Coopération et d'Action Culturelle, who eased our travels as well as the stations logistics between France and Morocco. We thank 3 reviewers and the associate editor, Michel Corsini, for their comments that improved the manuscript.

Appendix A. Supplementary data

Supplementary material related to this article can be found, in the online version, at http://dx.doi.org/10.1016/j.jog.2013.12.004.

References

Akoglu, A.M., Cakir, Z., Meghraoui, M., Bellabes, S., El Alami, S.O., Ergintav, S., Akyüz, H.S., 2006. The 1994–2004 Al Hoceima (Morocco) earthquake sequence: conjugate fault ruptures deduced from InSAR. Earth Planet. Sci. Lett. 252, 467–480.

Ait Brahim, L., Nakhcha, C., Tadili, B., El Mrabet, A., Jabour, N., 2004. Structural analysis and interpretation of the surface deformations of the February 24th, 2004 Al Hoceima earthquake. CSEM/EMSC Newslett. 21, 10–12.

Ait Brahim, L., Chotin, P., 1984. Mise en évidence d'un changement de direction de compression dans l'avant-pays rifain (Maroc) au cours du Tertiaire et du Quaternaire. Bull. Soc. Geol. France Paris Ser. 7 26 (4), 681–691.

Ait Brahim, L., Chotin, P., Tadili, B.A., Ramdani, M., 1990. Failles actives dans le Rif central et oriental (Maroc). C. R. Acad. Sci. Paris Ser. II 310, 1123–1129.

Andeweg, B., Cloetingh, S., 2001. Evidence for an active sinistral shear zone in the western Alboran region. Terra Nova 13, 44–50.

Andrieux, J., Fontbote, J.M., Mattauer, M., 1971. Sur un modèle explicatif de l'arc de Gibraltar. Earth Planet. Sci. Lett. 12, 191–198.

Andrieux, J., Mattauer, M., 1973. Précisions sur un modèle explicatif de l'arc de Gibraltar. Bull. Soc. Geol. France Ser. 7 XV, 115–118.

Armijo, R., Deschamps, A., Poirier, J.-P., 1986. Carte sismotectonique. Europe et Bassin Méditérranéen, Institut de Physique du Globe de Paris, Institut Géographique National, France.

Besse, P., 1986. Relocalisation relative d'événements sismiques appliquée àla region Sud du Lac Ghoubbet situé dans la République de Djibouti, *Rapport DEA*. Université Paris VII, Paris, France.

Bezzeghoud, M., Buforn, E., 1999. Source parameters of the 1992 Melilla (Spain, Mw = 4.8), 1994 Al Hoceima (Morocco Mw = 5. 8) and Mascara (Algeria, Mw = 5. 7) earthquakes and seismotectonic implications. Bull. Seismol. Soc. Am. 89, 359–372.

Biggs, J., Bergman, E., Emmerson, B., Funning, G.J., Jackson, J., Parsons, B., Wright, T., 2006. Fault identification for buried strike-slip earthquakes using InSAR: the 1994 and 2004 Al Hoceima, Morocco, earthquakes. Geophys. J. Int. 166, 1347–1362.

Bourgois, J., Mauffret, A., Ammar, A., Demnati, A., 1992. Multichannel seismic data imaging of inversion tectonics of the Alboran Ridge (Western Mediterranean Sea). Geo-Mar. Lett. 12, 117–122.

Buforn, E., Sanz de Galdeano, C.C., Udias, A., 1995. Seismotectonics of the Ibero-Maghrebian region. Tectonophysics 248, 247–261.

Cakir, Z., Meghraoui, M., Akoglu, A.M., Jabour, N., Belabbes, S., Ait-Brahim, L., 2006. Surface deformation associated with the Mw 6.4, 24 February 2004 Al Hoceima, Morocco, earthquake deduced from InSAR: implications for the active tectonics along North Africa. Bull. Seismol. Soc. Am. 96, 59–68, http://dx.doi.org/10.1785/0120050108.

Calvert, A., Gomez, F., Seber, D., Barazangi, M., Jabour, N., Ibenbrahim, A., Demnati, A., 1997. An integrated geophysical investigation of recent seismicity in the Al Hoceima region of North Morocco. Bull. Seismol. Soc. Am. 87, 637–651.

Cherkaoui, T.-E., Hatzfeld, D., Jebli, H., Medina, F., Caillot, V., 1990. Etude microsismique dela région d'Al Hoceima. Bull. Inst. Sci. Rabat 4, 25–34.

Chotin, P., Ait Brahim, L., 1988. Transpression et magmatisme au Néogène-Quaternaire dans le Maroc oriental, Magmatism and Neogene-Quaternary compressive tectonic episodes in northeastern Morocco. C. R. Acad. Sci., Ser. 2 – Méc. Phys. Chim. Sci. l'univ. Sci. Terre 306 (20), 1479–1485.

Choubert, G., Faure-Muret, A., Mégard, F., Hilali, E.A., Andrieux, J., 1984. Carte géologique du Rif, Al Hoceima 1/50000. Notes Mém. Serv. Géol. Maroc, 302.

Choubert, G., Faure-Muret, A., Frizon de Lamotte, D., Mourier, Th., Besson, F., 1987. Carte géologique du Rif, Rouadi 1/50000. Notes Mém. Serv. Géol. Maroc, 347.
CNRST, 2004. Centre National pour la Recherche Scientifique et Technique. Moroccan Seismic Network http://sismo-lag.cnrst.ma/
Das, S., Henry, C., 2003. Spatial relation between main earthquake slip and its aftershock distribution. Rev. Geophys. 41 (3), 1013, http://dx.doi.org/10.1029/2002RG000119.
DeMets, C., Gordon, R.G., Argus, D.F., Stein, S., 1990. Current plate motions. Geophys. J. Int. 101 (2), 425–478.
DeMets, C., Gordon, R.G., Argus, D.F., Stein, S., 1994. Effect of recent revisions to the geomagnetic reversal time scale on estimates of current plate motions. Geophys. Res. Lett. 21, 2191–2194.
Dorbath, L., Hahou, Y., Delouis, B., Dorbath, C., van der Woerd, J., Badrane, S., Frogneux, M., Haessler, H., Jacques, E., Menzhi, M., Tapponnier, P., 2005. Etude sismologique sur le séisme d'Al Hoceima: localisation et mécanisme du choc principal et des répliques, contraintes et structures de la zone épicentrale. In: Colloque International "Séisme d'Al Hoceima: bilan et perspectives", Al Hoceima, 24–26 Février 2005, Morocco, p. 22.
Dorbath, L., Evans, K., Cuenot, N., Valley, B., Charlety, J., Frogneux, M., 2010. The stress field at Soultz-Sous-Forêts from focal mechanisms of induced seismic events: cases of the wells GPK2 and GPK3. C. R. Geosci., http://dx.doi.org/10.1016/j.crte.2009.12.003.
Duffaud, F., Rothé, J.-P., Debrach, J., Erimesco, P., Choubert, G., Faure-Muret, A., 1962. Le séisme d'Agadir du 29 février 1960. Notes Mém. Serv. Géol. Maroc 154, 1–68.
Duputel, Z., Kanamoori, H., Tsai, V.C., Rivera, L., Meng, L., Ampuero, J.-P., Stock, J.M., 2012. The 2012 Sumatra great earthquake sequence. Earth Planet. Sci. Lett. 351–352, 247–257.
El Alami, S.O., Tadili, B.A., Cherkaoui, T.E., Medina, F., Ramdani, M., Ait Brahim, L., Harnafi, M., 1998. The Al Hoceima earthquake of May 26, 1994 and its aftershocks: a seismotectonic study. Ann. Geofisic. 41, 519–537.
El Mrabet, T., 2005a. La sismicité historique de la region d'Al Hoceima et la culture sismique locale. In: Colloque International "Séisme d'Al Hoceima: bilan et perspectives", Al Hoceima, 24–26 Février 2005, Morocco, p. 10.
El Mrabet, T., 2005b. The Great Earthquakes in the Maghreb Region and their Consequences on Man and Environment (in Arabic with Abstract in English), Edit. Centre National de Recheche Scientifique et Technique, Rabat, Morocco.
Fadil, A., Vernant, P., McClusky, S., Reilinger, R., Gomez, F., Ben Sari, D., Mourabit, T., Feigl, K., Baranzangi, M., 2006. Active tectonics of the western Mediterranean: geodetic evidence for rollback of a delaminated subcontinental lithospheric slab beneath the Rif Mountains, Morocco. Geology 34, 529–532, http://dx.doi.org/10.1130/G22291.1.
Frizon de Lamotte, D., Andrieux, J., Guezou, J.C., 1991. Cinématique des chevauchements néogènes dans l'Arc bético-rifain; discussion sur les modèles géodynamiques. Bull. Soc. Géol. France 162, 611–626.
Galindo-Zaldivar, J., Chalouan, A., Azzouz, O., Sanz de Galdeano, C., Anahnah, F., Ameza, L., Ruano, P., Pedrera, A., Ruiz-Constan, A., Marin-Lechado, C., Benmakhlouf, M., Lopez-Garrido, A.C., Ahmamou, M., Saji, R., Roldan-Garcia, F.J., Akil, M., Chabli, A., 2009. Are the seismological and geological observations of the Al Hoceima (Morocco, Rif) 2004 earthquake (M = 6.3) contradictory? Tectonophysics 475, 59–67.
Goula, X., Susagna, T., Gonzalez, M., Margarit, M., El Asbai, H., 2005. Site Effects Analysis from the Microtremors and Accelerograms Recorded after the Al Hoceima Earthquake of 24/02/04, in Séisme d'Al Hoceima: bilan et Perspectives. Université Mohamed Premier, Oujda.
Gutscher, M.A., Malod, J., Rehault, J.P., Contrucci, I., Klingelhoefer, F., Mendes-Victor, L., Spakman, W., 2002. Evidence for active subduction beneath Gibraltar. Geology 30, 1071–1074.
Hatzfeld, D., Caillot, V., Cherkaoui, T.-E., Jebli, H., Medina, F., 1993. Microearthquake seismicity and fault plane solutions around the Nékor strike-slip fault, Morocco. Earth Planet. Sci. Lett. 120, 31–41.
Hudnut, K., Seeber, L., Rockwell, T., Goodmacher, J., Klinger, R., Lindvall, S., McElwain, R., 1989. Surface ruptures on cross-faults in the 24 November 1987 Superstition Hills, California, earthquake sequence. B. Seismol. Soc. Am. 79 (2), 282–296.
Jabour, N., Kasmi, M., Menzhi, M., Birouk, A., Hni, L., Hahou, Y., Timoulali, Y., Badrane, S., 2004. The February 24th, 2004 Al Hoceima earthquake. CSEM/EMSC Newslett. 21, 7–10.
Kissling, E., Ellsworth, W.L., Eberhart-Phillips, D., Kradolfer, U., 1994. Initial reference models in local earthquake tomography. J. Geophys. Res. 99, 19,635–19,646.
Klein, F.W., 1978. Hypocentres Location Program HYPOINVERS, Open-file Rep. 78-694. US Geological Survey, Boulder, CO, USA.
Koulali, A., Ouazar, D., Tahayt, A., King, R.W., Vernant, P., Reilinger, R.E., McClusky, S., Mourabit, T., Davila, J.M., Amraoui, N., 2011. New GPS constraints on active deformation along the Africa–Iberia plate boundary. Earth Planet. Sci. Lett. 308, 211–217.
Leblanc, D., Olivier, P., 1984. Role of strike-slip faults in the Betic-Rifian orogeny. Tectonophysics 101, 345–355.
Lopez Casado, C., Sanz de Galdeano, C., Molina Palacios, S., Henares Romero, J., 2001. The structure of the Alboran Sea: an interpretation from seismological and geological data. Tectonophysics 338, 79–85.
Martinez-Garcia, P., Soto, J.I., Comas, M., 2011. Recent structures in the Alboran Ridge and Yusuf fault zones based on swath bathymetry and sub-bottom profiling: evidence of active tectonics. Geo-Mar. Lett. 31, 19–36.
Mattauer, M., 1964. Le style tectonique des chaînes tellienne et rifaine. Geolog. Rundschau 53, 296–313.
Meng, L., Ampuero, J.-P., Stock, J., Duputel, Z., Luo, Y., Tsai, V.C., 2012. Earthquake in a Maze: compressional rupture branching during the 2012 Mw 8.6 Sumatra earthquake. Science 337, 724–726.
Michael, A.J., 1984. Determination of stress from slip data: faults and folds. J. Geophys. Res. 89 (B13), 11517–11526.
Michael, A.J., 1987. Use of focal mechanisms to determine stress: a control study. J. Geophys. Res. 92, 357–368.
Morel, J.-L., (Ph.D. Thesis) 1988. Evolution récente de l'orogène rifain et de son avant-pays depuis la mise en place des nappes. University of Orsay, France, 584 pp.
Morel, J.L., Meghraoui, M., 1996. Goringe-Alboran-Tell tectonic zone: a transpression system along the Africa–Eurasia plate boundary. Geology 24, 755–758.
Morley, C.K., 1992. Notes on the Neogene basin history of the western Alboran Sea and its implications for the tectonic evolution of the Rif-Betic orogenic belt. J. Afr. Earth Sci. 14, 57–65.
Murphy Corella, P., 2005. Damage trends in RC buildings after the Al Hoceima 2004, earthquake, in Séisme d'Al Hoceima: bilan et perspectives. In: Colloque International "Séisme d'Al Hoceima: bilan et perspectives", Al Hoceima, 24–26 Février 2005, Morocco, p. 39.
Nabelek, J.L., (Ph.D. Thesis) 1984. Determination of earthquake source parameters from inversion of body waves. Mass. Inst. of Technol., Cambridge, USA.
Negro, F., Agard, P., Goffé, B., Saddiqi, O., 2007. Tectonic and metamorphic evolution of the Temsamaneunits, External Rif (northern Morocco). Implications for the evolution of the Rif and the Betic-Rif arc. J. Geol. Soc. Lond. 16, 824–842.
Nocquet, J.-M., Calais, E., 2003. Crustal velocity field of western Europe from permanent GPS array solutions, 1996–2001. Geophys. J. Int. 154, 72–88.
Nocquet, J.-M., 2012. Present-day kinematics of the Mediterranean: a comprehensive overview of GPS results. Tectonophysics 579, 220–242.
Payo, G., Ruiz de la Parte, E., 1974. Dispersion of surface waves in the Iberian Peninsula and the adjacent Atlantic and Mediterranean areas. Geofisic. Int. 14, 89–102.
Pelaez, J.A., Chourak, M., Tadili, B.A., Aït Brahim, L., Hamdache, M., Lopez Casado, C., Martinez Solares, J., 2007. A catalog of main Moroccan earthquakes from 1045 to 2005. Seismol. Res. Lett. 78, 614–621.
Platt, J.P., Vissers, R.L.M., 1989. Extensional collapse of thickened continental lithosphere: a working hypothesis for the Alboran Sea and Gibraltar Arc. Geology 17, 540–543.
Seber, D., Barazangi, M., Ibenbrahim, A., Demnati, A., 1996. Geophysical evidence for lithospheric delamination beneath the Alboran Sea and Rif-Betic mountains. Nature 379, 785–790, http://dx.doi.org/10.1038/379785a0.
Sébrier, M., Siame, L.L., Zouine, E., Winter, T., Missenard, Y., Leturmy, P., 2006. Active tectonics in the Moroccan High Atlas. C. R. Geosci. 338 (1–2), 65–79, http://dx.doi.org/10.1016/j.crte.2005.12.001.
Serrano, I., Zhao, D., Morales, J., Torcal, F., 2003. Seismic tomography from local crustal earthquakes beneath eastern Rif Mountains of Morocco. Tectonophysics 367, 187–201, http://dx.doi.org/10.1016/S0040-1951(03)00100-8.
Stich, D., Mancilla, F., Baumont, D., Morales, J., 2005. Source analysis of the Mw 6.3 2004 Al Hoceima earthquake (Morocco) using regional apparent source time functions. J. Geophys. Res. 110 (B06306), http://dx.doi.org/10.1029/2004/B003366.
Tahayt, A., Mourabit, T., Rigo, A., Feigl, K.L., Fadil, A., McClusky, S., Reilinger, R., Serroukh, M., Ouazzani-Touhami, A., Ben Sari, D., Vernant, P., 2008. Mouvements actuels des blocs tectoniques dans l'arc Bético-Rifain à partir des mesures GPS entre 1999 et 2005. C. R. Geosci. 340, 400–413 (in French with abridged English Version).
Tahayt, A., Feigl, K.L., Mourabit, T., Rigo, A., Reilinger, R., McKlusky, S., Fadil, A., Berthier, E., Dorbath, L., Serroukh, M., Gomez, F., Ben Sari, D., 2009. The Al Hoceima (Morocco) earthquake of 24 February 2004, analysis and interpretation of data from ENVISAT ASAR and SPOT5 validated by ground-based observations. Remote Sensing Environ. 113, 306–316.
Tapponnier, P., 1977. Evolution tectonique du système alpin en Méditerranée: poinçonnement et écrasement rigide plastique. Bull. Soc. Géol. France 19, 437–460.
Thurber, C.H., 1983. Earthquake locations and three-dimensional crustal structure in the Coyote Lake area, central California. J. Geophys. Res. 88, 8226–8236.
Van der Woerd, J., Tapponnier, P., Jacques, E., Dorbath, L., Hahou, Y., Menzhi, M., Cakir, Z., Badrane, S., Dorbath, C., Haessler, H., Frogneux, M., 2005. Le séisme d'Al Hoceima de Mw 6.4 du 24 février 2004. In: Colloque "Séisme d'Al Hoceima: bilan et perspectives", Al Hoceima, 24–26 février 2005.
Vernant, P., Fadil, A., Mourabit, T., Ouazar, D., Koulali, A., Davila, J.M., Garate, J., McClusky, S., Reilinger, R., 2010. Geodetic constraints on active tectonics of the Western Mediterranean: implications for the kinematics and dynamics of the Nubia-Eurasia plate boundary zone. J. Geodyn. 49, 123–129.
Waldhauser, F., Ellsworth, W.L., 2000. A double difference earthquake location algorithm: method and application to the northern Hayward fault, California. Bull. Seismol. Soc. Am. 90, 1353–1368.
Watts, A.B., Platt, J.P., Buhl, P., 1993. Tectonics evolution of the Alboran sea basin. Basin Res. 5, 153–177.
Woodside, J.M., Maldonado, A., 1992. Styles of compressional neotectonics in the eastern Alboran Sea. Geo-Mar. Lett. 12, 111–116.
Working Group for Deep Seismic Sounding in the Alboran Sea (W.G.D.S.S.A.S.), 1978. Crustal seismic profiles in the Alboran Sea-Preliminary results. Pageoph 116, 167–180.
Zhang, H., Thurber, C.H., 2003. Double-difference tomography: the method and its application to the Hayward fault, California. Bull. Seismol. Soc. Am. 93 (5), 1875–1889.

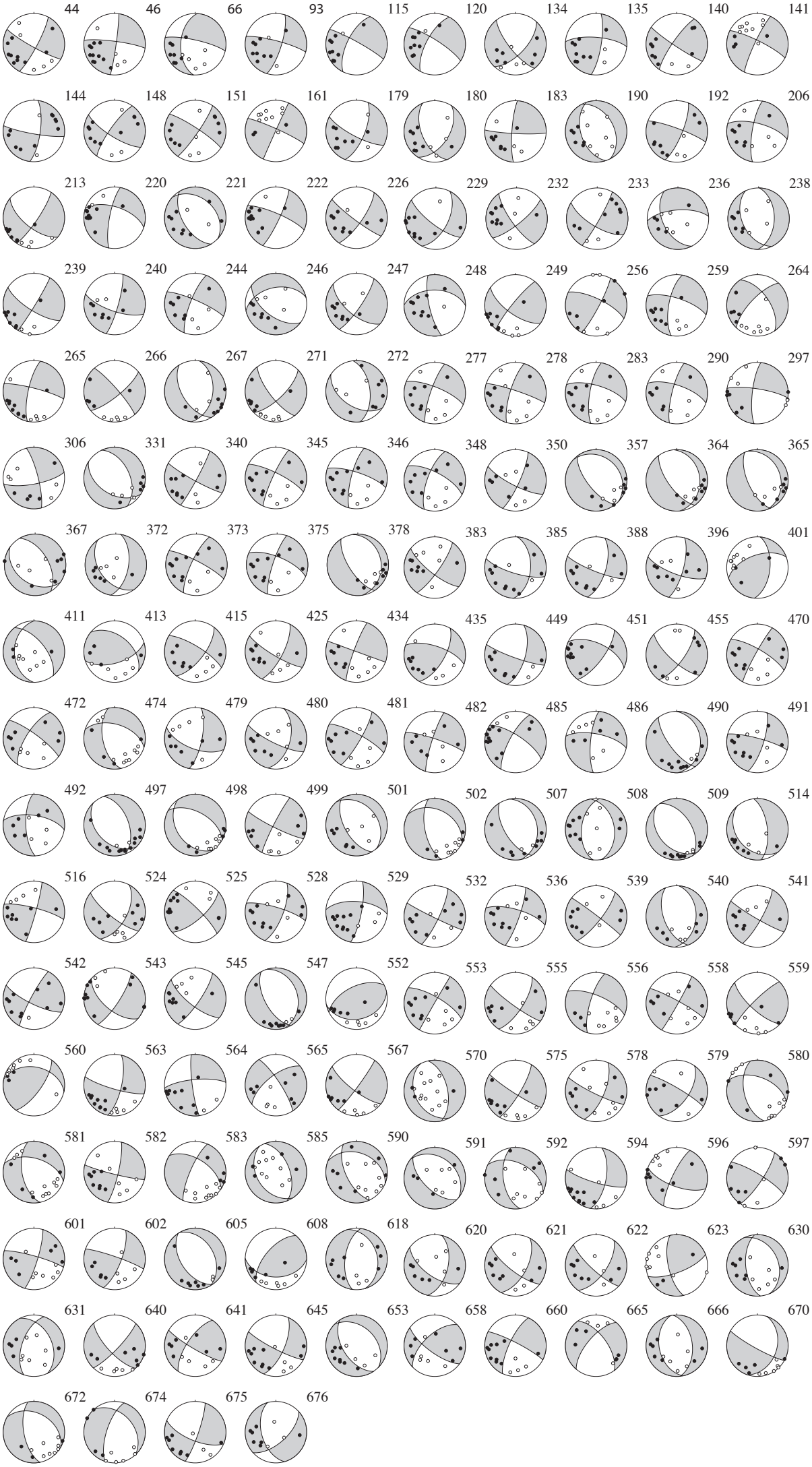
44 46 66 93 115 120 134 135 140 141
144 148 151 161 179 180 183 190 192 206
213 220 221 222 226 229 232 233 236 238
239 240 244 246 247 248 249 256 259 264
265 266 267 271 272 277 278 283 290 297
306 331 340 345 346 348 350 357 364 365
367 372 373 375 378 383 385 388 396 401
411 413 415 425 434 435 449 451 455 470
472 474 479 480 481 482 485 486 490 491
492 497 498 499 501 502 507 508 509 514
516 524 525 528 529 532 536 539 540 541
542 543 545 547 552 553 555 556 558 559
560 563 564 565 567 570 575 578 579 580
581 582 583 585 590 591 592 594 596 597
601 602 605 608 618 620 621 622 623 630
631 640 641 645 653 658 660 665 666 670
672 674 675 676

Table S1. List of 676 relocated events using tomoDD with the temporary network

N°	Latitude	Longitude	Depth	Year	M	D	H	M	Sec	Md	Rms
1	35.113978	-3.923148	9.461	2004	3	29	13	53	24.530	2.7	0.024
2	35.053204	-3.974342	6.664	2004	3	29	13	57	58.560	2.6	0.008
3	35.095557	-3.824766	9.167	2004	3	29	14	1	56.690	2.5	0.017
4	35.140399	-3.955907	8.003	2004	3	29	14	3	59.300	2.1	0.023
5	35.161441	-3.946708	8.791	2004	3	29	21	34	36.210	2.4	0.028
6	35.114048	-3.919255	9.164	2004	3	29	22	43	17.460	2.3	0.020
7	35.200094	-3.996153	6.463	2004	3	30	0	59	16.770	1.6	0.023
8	35.076144	-3.947094	9.229	2004	3	30	1	2	14.600	2.3	0.026
9	35.081963	-3.964051	10.918	2004	3	30	1	43	39.830	2.1	0.024
10	35.127648	-3.939148	6.259	2004	3	30	2	16	35.220	2.2	0.021
11	35.161545	-4.025844	4.438	2004	3	30	2	55	3.590	2.1	0.025
12	35.137523	-3.963760	7.227	2004	3	30	10	29	26.260	2.4	0.016
13	35.048356	-3.949323	9.370	2004	3	30	10	56	7.100	2.0	0.019
14	35.026775	-3.821060	2.298	2004	3	30	14	5	45.530	2.3	0.015
15	35.024730	-3.817168	6.460	2004	3	30	15	8	25.540	2.0	0.019
16	35.122833	-3.918051	7.982	2004	3	30	15	15	55.560	2.0	0.024
17	35.082382	-3.973568	8.217	2004	3	30	15	29	54.510	1.8	0.019
18	35.040404	-3.797945	1.544	2004	3	30	18	6	0.480	2.3	0.015
20	35.095648	-3.821450	9.060	2004	3	30	19	21	58.090	1.7	0.023
21	35.122906	-3.919197	8.959	2004	3	30	20	0	44.380	1.6	0.023
22	35.117719	-3.902268	6.567	2004	3	30	21	59	39.860	1.4	0.022
23	35.076904	-3.925557	3.057	2004	3	30	22	4	30.230	1.5	0.018
24	35.014974	-3.820712	2.126	2004	3	30	22	30	21.560	2.1	0.021
25	34.988103	-3.815100	1.943	2004	3	30	22	33	5.190	1.9	0.015
26	35.131109	-3.923898	7.566	2004	3	31	0	26	29.790	1.5	0.025
28	35.076914	-3.936048	6.135	2004	3	31	3	31	20.120	2.3	0.028
29	35.171988	-3.972423	6.648	2004	3	31	5	28	29.110	2.0	0.023
30	35.131457	-3.892607	6.703	2004	3	31	6	37	14.010	1.5	0.027
31	35.124045	-3.915586	8.746	2004	3	31	7	32	40.020	1.6	0.027
32	35.173112	-3.988445	8.760	2004	3	31	8	3	35.440	2.6	0.016
33	35.148244	-3.885625	11.619	2004	3	31	8	22	45.270	1.5	0.007
34	35.103494	-3.939584	10.865	2004	3	31	10	35	37.030	1.9	0.036
35	35.107021	-3.930128	9.504	2004	3	31	10	51	24.020	1.9	0.036
36	35.173306	-3.946399	10.518	2004	3	31	11	38	33.480	1.9	0.019
37	35.081176	-3.957466	14.612	2004	3	31	11	53	31.080	1.6	0.018
38	35.154105	-4.041200	11.797	2004	3	31	12	11	55.220	2.6	0.017
39	35.034349	-3.811461	8.451	2004	3	31	12	19	43.270	1.8	0.019
40	35.045326	-3.833223	6.806	2004	3	31	12	28	17.660	1.5	0.020
41	35.171829	-4.072251	15.647	2004	3	31	12	49	51.900	2.7	0.011
42	35.092164	-3.966001	7.156	2004	3	31	14	28	56.150	2.1	0.030
43	35.096222	-3.821906	8.234	2004	3	31	17	17	19.070	1.5	0.025
44	35.118371	-3.931996	3.795	2004	3	31	17	40	44.220	1.7	0.028
45	35.259111	-3.910140	10.689	2004	3	31	19	48	47.390	0.9	0.012
46	35.098479	-3.963798	9.254	2004	3	31	20	15	38.070	1.7	0.030
47	35.195758	-4.078992	6.920	2004	3	31	20	39	12.440	1.4	0.022

48	35.106841	-3.919397	8.297	2004	3	31	21	23	42.480	1.0	0.027
49	35.189652	-4.080516	10.777	2004	3	31	21	29	35.460	1.5	0.022
50	35.036396	-3.975586	6.673	2004	3	31	21	48	35.280	1.2	0.029
51	35.048862	-3.983136	7.191	2004	3	31	22	57	57.520	1.8	0.020
52	35.121965	-3.927269	7.162	2004	3	31	23	10	7.530	1.2	0.025
53	35.094284	-3.893388	5.138	2004	3	31	23	16	27.800	1.2	0.026
54	35.039517	-3.768099	7.703	2004	3	31	23	24	51.730	2.1	0.024
55	35.038387	-3.766637	7.758	2004	3	31	23	50	32.140	2.5	0.028
56	35.034493	-3.790836	4.733	2004	4	1	0	0	4.730	1.0	0.023
57	35.302824	-3.949883	2.291	2004	4	1	0	2	10.940	2.3	0.014
58	35.306201	-3.954308	5.487	2004	4	1	0	8	8.480	1.1	0.009
59	35.179836	-4.119803	10.354	2004	4	1	0	25	35.980	3.8	0.008
60	35.181897	-4.077251	8.566	2004	4	1	0	52	18.010	1.8	0.021
61	35.101459	-3.971044	12.010	2004	4	1	1	6	4.890	1.8	0.027
62	35.259014	-3.911928	10.744	2004	4	1	1	11	4.440	1.4	0.020
63	35.181210	-4.055810	5.910	2004	4	1	1	19	28.790	1.2	0.025
64	35.020725	-3.947113	8.839	2004	4	1	1	19	38.230	1.5	0.020
65	35.102751	-3.964704	9.371	2004	4	1	1	22	40.140	1.5	0.020
66	35.117370	-3.924976	8.190	2004	4	1	1	33	54.320	2.1	0.021
67	35.095942	-3.901521	6.620	2004	4	1	1	37	29.020	1.1	0.021
68	35.111192	-3.924506	6.510	2004	4	1	1	38	52.910	1.4	0.025
69	35.154799	-4.090014	6.177	2004	4	1	2	20	32.180	1.5	0.020
70	35.119824	-3.916102	8.875	2004	4	1	2	29	56.160	1.1	0.018
72	35.045446	-3.955798	4.900	2004	4	1	2	52	27.150	1.3	0.013
73	35.104536	-3.967568	11.379	2004	4	1	3	8	49.020	1.7	0.020
74	35.079116	-3.971397	9.573	2004	4	1	3	12	10.500	1.3	0.020
75	35.171762	-4.089065	8.882	2004	4	1	3	24	41.860	1.4	0.022
76	35.177617	-4.069289	8.335	2004	4	1	3	40	51.070	1.6	0.021
77	35.139572	-3.977841	14.007	2004	4	1	4	13	4.180	1.4	0.021
78	35.013852	-3.787192	3.128	2004	4	1	4	14	20.570	1.5	0.022
79	35.194301	-4.071741	10.134	2004	4	1	4	26	34.890	1.8	0.019
80	35.099079	-3.822965	9.260	2004	4	1	4	27	45.890	1.3	0.029
81	35.115486	-3.930357	9.737	2004	4	1	4	31	3.800	1.4	0.033
82	35.078216	-3.975997	7.771	2004	4	1	4	47	56.190	1.3	0.019
83	35.002376	-3.783208	4.839	2004	4	1	4	51	22.570	1.4	0.028
84	34.947324	-4.065286	8.937	2004	4	1	5	0	32.750	2.0	0.019
85	35.207422	-4.082364	6.132	2004	4	1	6	4	33.260	1.9	0.023
86	35.120059	-3.925082	9.504	2004	4	1	6	32	9.650	1.6	0.030
87	35.094160	-3.950965	6.300	2004	4	1	7	14	5.650	1.8	0.022
89	35.078336	-3.951567	10.304	2004	4	1	10	42	8.640	2.3	0.019
90	35.064403	-3.949269	5.276	2004	4	1	11	6	10.820	2.0	0.020
91	35.125900	-3.912974	8.426	2004	4	1	11	51	49.550	1.9	0.023
92	35.177324	-4.073228	8.724	2004	4	1	12	5	40.110	1.9	0.029
93	35.121103	-3.923893	10.594	2004	4	1	12	36	22.200	1.5	0.031
94	35.020804	-3.985868	8.783	2004	4	1	12	43	11.510	2.1	0.030
95	35.123137	-3.917083	8.728	2004	4	1	12	44	44.110	1.6	0.023
96	35.114074	-3.911454	4.535	2004	4	1	13	9	52.570	1.5	0.025
97	35.139949	-3.965377	12.812	2004	4	1	13	21	39.990	1.3	0.025

98	35.197375	-3.944387	9.312	2004	4	1	13	26	26.130	1.6	0.018
99	35.021557	-3.969052	6.811	2004	4	1	13	29	3.550	2.0	0.022
100	35.115671	-3.926599	9.912	2004	4	1	14	51	43.050	1.8	0.024
101	35.036602	-3.984997	5.721	2004	4	1	15	22	10.280	2.0	0.026
102	35.183073	-4.044997	11.987	2004	4	1	15	41	24.550	1.8	0.018
103	35.029338	-3.980386	7.479	2004	4	1	17	36	21.960	1.6	0.025
104	35.230777	-4.161925	13.502	2004	4	1	18	35	20.790	2.1	0.015
105	35.024971	-4.003998	5.367	2004	4	1	18	54	5.790	1.7	0.023
106	35.106752	-3.920090	5.904	2004	4	1	19	24	24.770	1.6	0.025
107	35.106803	-3.920336	5.911	2004	4	1	19	24	46.350	2.3	0.025
108	34.964226	-3.802177	4.925	2004	4	1	20	10	15.660	2.0	0.020
109	35.094756	-3.970181	6.902	2004	4	1	22	22	36.770	1.5	0.023
110	35.175460	-4.034006	8.441	2004	4	1	22	40	1.520	1.7	0.021
111	35.121507	-3.921426	9.898	2004	4	1	23	19	43.410	1.3	0.026
112	35.033385	-3.975313	7.305	2004	4	1	23	22	47.510	1.5	0.027
113	35.333690	-3.843518	13.170	2004	4	1	23	29	24.700	2.1	0.019
114	35.114056	-3.907668	8.041	2004	4	2	1	16	33.520	1.6	0.024
115	35.132449	-3.948705	7.371	2004	4	2	1	36	0.250	1.5	0.022
116	35.024016	-3.977123	7.571	2004	4	2	3	52	39.090	1.7	0.021
117	35.116966	-3.925663	10.319	2004	4	2	4	46	24.490	1.8	0.033
118	35.087415	-3.987445	12.990	2004	4	2	4	53	20.280	1.6	0.019
119	35.170178	-3.960660	13.979	2004	4	2	5	56	6.240	1.5	0.019
120	35.165540	-3.947222	12.206	2004	4	2	5	56	45.040	2.0	0.018
121	35.165627	-4.047592	9.069	2004	4	2	6	39	40.040	2.6	0.022
122	35.170339	-4.077593	14.847	2004	4	2	7	2	26.790	2.5	0.022
123	35.052024	-3.971127	7.341	2004	4	2	8	32	42.610	1.9	0.021
124	35.114162	-3.904802	8.555	2004	4	2	9	3	17.540	1.4	0.023
125	35.202024	-4.081613	13.915	2004	4	2	9	30	26.860	1.8	0.023
126	35.257883	-3.920090	12.605	2004	4	2	11	13	25.020	1.4	0.017
127	35.029189	-3.973636	7.161	2004	4	2	11	17	4.660	2.0	0.027
128	35.107003	-3.893344	6.325	2004	4	2	11	41	59.430	2.0	0.016
129	35.114556	-3.903263	7.202	2004	4	2	13	48	32.070	1.2	0.024
130	35.016980	-3.992282	7.823	2004	4	2	14	54	39.560	2.1	0.029
131	35.009273	-3.973502	6.002	2004	4	2	16	15	36.580	1.8	0.022
132	35.069407	-3.968635	6.390	2004	4	2	16	50	27.990	1.8	0.030
133	35.166214	-4.030061	8.998	2004	4	2	17	13	53.500	1.9	0.024
134	35.078549	-3.841144	9.757	2004	4	2	18	7	6.180	1.5	0.030
135	35.116065	-3.924402	9.635	2004	4	2	18	13	15.100	1.7	0.035
136	35.115921	-3.924969	9.404	2004	4	2	18	30	52.350	1.5	0.028
137	35.194600	-4.022157	7.697	2004	4	2	18	42	25.240	1.6	0.024
138	35.181373	-4.065233	5.574	2004	4	2	19	12	54.270	1.9	0.023
139	35.113365	-3.927030	11.470	2004	4	2	19	13	54.220	1.3	0.028
140	35.112661	-3.915028	3.611	2004	4	2	19	27	35.090	1.8	0.022
141	35.256379	-3.918562	11.903	2004	4	2	19	41	53.250	1.8	0.018
142	35.098704	-3.900973	6.152	2004	4	2	20	23	23.350	1.4	0.025
143	35.098063	-3.901211	6.594	2004	4	2	20	23	49.940	1.5	0.022
144	35.096759	-3.971764	5.763	2004	4	2	20	27	50.440	1.9	0.019
145	35.023705	-3.996514	8.609	2004	4	2	20	44	44.660	1.7	0.027

146	35.175467	-4.028054	5.965	2004	4	2	20	49	15.410	1.6	0.021
147	35.009629	-3.992076	8.532	2004	4	2	20	49	58.040	2.0	0.030
148	35.137239	-3.954178	3.547	2004	4	2	21	2	32.890	1.9	0.019
149	35.202008	-4.053482	8.778	2004	4	2	21	7	3.490	1.7	0.030
150	35.030171	-3.790151	5.609	2004	4	2	21	8	35.080	1.2	0.021
151	35.132458	-3.961817	4.291	2004	4	2	21	43	0.370	2.8	0.018
152	35.190151	-4.074026	12.849	2004	4	2	21	46	58.130	1.2	0.032
153	35.115338	-3.944169	10.888	2004	4	2	21	53	9.110	1.4	0.028
154	35.012710	-3.786179	5.497	2004	4	2	22	2	26.130	1.7	0.029
155	35.021228	-3.789321	4.771	2004	4	2	22	18	46.130	1.5	0.028
156	35.125526	-3.918469	9.514	2004	4	2	23	16	45.410	1.5	0.022
157	35.081149	-3.959145	6.198	2004	4	2	23	33	2.930	1.1	0.030
158	35.072839	-3.979927	10.275	2004	4	2	23	33	5.860	1.8	0.026
159	35.124342	-3.935322	9.149	2004	4	3	0	36	9.120	1.9	0.036
160	35.074657	-3.830646	7.928	2004	4	3	1	16	27.820	1.6	0.027
161	35.255819	-3.918757	11.790	2004	4	3	2	14	52.320	1.7	0.019
162	35.134367	-3.913330	9.477	2004	4	3	3	6	14.610	1.4	0.027
163	34.992672	-3.873228	1.163	2004	4	3	4	2	45.250	1.6	0.016
164	35.156334	-3.966765	8.357	2004	4	3	4	37	21.420	1.4	0.023
165	35.121515	-3.865055	10.468	2004	4	3	4	43	54.310	1.4	0.023
166	35.103959	-3.849363	8.387	2004	4	3	5	10	16.100	1.4	0.030
167	35.190100	-4.042903	7.927	2004	4	3	5	26	49.610	2.0	0.021
168	35.261603	-3.628431	8.552	2004	4	3	5	43	0.140	1.8	0.009
169	35.047205	-3.953001	6.383	2004	4	3	6	12	18.410	1.8	0.022
170	35.052521	-3.948648	4.714	2004	4	3	6	14	15.760	1.4	0.019
171	35.184654	-4.062944	6.937	2004	4	3	6	31	45.800	1.6	0.027
172	35.183595	-4.064263	7.286	2004	4	3	6	37	44.970	1.8	0.031
173	35.083613	-3.970104	10.085	2004	4	3	6	48	31.660	1.4	0.022
174	35.189540	-4.068865	10.757	2004	4	3	7	20	14.010	1.7	0.030
175	35.179603	-4.037249	7.039	2004	4	3	7	26	3.240	1.9	0.028
176	35.048519	-3.971012	7.020	2004	4	3	8	58	23.160	2.2	0.029
177	35.040899	-3.977831	8.486	2004	4	3	9	0	3.420	1.9	0.015
178	35.181995	-4.055205	6.821	2004	4	3	10	3	12.460	1.6	0.025
179	35.109416	-3.916469	8.764	2004	4	3	13	16	44.180	2.1	0.026
180	35.113659	-3.926871	5.979	2004	4	3	14	46	38.080	1.7	0.018
181	35.099854	-3.878348	10.921	2004	4	3	14	52	51.740	1.8	0.021
182	35.084348	-3.900624	5.405	2004	4	3	17	26	14.810	1.7	0.026
183	35.059532	-3.975769	10.979	2004	4	3	17	58	21.530	2.0	0.032
184	35.053244	-3.948847	4.627	2004	4	3	18	21	16.800	1.8	0.023
185	35.115906	-3.913581	7.315	2004	4	3	18	24	45.320	1.3	0.019
186	35.078385	-3.968763	3.059	2004	4	3	18	46	34.030	1.3	0.020
187	35.118472	-3.923196	7.943	2004	4	3	18	49	7.290	1.1	0.028
188	35.069760	-3.958395	10.815	2004	4	3	19	13	41.930	1.1	0.024
189	35.051536	-3.949483	4.963	2004	4	3	19	14	47.060	1.4	0.022
190	35.115566	-3.924487	9.555	2004	4	3	19	24	21.900	1.6	0.034
191	35.187468	-4.077596	6.125	2004	4	3	19	33	5.720	1.7	0.029
192	35.029177	-3.969335	6.100	2004	4	3	19	45	25.270	1.6	0.037
193	35.065161	-3.972457	10.173	2004	4	3	19	49	10.710	1.2	0.034

194	34.993655	-3.830305	8.374	2004	4	3	20	46	2.550	1.5	0.024
195	35.080085	-3.794731	5.970	2004	4	3	21	23	23.530	1.1	0.024
196	35.088293	-3.970141	7.797	2004	4	3	21	23	28.030	1.4	0.025
197	35.035843	-3.965120	7.639	2004	4	3	21	25	40.710	1.5	0.023
198	35.100968	-3.975061	8.988	2004	4	3	21	26	49.560	1.2	0.022
199	35.119043	-3.908161	7.478	2004	4	3	21	27	38.930	1.2	0.024
200	35.109868	-3.916347	6.333	2004	4	3	21	27	52.190	1.5	0.029
201	35.035783	-3.979706	8.287	2004	4	3	21	30	3.290	1.5	0.029
202	35.215377	-4.054984	6.609	2004	4	3	21	33	10.910	2.0	0.029
203	35.211450	-4.071257	11.662	2004	4	3	21	58	48.370	1.8	0.027
204	35.182136	-4.048695	6.803	2004	4	3	22	0	50.610	1.7	0.032
205	35.206751	-4.067909	10.912	2004	4	3	22	15	21.980	1.7	0.034
206	35.118416	-3.920440	8.848	2004	4	3	22	20	39.070	1.7	0.030
207	35.043219	-3.972096	7.339	2004	4	3	22	39	26.690	1.7	0.024
208	35.001410	-3.818910	7.454	2004	4	3	22	55	40.680	1.7	0.034
209	35.118375	-3.923301	7.479	2004	4	3	23	11	41.990	1.5	0.027
210	35.043202	-3.980466	8.561	2004	4	4	14	19	3.380	1.8	0.022
211	35.034431	-3.988343	5.908	2004	4	4	15	31	22.480	1.8	0.020
212	35.183803	-4.048492	4.571	2004	4	4	16	9	9.060	2.3	0.028
213	35.023502	-3.986938	7.254	2004	4	4	16	11	2.010	1.9	0.033
214	35.240618	-4.190053	6.892	2004	4	4	17	30	46.320	1.8	0.022
215	35.176199	-4.039331	7.021	2004	4	4	17	32	43.300	1.7	0.028
216	35.031126	-3.978412	10.428	2004	4	4	17	46	27.950	2.0	0.035
217	35.055844	-3.984770	8.722	2004	4	4	17	48	50.990	1.5	0.023
218	35.030183	-3.978200	10.657	2004	4	4	19	43	59.280	2.5	0.029
219	35.081077	-3.972823	5.345	2004	4	4	19	51	18.140	1.4	0.024
220	35.184746	-4.067775	7.087	2004	4	4	20	8	15.320	2.8	0.026
221	35.116240	-3.915529	7.877	2004	4	4	20	50	15.400	1.5	0.031
222	35.178426	-4.061867	8.072	2004	4	4	21	15	26.620	2.6	0.030
223	35.216472	-4.096652	15.610	2004	4	4	21	35	31.040	1.5	0.018
224	35.256218	-4.166503	10.098	2004	4	4	21	41	51.840	1.6	0.021
225	35.027254	-3.978647	11.174	2004	4	4	21	47	19.560	1.8	0.026
226	35.119362	-3.923868	8.058	2004	4	4	22	30	49.180	0.9	0.028
227	35.055100	-3.885215	1.697	2004	4	4	22	43	37.850	1.1	0.012
228	35.028798	-3.980283	10.441	2004	4	4	22	54	24.910	1.5	0.031
229	35.097278	-3.975416	6.191	2004	4	4	23	13	51.030	1.6	0.027
230	35.096138	-3.975146	6.250	2004	4	4	23	19	24.550	1.2	0.026
231	35.054355	-3.885208	1.808	2004	4	4	23	35	2.130	1.3	0.014
232	35.160444	-3.975286	9.479	2004	4	5	0	12	48.410	1.5	0.015
233	35.057019	-3.966323	6.119	2004	4	5	0	26	1.210	2.8	0.024
234	35.042870	-3.963438	7.013	2004	4	5	0	37	55.530	1.8	0.023
235	35.054972	-3.885556	2.014	2004	4	5	1	10	16.090	1.2	0.010
236	35.112858	-3.918717	9.979	2004	4	5	1	11	39.620	1.4	0.027
237	35.000305	-3.997718	9.253	2004	4	5	1	44	58.820	1.2	0.029
238	35.121890	-3.936404	8.153	2004	4	5	1	51	21.060	1.4	0.031
239	35.056776	-3.968625	6.300	2004	4	5	2	41	49.610	2.5	0.024
240	35.113460	-3.924507	9.680	2004	4	5	3	1	52.780	2.5	0.030
241	35.055130	-3.973647	7.022	2004	4	5	3	6	48.280	1.3	0.024

242	35.053866	-3.720424	6.444	2004	4	5	3	47	31.870	1.5	0.026
243	35.175692	-4.044312	6.506	2004	4	5	4	35	43.830	1.8	0.032
244	35.118821	-3.906283	8.093	2004	4	5	4	40	57.640	1.7	0.027
245	35.108940	-3.916927	8.287	2004	4	5	5	31	18.700	1.3	0.026
246	35.117709	-3.934956	9.651	2004	4	5	6	15	45.120	1.9	0.029
247	35.094710	-3.951446	9.766	2004	4	5	6	29	19.010	1.8	0.027
248	35.133235	-3.922351	9.541	2004	4	5	7	1	32.900	1.8	0.026
249	35.055569	-3.964111	6.270	2004	4	5	9	53	58.350	1.7	0.029
250	35.193261	-4.100907	13.245	2004	4	5	10	24	28.860	2.3	0.030
251	35.014829	-3.790905	2.789	2004	4	5	10	52	38.770	1.6	0.023
252	35.203761	-4.073427	11.317	2004	4	5	11	20	6.490	1.4	0.024
253	34.971241	-3.915081	12.310	2004	4	5	11	22	48.060	1.6	0.018
254	35.193552	-3.947206	9.801	2004	4	5	11	27	14.430	1.2	0.008
255	35.193521	-3.946208	9.495	2004	4	5	11	45	5.210	1.4	0.018
256	35.059142	-3.965831	5.671	2004	4	5	12	15	28.110	1.8	0.024
258	35.178514	-4.038925	7.905	2004	4	5	14	54	43.130	1.6	0.025
259	35.075325	-3.966469	8.890	2004	4	5	15	12	17.220	1.4	0.030
260	35.031631	-3.764440	8.030	2004	4	5	15	13	56.750	1.5	0.029
261	35.136445	-3.935965	10.619	2004	4	5	15	15	53.720	1.4	0.022
262	35.042004	-3.968711	5.769	2004	4	5	15	57	27.560	2.0	0.025
263	35.286881	-4.156984	7.036	2004	4	5	16	12	21.430	1.7	0.016
264	35.058493	-3.963785	5.901	2004	4	5	16	23	25.060	1.8	0.025
265	35.045856	-3.963271	4.054	2004	4	5	16	28	10.100	3.4	0.015
266	35.044298	-3.964480	3.999	2004	4	5	16	34	24.550	1.6	0.025
267	35.059249	-3.766316	7.024	2004	4	5	16	43	51.670	1.9	0.025
268	35.015787	-3.995534	7.808	2004	4	5	16	45	30.860	1.7	0.032
269	35.018558	-3.988989	12.340	2004	4	5	16	59	19.740	1.5	0.025
270	35.194128	-3.946992	9.738	2004	4	5	17	30	31.040	0.9	0.015
271	35.042015	-3.963483	4.422	2004	4	5	18	54	40.890	2.5	0.017
272	35.116736	-3.794190	3.925	2004	4	5	19	31	47.560	1.6	0.017
273	35.034694	-3.766200	9.186	2004	4	5	19	58	0.490	1.5	0.020
274	35.010117	-4.088866	10.318	2004	4	5	20	25	3.450	1.9	0.009
275	35.211120	-4.077445	12.356	2004	4	5	20	46	46.240	1.2	0.024
276	35.060412	-3.977507	5.177	2004	4	5	21	22	25.390	1.2	0.025
277	35.113733	-3.921342	7.374	2004	4	5	21	28	51.030	2.4	0.026
278	35.110840	-3.919560	7.229	2004	4	5	21	34	42.280	1.4	0.024
279	35.104824	-3.915709	6.119	2004	4	5	21	48	2.560	0.8	0.022
280	35.114673	-3.924246	9.206	2004	4	5	22	34	21.860	1.1	0.016
281	35.092629	-3.941631	6.666	2004	4	5	22	34	33.920	1.0	0.031
282	35.235445	-4.134252	10.052	2004	4	5	22	40	34.750	1.8	0.022
283	35.113134	-3.920178	7.333	2004	4	5	22	42	53.320	2.1	0.034
284	35.091702	-3.865889	7.827	2004	4	5	22	54	14.080	0.8	0.024
285	35.037726	-3.964545	4.876	2004	4	5	23	14	54.830	1.4	0.024
286	35.040920	-3.959760	4.605	2004	4	5	23	35	20.740	1.8	0.025
287	35.070372	-3.854214	4.295	2004	4	6	0	29	6.550	1.0	0.015
288	35.195467	-4.047128	8.416	2004	4	6	0	32	28.350	1.6	0.032
289	35.100503	-3.963966	6.752	2004	4	6	0	34	40.360	1.3	0.025
290	35.112722	-3.919818	6.906	2004	4	6	0	56	56.390	1.0	0.027

291	35.218504	-4.122710	6.132	2004	4	6	1	4	29.600	1.7	0.033
292	35.173149	-4.063675	5.625	2004	4	6	1	46	24.340	1.3	0.028
293	35.016338	-3.754273	8.451	2004	4	6	1	51	30.280	1.7	0.018
294	35.173399	-4.055058	5.216	2004	4	6	1	53	10.500	3.5	0.019
295	35.163663	-4.026880	9.653	2004	4	6	1	57	42.090	1.6	0.017
296	35.172413	-4.051345	4.445	2004	4	6	2	0	15.100	3.0	0.028
297	35.174101	-4.051053	5.027	2004	4	6	2	45	36.420	2.1	0.025
298	35.199035	-4.055056	6.842	2004	4	6	3	42	13.600	2.0	0.024
299	35.019776	-3.990031	7.772	2004	4	6	3	43	29.830	1.7	0.034
300	35.086552	-3.968377	8.721	2004	4	6	3	45	5.520	1.5	0.029
301	35.200983	-4.080276	8.198	2004	4	6	3	47	6.220	1.2	0.022
302	35.055841	-3.733675	8.379	2004	4	6	3	50	51.450	1.8	0.027
303	35.056028	-3.732681	8.351	2004	4	6	3	52	55.320	1.3	0.027
304	35.115410	-3.927006	9.029	2004	4	6	3	54	35.740	1.1	0.026
305	35.175746	-4.065234	5.987	2004	4	6	4	2	25.670	1.5	0.030
306	35.118329	-3.871869	4.222	2004	4	6	4	8	29.470	1.3	0.025
307	35.174622	-4.048930	4.971	2004	4	6	4	13	26.230	2.0	0.021
308	35.062887	-3.741908	7.786	2004	4	6	4	23	20.240	1.9	0.024
309	35.179063	-4.060910	6.462	2004	4	6	4	24	55.890	2.0	0.028
310	35.178655	-4.063849	7.073	2004	4	6	4	34	24.930	2.1	0.026
311	35.025892	-3.970200	6.582	2004	4	6	5	2	26.780	1.2	0.021
312	35.172863	-4.054316	4.669	2004	4	6	5	29	40.700	1.8	0.027
313	35.175334	-4.061713	5.405	2004	4	6	5	54	53.030	2.0	0.027
314	35.052174	-3.727649	8.504	2004	4	6	5	58	18.040	1.6	0.025
315	35.173242	-4.050098	5.112	2004	4	6	5	59	20.930	1.4	0.026
316	35.033116	-3.973382	6.216	2004	4	6	6	3	45.220	1.1	0.030
318	35.055467	-4.033307	4.921	2004	4	6	6	19	47.390	1.7	0.019
319	35.176588	-4.063805	6.386	2004	4	6	6	23	17.740	1.4	0.023
320	35.140336	-3.922060	12.108	2004	4	6	6	36	0.710	0.9	0.023
321	35.175443	-4.064373	6.202	2004	4	6	7	10	14.860	2.6	0.030
322	35.174979	-4.058574	5.768	2004	4	6	7	56	56.870	2.3	0.028
323	35.058740	-3.978253	11.482	2004	4	6	8	35	25.720	1.6	0.027
324	34.999639	-3.994571	10.191	2004	4	6	10	14	12.380	1.8	0.041
325	35.012333	-3.970466	5.442	2004	4	6	11	42	29.750	1.9	0.018
326	35.009272	-3.998847	8.078	2004	4	6	12	26	55.700	1.6	0.025
328	35.086494	-3.868094	8.537	2004	4	6	13	7	21.500	1.1	0.022
329	35.050089	-3.725832	8.464	2004	4	6	13	37	23.970	1.5	0.026
330	35.053990	-3.731046	8.108	2004	4	6	13	41	37.920	1.2	0.031
331	35.054678	-3.734247	7.481	2004	4	6	13	43	17.100	1.8	0.025
332	35.058779	-3.730455	8.163	2004	4	6	13	43	35.050	1.2	0.043
333	35.054096	-3.728575	8.096	2004	4	6	13	43	55.530	1.6	0.034
334	35.042410	-3.965841	7.230	2004	4	6	14	4	40.810	1.3	0.021
335	35.111398	-3.925493	8.744	2004	4	6	14	6	17.460	1.1	0.019
336	35.089198	-3.948462	8.717	2004	4	6	14	28	10.000	1.4	0.026
337	35.021039	-3.988381	6.954	2004	4	6	14	36	8.790	1.4	0.023
338	35.064818	-3.743151	7.109	2004	4	6	15	1	12.550	1.6	0.025
339	35.051832	-3.725543	8.601	2004	4	6	15	30	18.330	1.2	0.024
340	35.093001	-3.968691	5.094	2004	4	6	15	34	19.670	1.7	0.024

341	35.079869	-3.968692	8.678	2004	4	6	16	37	50.980	1.6	0.027
342	35.105029	-3.968503	5.467	2004	4	6	16	41	16.400	1.2	0.020
343	35.125654	-3.930282	8.422	2004	4	6	16	42	22.370	1.1	0.019
344	35.084810	-3.966027	9.141	2004	4	6	16	45	54.330	1.2	0.024
345	35.112597	-3.921342	7.708	2004	4	6	17	25	40.480	2.8	0.016
346	35.114177	-3.922087	7.427	2004	4	6	17	42	32.780	2.0	0.023
347	35.111943	-3.920299	7.681	2004	4	6	18	6	1.240	1.2	0.024
348	35.114366	-3.922749	7.399	2004	4	6	18	47	27.760	0.9	0.020
349	35.056540	-3.731891	7.675	2004	4	6	18	47	31.770	1.8	0.032
350	35.112013	-3.923887	7.971	2004	4	6	19	16	33.030	1.5	0.024
351	35.068453	-3.747853	6.782	2004	4	6	19	27	21.230	1.4	0.027
352	35.112272	-3.919929	7.346	2004	4	6	19	34	27.080	0.9	0.030
353	35.088916	-3.961029	10.285	2004	4	6	19	51	44.730	1.4	0.029
354	35.138017	-3.957053	4.744	2004	4	6	20	5	7.900	1.1	0.015
355	35.035127	-3.763730	8.392	2004	4	6	20	5	17.100	0.8	0.020
356	35.031848	-3.984106	8.427	2004	4	6	20	12	46.760	1.2	0.019
357	35.060496	-3.740711	6.858	2004	4	6	20	17	31.600	1.9	0.021
358	35.016181	-3.791061	4.627	2004	4	6	21	3	18.920	1.2	0.021
359	35.034504	-3.979933	10.664	2004	4	6	21	16	33.730	1.4	0.029
360	35.062057	-3.740563	7.032	2004	4	6	21	21	15.960	1.4	0.029
361	35.051251	-3.725386	8.429	2004	4	6	21	42	37.630	1.8	0.022
362	35.064542	-3.741367	7.907	2004	4	6	21	43	48.880	1.4	0.032
363	35.059491	-3.734873	8.197	2004	4	6	21	47	24.250	1.3	0.021
364	35.051073	-3.724896	8.510	2004	4	6	21	48	38.820	1.8	0.027
365	35.058173	-3.736623	7.457	2004	4	6	21	48	56.550	2.4	0.033
366	35.054374	-3.729745	8.225	2004	4	6	22	4	25.080	2.0	0.029
367	35.115848	-3.792279	4.642	2004	4	6	22	8	34.360	1.8	0.014
368	35.263831	-4.183188	1.409	2004	4	6	22	15	0.230	3.0	0.014
370	35.235146	-4.173282	7.855	2004	4	6	22	19	16.770	1.5	0.021
371	35.055782	-3.732812	8.642	2004	4	6	22	24	17.050	1.4	0.021
372	35.071522	-3.980940	11.511	2004	4	6	23	4	37.220	1.3	0.021
373	35.115986	-3.923625	7.527	2004	4	6	23	24	9.250	1.4	0.020
374	35.082350	-3.980352	10.888	2004	4	6	23	35	43.940	1.3	0.022
375	35.112754	-3.921946	7.388	2004	4	6	23	39	20.110	2.5	0.016
376	35.068456	-3.747647	5.540	2004	4	7	0	14	19.040	1.5	0.028
377	35.065241	-3.970426	9.736	2004	4	7	0	18	43.060	1.5	0.024
378	35.053152	-3.727549	8.399	2004	4	7	0	19	33.530	1.8	0.031
379	35.253632	-3.919582	11.508	2004	4	7	0	51	45.740	1.3	0.007
380	35.067196	-3.744984	7.602	2004	4	7	0	54	18.350	1.8	0.023
381	35.068316	-3.747099	7.055	2004	4	7	1	0	41.830	1.4	0.020
382	35.096263	-3.902627	5.239	2004	4	7	1	7	30.940	1.2	0.022
383	35.167979	-3.949609	9.207	2004	4	7	1	12	53.700	1.7	0.020
384	35.096647	-3.895346	5.234	2004	4	7	1	14	47.240	1.2	0.018
385	35.097051	-3.901860	5.065	2004	4	7	1	34	12.730	1.4	0.024
386	35.398548	-3.841510	14.915	2004	4	7	1	37	48.490	2.4	0.012
387	35.097428	-3.901449	4.929	2004	4	7	1	44	59.310	1.0	0.020
388	35.095550	-3.902369	5.562	2004	4	7	2	9	1.880	1.6	0.026
389	35.109146	-3.949367	10.925	2004	4	7	2	19	55.990	1.3	0.019

390	35.107876	-3.917317	8.276	2004	4	7	2	45	4.110	1.5	0.012
391	35.062157	-3.736996	8.013	2004	4	7	2	45	22.330	1.2	0.023
392	35.063983	-3.744437	7.314	2004	4	7	2	55	24.950	1.6	0.021
393	35.061668	-3.740715	7.702	2004	4	7	2	56	24.490	2.6	0.029
394	35.051481	-3.949828	9.630	2004	4	7	3	7	39.600	1.3	0.020
395	35.015692	-3.789041	5.105	2004	4	7	3	17	58.850	1.5	0.020
396	35.122501	-3.915235	10.663	2004	4	7	3	34	25.920	1.4	0.027
397	35.168193	-4.016654	8.913	2004	4	7	3	50	10.310	1.4	0.022
398	35.033239	-3.965876	5.479	2004	4	7	4	27	17.960	2.7	0.022
399	35.035866	-3.700402	7.244	2004	4	7	4	33	1.120	1.4	0.028
400	35.087687	-3.963096	7.262	2004	4	7	4	39	28.350	1.0	0.021
401	35.182751	-4.045546	8.366	2004	4	7	4	42	54.890	2.0	0.025
402	35.194124	-4.071909	9.600	2004	4	7	4	43	38.700	1.4	0.024
403	35.065220	-3.743950	7.533	2004	4	7	4	53	31.250	1.1	0.019
404	35.104036	-3.964667	10.626	2004	4	7	5	3	48.100	1.7	0.015
405	35.037885	-3.971127	6.404	2004	4	7	6	16	11.530	2.0	0.017
406	35.039823	-3.975691	7.135	2004	4	7	6	56	4.220	2.0	0.019
407	35.039698	-3.712210	8.148	2004	4	7	8	26	56.270	2.0	0.023
408	35.062287	-3.846352	7.509	2004	4	7	10	5	47.280	2.5	0.014
409	35.025311	-3.968729	5.799	2004	4	7	11	29	35.190	1.9	0.022
410	35.068769	-3.851337	5.399	2004	4	7	11	42	23.320	1.6	0.014
411	35.139627	-3.965776	12.384	2004	4	7	11	52	43.760	2.2	0.022
412	35.140678	-3.965548	12.728	2004	4	7	11	53	1.180	1.4	0.019
413	35.115491	-3.921460	7.011	2004	4	7	12	4	18.520	2.2	0.021
414	35.036324	-3.968941	5.154	2004	4	7	12	15	14.940	1.5	0.024
415	35.115524	-3.918581	8.320	2004	4	7	12	49	43.850	1.5	0.019
416	35.189681	-3.947300	10.650	2004	4	7	13	2	44.750	1.5	0.017
417	35.085565	-3.854054	6.633	2004	4	7	13	16	33.390	1.2	0.024
418	35.005274	-3.743008	7.499	2004	4	7	13	33	44.470	1.8	0.022
419	35.014267	-3.749705	7.254	2004	4	7	13	34	13.730	1.9	0.022
420	35.004824	-3.742647	7.324	2004	4	7	13	53	15.990	1.5	0.021
421	35.069478	-3.849995	5.540	2004	4	7	14	56	42.940	1.5	0.022
422	35.013250	-3.750179	8.135	2004	4	7	15	36	9.760	2.0	0.020
423	35.012064	-3.747134	8.282	2004	4	7	15	38	4.390	1.3	0.018
424	35.081812	-3.932170	6.142	2004	4	7	15	52	25.230	1.6	0.023
425	35.127648	-3.959677	9.917	2004	4	7	17	51	26.240	1.9	0.024
426	35.036857	-3.790923	4.762	2004	4	7	18	7	56.930	1.3	0.021
427	35.046556	-3.962992	4.754	2004	4	7	18	30	30.130	2.6	0.021
428	35.231658	-4.162408	7.673	2004	4	7	18	39	31.440	2.8	0.019
429	35.029666	-3.974214	6.758	2004	4	7	18	46	10.710	1.2	0.024
430	35.238300	-4.153753	5.753	2004	4	7	18	55	56.140	2.6	0.028
431	35.044165	-3.775698	5.271	2004	4	7	19	33	11.260	1.2	0.026
432	35.043622	-3.775753	6.282	2004	4	7	19	50	20.480	1.4	0.026
433	35.076206	-3.913208	4.411	2004	4	7	20	12	28.440	1.7	0.016
434	35.113710	-3.914467	7.938	2004	4	7	20	15	45.190	1.7	0.017
435	35.076688	-3.974999	10.057	2004	4	7	20	18	12.320	1.3	0.018
436	35.080226	-3.946862	9.354	2004	4	7	20	31	39.180	1.3	0.019
437	35.039333	-3.767640	7.316	2004	4	7	20	37	27.430	1.1	0.023

438	35.036681	-3.964810	5.429	2004	4	7	20	48	30.000	1.6	0.024
439	35.036323	-3.964665	5.075	2004	4	7	20	49	51.710	1.9	0.018
440	35.075232	-3.913579	4.701	2004	4	7	20	54	39.150	1.5	0.025
441	35.042564	-3.963895	7.524	2004	4	7	21	0	43.790	2.0	0.027
442	35.029883	-3.976938	9.941	2004	4	7	21	45	6.100	2.5	0.025
443	35.032623	-3.979149	8.172	2004	4	7	21	56	59.470	1.4	0.025
444	35.034427	-3.805812	4.201	2004	4	7	22	34	41.860	1.8	0.030
445	35.267414	-4.200638	10.458	2004	4	7	22	42	37.740	1.7	0.021
446	35.111847	-3.922465	9.437	2004	4	8	0	23	54.370	1.5	0.027
447	35.227108	-4.106398	4.825	2004	4	8	0	25	59.520	1.1	0.024
448	35.078646	-3.958209	10.683	2004	4	8	0	26	11.370	2.4	0.029
449	35.097795	-3.901898	4.884	2004	4	8	0	47	51.790	1.8	0.027
450	35.083476	-3.965890	7.116	2004	4	8	0	53	47.760	1.5	0.025
451	35.171878	-4.029581	7.227	2004	4	8	1	2	44.660	2.0	0.022
452	35.110582	-3.922539	9.252	2004	4	8	1	44	13.220	1.2	0.024
453	35.093814	-3.969877	9.685	2004	4	8	1	53	54.610	1.5	0.028
454	35.133343	-3.917020	8.512	2004	4	8	2	6	38.910	1.7	0.022
455	35.028194	-3.969412	5.657	2004	4	8	2	9	36.910	1.9	0.029
456	35.031208	-3.980446	8.457	2004	4	8	2	20	43.910	1.6	0.023
457	35.102629	-3.966542	11.193	2004	4	8	3	25	40.810	2.7	0.023
458	35.028324	-3.813394	2.350	2004	4	8	3	44	27.790	1.9	0.028
459	35.132215	-3.911870	9.140	2004	4	8	4	8	26.570	1.8	0.024
460	35.037149	-3.988004	9.945	2004	4	8	5	8	25.870	1.8	0.028
461	35.023081	-3.971832	5.422	2004	4	8	5	47	36.880	1.7	0.026
462	35.122077	-3.933350	8.727	2004	4	8	6	3	8.260	1.8	0.023
463	35.213655	-4.132111	6.191	2004	4	8	6	14	7.920	2.0	0.027
464	35.035873	-3.756733	4.295	2004	4	8	7	13	54.220	1.9	0.028
465	35.026848	-3.970940	5.596	2004	4	8	8	30	23.960	1.9	0.021
466	35.102373	-3.965190	10.670	2004	4	8	9	5	24.360	1.9	0.023
467	35.199512	-4.042309	11.796	2004	4	8	10	49	33.640	2.0	0.022
468	35.045222	-3.963633	6.778	2004	4	8	11	6	9.690	1.8	0.023
469	35.104931	-3.887111	4.225	2004	4	8	11	20	55.200	1.6	0.027
470	35.121072	-3.922239	8.666	2004	4	8	14	22	55.880	1.8	0.025
471	35.028901	-3.968672	5.696	2004	4	8	14	26	12.640	1.8	0.029
472	35.120365	-3.921969	8.449	2004	4	8	14	39	39.770	1.9	0.024
473	35.076683	-3.976670	10.864	2004	4	8	15	27	33.910	1.7	0.027
474	35.039397	-3.769781	6.400	2004	4	8	16	20	27.320	1.7	0.032
475	35.032256	-3.766191	7.940	2004	4	8	16	20	27.500	1.9	0.029
476	35.018744	-3.752677	8.782	2004	4	8	16	21	3.170	1.7	0.018
477	35.040859	-3.770656	6.020	2004	4	8	16	21	7.840	1.7	0.030
478	35.031484	-3.764853	7.665	2004	4	8	16	24	20.510	1.5	0.025
479	35.134776	-3.950060	5.600	2004	4	8	17	0	35.780	1.8	0.034
480	35.108729	-3.917471	8.317	2004	4	8	17	21	13.730	1.7	0.023
481	35.108248	-3.918118	6.735	2004	4	8	17	47	7.020	1.9	0.036
482	35.121975	-3.933887	8.831	2004	4	8	18	0	43.040	1.8	0.029
483	35.073009	-3.973579	6.766	2004	4	8	18	15	11.110	1.5	0.020
484	35.028405	-3.980591	6.452	2004	4	8	19	18	48.990	1.9	0.035
485	35.185378	-4.046469	6.794	2004	4	8	19	20	44.950	2.4	0.034

486	35.187175	-3.948688	9.661	2004	4	8	20	18	31.030	1.9	0.021
487	35.184193	-4.120132	1.935	2004	4	8	20	28	8.160	1.9	0.018
488	35.021133	-3.809449	4.933	2004	4	8	21	12	17.470	1.9	0.043
489	35.025454	-3.811256	5.734	2004	4	8	21	13	34.970	1.2	0.021
490	35.023250	-3.811863	5.482	2004	4	8	21	16	24.090	1.8	0.032
491	35.120313	-3.929571	7.997	2004	4	8	21	30	34.410	2.0	0.030
492	35.120673	-3.906057	8.793	2004	4	8	21	32	35.980	1.1	0.024
493	35.015503	-3.750378	8.682	2004	4	8	21	36	57.990	1.6	0.024
494	35.095903	-3.901641	5.479	2004	4	8	21	42	18.570	1.2	0.031
495	35.043555	-3.975578	10.308	2004	4	8	21	47	44.740	1.5	0.032
496	35.022018	-3.808103	4.973	2004	4	8	21	59	29.290	1.5	0.029
497	35.024487	-3.811620	5.314	2004	4	8	22	22	46.940	1.8	0.030
498	35.021480	-3.758301	7.773	2004	4	8	22	31	7.860	1.7	0.030
499	35.084278	-3.881290	2.312	2004	4	8	23	6	15.030	1.5	0.026
501	35.080031	-3.914195	5.335	2004	4	8	23	19	14.190	1.5	0.023
502	35.026042	-3.762626	7.477	2004	4	8	23	31	14.660	1.8	0.029
503	35.094017	-3.968148	8.542	2004	4	8	23	32	2.510	1.6	0.027
504	35.180851	-4.060010	6.854	2004	4	8	23	34	31.960	1.5	0.029
505	35.227858	-4.140484	0.950	2004	4	8	23	40	56.310	2.0	0.013
506	35.094376	-3.862167	9.909	2004	4	9	0	9	41.730	1.0	0.026
507	35.022588	-3.793137	4.958	2004	4	9	0	27	14.960	1.6	0.030
508	35.140580	-3.969546	7.464	2004	4	9	0	28	51.100	1.9	0.032
509	34.964427	-3.812053	4.578	2004	4	9	0	50	43.310	1.8	0.021
510	35.042372	-3.970479	5.884	2004	4	9	1	9	38.940	1.7	0.032
512	35.206838	-4.073710	9.277	2004	4	9	1	41	39.070	2.4	0.028
513	35.201021	-4.073754	8.607	2004	4	9	1	42	34.740	1.8	0.027
514	35.033597	-3.966461	5.914	2004	4	9	1	51	17.580	1.7	0.031
515	35.202116	-4.072529	8.794	2004	4	9	1	55	47.780	1.8	0.026
516	35.150910	-3.981888	7.623	2004	4	9	2	2	39.300	1.6	0.026
517	35.092742	-3.968406	4.883	2004	4	9	2	23	32.760	1.3	0.023
518	35.100777	-3.964334	9.729	2004	4	9	2	25	14.000	1.2	0.027
519	35.101411	-3.877274	9.651	2004	4	9	2	26	12.330	1.1	0.027
520	35.102569	-3.876423	9.530	2004	4	9	2	26	25.930	1.2	0.031
521	35.031107	-3.765137	7.910	2004	4	9	2	50	19.600	1.7	0.026
522	35.186561	-4.052646	7.528	2004	4	9	2	54	5.120	1.4	0.027
523	35.159007	-3.968664	9.033	2004	4	9	3	0	53.760	1.1	0.027
524	35.081321	-3.845625	7.988	2004	4	9	3	8	17.550	1.7	0.021
525	35.022892	-3.760897	1.471	2004	4	9	3	13	59.530	1.6	0.023
526	35.169004	-4.021044	8.773	2004	4	9	3	14	23.240	1.3	0.024
527	35.182498	-4.046915	4.539	2004	4	9	3	41	45.870	2.0	0.024
528	35.116855	-3.916621	8.002	2004	4	9	3	46	18.460	1.4	0.036
529	35.071468	-3.957710	10.465	2004	4	9	4	9	56.010	1.6	0.027
530	35.111943	-3.920217	7.457	2004	4	9	4	13	48.070	1.2	0.019
531	35.106138	-3.877030	2.865	2004	4	9	4	44	29.970	1.3	0.022
532	35.096804	-3.895167	5.291	2004	4	9	4	46	0.540	1.3	0.028
533	35.105650	-3.932923	9.855	2004	4	9	5	35	34.920	1.4	0.019
534	35.029242	-4.014227	5.152	2004	4	9	5	51	8.890	1.9	0.025
535	35.130315	-3.909207	8.863	2004	4	9	5	57	4.330	1.5	0.028

536	35.132433	-3.922690	9.029	2004	4	9	6	2	16.990	1.7	0.028
537	35.027286	-3.762019	7.955	2004	4	9	6	4	39.380	1.4	0.029
538	35.087938	-3.944554	7.309	2004	4	9	6	11	27.970	0.5	0.029
539	35.115746	-3.960787	5.086	2004	4	9	6	11	32.030	1.5	0.028
540	35.059646	-3.840001	5.470	2004	4	9	6	13	53.310	1.4	0.015
541	35.119675	-3.935615	9.627	2004	4	9	7	8	14.810	1.5	0.024
542	35.107008	-3.915573	7.021	2004	4	9	7	12	44.010	1.5	0.031
543	35.186353	-4.041333	4.706	2004	4	9	7	23	59.760	2.5	0.025
544	35.129486	-3.945454	8.478	2004	4	9	7	38	15.030	1.5	0.018
545	35.165258	-4.011219	8.744	2004	4	9	7	45	49.230	1.9	0.027
546	35.041811	-3.735977	3.593	2004	4	9	7	46	29.930	1.5	0.025
547	34.967112	-3.812546	4.389	2004	4	9	8	40	32.340	2.0	0.018
548	34.991125	-3.818293	2.411	2004	4	9	8	54	12.510	1.8	0.017
549	35.112862	-3.922710	7.325	2004	4	9	10	16	10.490	1.5	0.017
550	35.115643	-3.932010	7.505	2004	4	9	10	28	11.860	1.1	0.027
551	35.089181	-3.969925	8.348	2004	4	9	10	28	21.390	1.2	0.022
552	35.034835	-3.965392	5.429	2004	4	9	10	46	19.710	1.8	0.032
553	35.113962	-3.923853	7.443	2004	4	9	11	33	51.830	1.6	0.026
554	35.043807	-3.983884	6.115	2004	4	9	11	54	15.990	1.6	0.026
555	35.086181	-3.916360	3.252	2004	4	9	12	0	53.090	1.9	0.028
556	35.068947	-3.847926	5.760	2004	4	9	12	13	14.830	1.9	0.028
557	35.097705	-3.950039	8.473	2004	4	9	12	54	8.460	1.4	0.027
558	35.121023	-3.921604	7.966	2004	4	9	13	2	40.250	1.6	0.030
559	35.038668	-3.977830	6.163	2004	4	9	13	24	36.040	1.7	0.032
560	35.245538	-4.123464	3.614	2004	4	9	13	42	17.710	1.9	0.024
561	35.091360	-3.978584	6.601	2004	4	9	14	4	49.360	1.2	0.026
562	35.077426	-3.855609	7.642	2004	4	9	14	10	28.060	1.0	0.019
563	35.039054	-3.964042	4.850	2004	4	9	14	11	57.720	2.0	0.029
564	35.067726	-3.979112	6.300	2004	4	9	14	34	7.150	1.9	0.026
565	35.088100	-3.900705	5.832	2004	4	9	14	36	34.180	1.7	0.026
566	35.131442	-3.936557	8.647	2004	4	9	14	44	23.720	1.5	0.028
567	35.025949	-3.983868	6.618	2004	4	9	14	54	19.560	1.7	0.022
568	35.112035	-3.916178	7.539	2004	4	9	15	4	33.220	1.3	0.030
569	35.115929	-3.925607	9.158	2004	4	9	15	21	46.010	1.7	0.025
570	35.137613	-3.951293	12.231	2004	4	9	15	39	46.660	1.8	0.033
571	35.082735	-3.975322	6.599	2004	4	9	15	58	19.740	1.6	0.030
572	35.126363	-3.923354	7.989	2004	4	9	16	38	25.750	1.6	0.032
574	35.074854	-3.934411	7.495	2004	4	9	18	39	29.460	1.6	0.031
575	35.041028	-3.964732	4.252	2004	4	9	19	13	58.160	1.7	0.031
576	35.048799	-3.951279	5.505	2004	4	9	19	20	8.030	1.7	0.026
577	35.078429	-3.955584	9.946	2004	4	9	19	20	0.410	1.1	0.032
578	35.098197	-3.901804	5.041	2004	4	9	19	30	42.560	1.5	0.033
579	35.095568	-3.975619	5.895	2004	4	9	19	37	5.690	1.5	0.027
580	35.041532	-3.771814	6.143	2004	4	9	20	31	37.060	1.8	0.032
581	35.042679	-3.773983	6.578	2004	4	9	20	41	21.430	2.3	0.033
582	35.094424	-3.948852	8.893	2004	4	9	20	44	7.580	2.1	0.033
583	35.038599	-3.770038	7.260	2004	4	9	21	11	4.250	1.8	0.036
584	35.102264	-3.912844	3.955	2004	4	9	21	50	12.310	1.7	0.022

585	35.156529	-3.946129	11.079	2004	4	9	22	6	12.480	1.6	0.034
586	35.040162	-3.772209	6.278	2004	4	9	22	25	18.540	1.4	0.022
587	35.200575	-4.114264	6.224	2004	4	9	22	37	41.220	1.8	0.024
588	35.198748	-4.110990	5.887	2004	4	9	22	38	2.390	1.8	0.029
589	35.096938	-3.951999	9.454	2004	4	9	23	4	36.200	1.4	0.026
590	35.116167	-3.852912	6.935	2004	4	9	23	11	8.390	3.0	0.013
591	35.118292	-3.853469	7.871	2004	4	9	23	13	57.530	1.5	0.022
592	35.117023	-3.853793	6.557	2004	4	9	23	15	52.340	1.8	0.027
593	35.116676	-3.925611	5.131	2004	4	9	23	50	47.020	1.8	0.034
594	35.035331	-3.980460	6.561	2004	4	10	0	17	8.340	1.9	0.037
595	35.083077	-3.799548	9.098	2004	4	10	0	33	9.350	1.7	0.020
596	35.182610	-4.039365	5.602	2004	4	10	1	1	18.270	1.8	0.026
597	35.039815	-3.970681	6.012	2004	4	10	1	4	40.600	1.5	0.031
598	35.181032	-4.037988	4.964	2004	4	10	1	5	44.510	1.4	0.025
599	35.025384	-3.760498	8.697	2004	4	10	1	50	29.270	1.6	0.030
600	35.027089	-3.972732	5.658	2004	4	10	2	5	12.250	1.4	0.022
601	35.115063	-3.852263	7.926	2004	4	10	2	10	11.880	1.5	0.021
602	35.070746	-3.953833	10.048	2004	4	10	2	16	0.930	1.2	0.034
603	35.025361	-3.985941	7.481	2004	4	10	2	51	55.610	1.5	0.038
604	35.099497	-3.902492	5.301	2004	4	10	3	3	59.980	1.5	0.026
605	34.988028	-3.811160	3.051	2004	4	10	3	19	58.460	1.6	0.020
606	35.117033	-3.853627	6.417	2004	4	10	3	22	52.440	1.2	0.016
607	35.016238	-3.791922	4.071	2004	4	10	3	43	54.550	1.6	0.026
608	35.039680	-3.965845	4.477	2004	4	10	3	52	29.380	1.9	0.027
609	35.210345	-4.096925	3.875	2004	4	10	3	55	16.670	1.8	0.029
610	35.125420	-3.915763	9.062	2004	4	10	4	3	36.760	1.6	0.020
611	35.035339	-3.961782	4.948	2004	4	10	5	12	6.270	1.3	0.027
612	35.196631	-4.059759	10.858	2004	4	10	5	37	28.360	1.8	0.029
613	35.096695	-3.972735	6.346	2004	4	10	5	47	35.990	1.5	0.024
614	35.167363	-4.037161	10.038	2004	4	10	5	50	16.800	1.6	0.023
615	35.039075	-3.964814	4.820	2004	4	10	6	11	0.330	1.2	0.022
616	35.214838	-4.158468	6.716	2004	4	10	6	11	7.380	2.2	0.033
617	35.224041	-4.194675	7.943	2004	4	10	6	56	1.220	2.0	0.020
618	35.088603	-3.972655	4.900	2004	4	10	7	25	49.390	1.6	0.029
619	35.218374	-4.169432	6.925	2004	4	10	7	33	49.180	2.1	0.025
620	35.114291	-3.923469	9.328	2004	4	10	7	42	16.700	1.6	0.033
621	35.120199	-3.934994	9.087	2004	4	10	9	4	51.110	1.9	0.025
622	35.120143	-3.935424	9.607	2004	4	10	11	12	51.680	1.7	0.034
623	35.175927	-4.044282	6.710	2004	4	10	11	45	3.180	2.0	0.027
624	35.124200	-3.903930	8.508	2004	4	10	11	48	9.680	1.6	0.025
625	35.066929	-3.966293	9.310	2004	4	10	11	53	25.710	1.9	0.027
626	35.237062	-4.116364	3.490	2004	4	10	13	58	0.180	1.8	0.016
627	35.116941	-3.916706	8.492	2004	4	10	14	18	35.690	1.1	0.024
628	35.192187	-4.086378	13.734	2004	4	10	14	58	52.180	1.7	0.027
629	35.035522	-3.955642	6.642	2004	4	10	15	14	24.140	1.7	0.026
630	35.122695	-3.916952	8.506	2004	4	10	15	54	4.710	1.7	0.028
631	35.122053	-3.917491	8.824	2004	4	10	15	57	25.620	1.5	0.031
632	35.020082	-3.756045	8.072	2004	4	10	16	56	56.170	1.6	0.020

633	35.118758	-3.925442	8.166	2004	4	10	17	20	42.320	1.7	0.028
634	35.028560	-3.967486	5.615	2004	4	10	17	50	37.580	1.4	0.027
635	35.189230	-4.045483	8.004	2004	4	10	18	22	35.190	1.9	0.043
636	35.255162	-4.106542	6.868	2004	4	10	18	45	41.560	1.9	0.021
637	34.978022	-3.813618	3.484	2004	4	10	19	14	45.410	1.7	0.019
638	35.033094	-3.981789	6.687	2004	4	10	19	29	56.150	1.5	0.025
640	35.075024	-3.851946	6.563	2004	4	10	20	39	1.430	2.0	0.027
641	35.116335	-3.923679	8.572	2004	4	10	20	49	30.790	1.5	0.033
642	35.082609	-3.972308	7.596	2004	4	10	21	16	43.250	1.6	0.023
643	35.127094	-3.912848	9.012	2004	4	10	22	1	11.690	1.5	0.021
644	35.191405	-3.952695	9.745	2004	4	10	22	11	51.110	1.4	0.012
645	35.080892	-3.931946	6.921	2004	4	10	22	50	58.340	1.6	0.026
646	35.198001	-4.073556	11.120	2004	4	10	23	38	27.770	1.7	0.038
647	35.038374	-3.977167	10.244	2004	4	11	0	31	52.920	1.8	0.031
648	35.121038	-3.870588	9.409	2004	4	11	1	34	34.240	1.2	0.028
649	35.051313	-3.941936	4.135	2004	4	11	2	19	41.690	1.5	0.028
650	35.060301	-3.959343	8.240	2004	4	11	2	27	14.400	1.3	0.044
651	35.040538	-3.978086	10.256	2004	4	11	2	27	43.900	1.4	0.024
652	35.102862	-3.913733	7.162	2004	4	11	2	28	16.930	1.0	0.020
653	35.079744	-3.975928	10.096	2004	4	11	4	35	11.470	1.5	0.026
654	35.105919	-3.946517	9.594	2004	4	11	4	43	36.420	1.3	0.031
655	35.036489	-3.796558	3.493	2004	4	11	4	59	28.600	1.5	0.028
656	35.053489	-3.809950	2.617	2004	4	11	5	15	41.030	1.4	0.019
657	35.030007	-3.987125	10.536	2004	4	11	5	52	29.560	1.5	0.031
658	35.120266	-3.924462	7.763	2004	4	11	6	6	19.520	1.3	0.026
659	35.120279	-3.923803	8.194	2004	4	11	6	6	28.610	1.0	0.027
660	35.099220	-3.971730	7.403	2004	4	11	6	16	33.580	1.5	0.030
661	35.046316	-3.964733	8.864	2004	4	11	6	22	56.340	2.7	0.013
662	35.230839	-4.101383	5.501	2004	4	11	6	31	40.650	1.8	0.031
663	35.090873	-3.978500	6.702	2004	4	11	6	44	14.510	1.3	0.024
664	35.044884	-3.963926	9.099	2004	4	11	6	50	41.630	1.6	0.026
665	35.266516	-4.018048	5.128	2004	4	11	6	56	31.110	1.8	0.015
666	35.119746	-3.924584	7.996	2004	4	11	7	6	34.620	1.8	0.026
667	35.117927	-3.905147	7.197	2004	4	11	7	12	6.930	1.8	0.024
668	34.992427	-3.869890	5.726	2004	4	11	7	58	0.130	1.4	0.014
669	35.097208	-3.856468	6.077	2004	4	11	8	42	22.250	1.5	0.026
670	35.024994	-3.837886	6.943	2004	4	11	8	44	5.760	1.6	0.018
671	35.019917	-3.837604	7.343	2004	4	11	8	45	54.530	1.4	0.020
672	35.057237	-3.782805	7.815	2004	4	11	9	6	3.180	1.7	0.026
673	35.237461	-4.103842	6.493	2004	4	11	9	28	49.030	1.6	0.022
674	35.018769	-3.837708	6.953	2004	4	11	9	37	36.030	1.4	0.026
675	35.076994	-3.935800	6.958	2004	4	11	10	13	28.820	1.7	0.027
676	35.119489	-3.932798	8.269	2004	4	11	10	45	51.510	1.6	0.025

Table S2. List of 164 constructed focal mechanisms

N°	strike	deep	rake
44	119.1	82.6	-171.3
46	277.4	82.2	175.9
66	282.7	79	-140
93	284.7	80.8	165.1
115	206.2	65.2	-6.8
120	208.1	67.6	-11.9
134	141.7	73.4	-152.6
135	274.7	71.7	165.9
140	214.7	79.2	5.9
141	296.4	80.7	-172.4
144	100	82.4	-162.9
148	215.3	78.2	15.8
151	303.4	81.7	172.4
161	294.3	84.2	-179.3
179	117.7	75.8	-157.1
180	156.5	55	-130.9
183	183.8	80.6	5.7
190	332.3	41.3	-97
192	290.2	81.8	165.6
206	284.8	68.7	-165
213	129	63.7	-169
220	288.3	61	-164.7
221	311.9	34.9	-104.3
222	293.3	78.3	170.9
226	126.8	83	-164.8
229	127.5	74.1	-145.7
232	144.7	75.3	-165.8
233	121.6	69.5	-173.9
236	265.7	66.8	-134.2
238	154.5	45.7	-109.6
239	122.5	72.8	-175.9
240	109.1	71.2	-169.6
244	293.5	80.1	-166.2
246	257.2	45.4	-130
247	130.5	61.9	-167.1
248	270.6	48.5	-160.3
249	125.6	66.4	171.2
256	295.5	72.2	172.2
259	288	71.2	-157.5
264	325.8	57.9	-157.5
265	284.4	81.9	-164.8
266	318.9	81.8	-14.1
267	148.4	54.9	-115
271	142.6	72.8	-159.2
272	353.3	54	-54.7
277	292.1	74.1	-168.2
278	288.4	83.5	-165.5
283	286.2	69.6	-162.1
290	288.7	69.1	-166.5
297	279.1	78.7	-166.1
306	345.9	78.8	-16.1
331	335.5	49.1	-66.3
340	118.9	83.4	-175.2
345	296.7	77.1	-171.1
346	288.2	75	-165

N°	strike	deep	rake
348	297.8	69.1	-158.7
350	117	76.6	-168.8
357	312.6	22.8	-98.6
364	354.4	25.8	-62.1
365	341.2	25.4	-84.8
367	329.8	54.7	-75
372	144.1	43.9	-126.1
373	297.4	80.2	-165.9
375	292.5	69.2	-167.7
378	351.7	24.9	-67.3
383	128.5	74.3	-168
385	107	74.8	-137.4
388	111.6	79.7	-153.3
396	110.6	72.7	-161.4
401	250	56.9	138.8
411	321.1	60.1	-112.1
413	308.9	46.6	135.6
415	301.5	75.7	156.3
425	120.9	79.1	-160.9
434	200.1	82.6	0.2
435	288.2	66.9	151.8
449	109.7	82.1	-153.4
451	295	59	158.2
455	132.1	72.4	-159.5
470	300.3	75.3	-174.3
472	306.4	79	-159.2
474	286.8	52	-138.4
479	11.3	72.2	-29.4
480	115.9	76.9	-140.2
481	298.1	78.1	169.9
482	288.6	81.6	-171.8
485	303.3	72.3	-162.6
486	281.2	68.4	-164
490	358.4	23.9	-57.4
491	285.1	80	163.9
492	278.9	64	-155.9
497	339.3	52.3	-74.9
498	298.6	54.5	-106.1
499	207	84.4	7.3
501	319.3	32.1	-99.4
502	298.9	36.5	-132.7
507	349.8	29.6	-71
508	349.9	40.5	-102.4
509	327.2	50.9	-84.6
514	353	63.5	-72.6
516	284.5	79.2	175.2
524	128.4	75.4	-145.2
525	314.8	80	158.9
528	286.6	77.8	160.3
529	274.3	62.3	165.5
532	116	86.7	-169.3
536	286.1	71.2	169.8
539	307.3	87	166.8
540	158.3	55.5	-105.1
541	120.2	84.1	-168.5

N°	strike	deep	rake
542	208	82.2	14.5
543	130.7	59.4	-164.9
545	128.4	71.5	-167.4
547	343.1	29.8	-79.7
552	243.9	57.3	82.4
553	300.2	73.5	-179.1
555	125.7	82.4	-160
556	292.7	69.3	-162.9
558	298.9	83.2	176.8
559	225.5	80.6	18.6
560	281.4	40.5	149.5
563	106.2	79.8	-161.3
564	264.7	74.9	-171.9
565	326.8	78.6	-154.6
567	127.5	75.3	-175.1
570	347.6	55.8	-80.9
575	122.7	83.6	-167.9
578	116	82.1	-157.5
579	300.6	82.3	147.6
580	290.5	52.7	-132.5
581	286.7	52.7	-138.7
582	103.9	84.6	-170.1
583	302.9	55.2	-163.8
585	338.8	53.3	-83
590	291.1	36.9	-127.1
591	308.1	31.2	-95.6
592	296.1	48.4	-134.1
594	106.6	78.2	-152.9
596	205.3	77.6	22.7
597	301.5	79	167.8
601	285.7	82	170.5
602	289.1	83.6	162.2
605	329.9	38.4	-87.1
608	220.3	61.2	59.7
618	343.8	33	-110.5
620	126	61.4	-138.8
621	127.7	74.2	-148.2
622	132.5	76.9	-151.6
623	167.3	67.7	20.4
630	335.1	32.9	-106.6
631	333.4	41.5	-127.8
640	137.2	71.5	-169.1
641	213.9	68.4	9.4
645	117.2	81.4	-157
653	314.2	37.3	-100
658	226.6	60.8	20.8
660	297.3	82	-163.2
665	323.6	61.8	-153.7
666	353.5	48	-86.6
670	118.8	82.3	-126.1
672	299.1	37.9	-133
674	317.5	37.9	-144.4
675	112.4	67.6	-170.8
676	163.9	51.5	-142.2

Table S3. List of 150 relocated aftershocks for events that occurred before the installation of the temporary network

Year	M	D	H	M	Sec	Latitude		Longitude		Mag
						°	‘	°	‘	
2004	02	24	2	27	46.68	35	7.72	-3	57.31	6.4
2004	02	24	2	36	38.93	35	10.07	-3	57.63	4.5
2004	02	24	2	38	59.55	35	8.15	-3	53.54	4.4
2004	02	24	2	41	10.40	35	10.61	-3	59.79	3.7
2004	02	24	2	48	2.64	35	4.23	-3	56.69	4.7
2004	02	24	2	59	02.68	35	11.28	-4	0.76	4.9
2004	02	24	3	17	44.97	35	7.83	-3	58.62	4.7
2004	02	24	3	25	10.57	35	9.43	-3	57.56	3.8
2004	02	24	3	27	14.14	35	3.20	-3	59.74	4.4
2004	02	24	3	43	24.83	35	6.79	-3	59.25	4.3
2004	02	24	3	53	57.74	35	3.75	-3	55.41	4.0
2004	02	24	4	4	45.61	35	10.66	-3	57.62	3.6
2004	02	24	4	6	37.61	35	4.37	-3	57.59	4.4
2004	02	24	4	13	53.25	35	7.07	-3	55.80	4.5
2004	02	24	4	16	26.43	35	8.95	-3	58.99	3.6
2004	02	24	4	18	40.17	35	7.83	-3	55.08	3.7
2004	02	24	4	22	58.94	35	7.12	-3	54.49	3.8
2004	02	24	4	31	13.47	35	3.76	-3	59.72	3.6
2004	02	24	4	32	42.44	35	9.89	-4	0.02	4.4
2004	02	24	4	39	29.24	35	9.74	-3	56.54	3.5
2004	02	24	4	50	54.01	35	4.31	-3	56.94	3.5
2004	02	24	4	55	36.04	35	7.80	-3	56.88	4.2
2004	02	24	4	58	26.97	35	1.63	-3	58.53	3.3
2004	02	24	5	1	24.78	35	8.09	-3	57.25	3.3
2004	02	24	5	4	59.70	35	3.54	-3	56.56	3.9
2004	02	24	5	34	27.30	35	8.30	-3	54.76	3.7
2004	02	24	5	36	18.07	35	8.10	-3	54.76	3.5
2004	02	24	5	41	34.05	35	11.59	-3	56.98	3.7
2004	02	24	6	3	0.16	35	4.85	-3	59.46	3.5
2004	02	24	6	20	17.48	35	6.47	-3	56.93	4.3
2004	02	24	7	0	13.03	35	7.70	-3	59.29	3.9
2004	02	24	7	7	58.50	35	11.36	-4	3.40	4.0
2004	02	24	7	21	35.21	35	9.75	-3	58.88	3.7
2004	02	24	7	28	22.92	35	8.10	-3	57.64	3.6
2004	02	24	7	38	48.62	35	5.97	-3	58.66	4.4
2004	02	24	8	5	26.23	35	12.69	-4	2.51	3.4
2004	02	24	8	16	46.72	35	2.67	-3	57.70	3.8
2004	02	24	8	33	27.93	35	8.81	-3	55.62	3.5
2004	02	24	8	44	37.36	35	7.50	-3	57.40	3.7
2004	02	24	9	1	51.18	35	5.63	-3	56.95	4.6
2004	02	24	9	47	16.12	35	12.58	-3	57.81	3.6
2004	02	24	10	50	33.39	35	5.62	-3	56.01	3.7
2004	02	24	11	4	44.33	35	10.91	-4	3.22	4.9
2004	02	24	11	25	8.11	35	10.83	-3	56.31	3.8
2004	02	24	11	31	41.39	35	8.65	-3	57.30	3.9
2004	02	24	11	51	49.84	35	12.13	-3	57.16	3.9
2004	02	24	12	7	23.68	35	5.55	-3	53.83	3.7
2004	02	24	13	9	44.36	35	3.17	-3	56.97	3.8
2004	02	24	13	29	20.91	35	11.27	-4	1.73	3.7
2004	02	24	13	43	33.66	35	10.66	-3	58.24	3.9
2004	02	24	14	6	13.57	35	5.20	-3	54.35	3.8
2004	02	24	14	10	58.94	35	3.31	-3	56.68	4.1
2004	02	24	15	35	13.63	35	1.63	-3	57.89	3.5
2004	02	24	15	42	16.79	35	7.83	-3	56.65	4.0
2004	02	24	18	53	02.38	35	9.69	-3	56.71	4.7
2004	02	24	20	37	1.16	35	2.70	-3	58.56	4.7
2004	02	24	22	24	18.86	35	11.61	-3	57.54	3.2

2004	02	24	23	58	44.99	35	10.77	-3	57.62	4.0
2004	02	25	0	11	15.40	35	10.60	-3	58.90	4.1
2004	02	25	0	13	31.52	35	7.08	-3	55.75	4.0
2004	02	25	10	5	20.02	35	7.69	-3	58.09	4.4
2004	02	25	12	44	55.25	35	4.16	-3	48.37	5.2
2004	02	25	16	33	28.07	35	7.72	-3	56.07	4.5
2004	02	25	21	39	35.12	35	5.31	-3	58.78	3.5
2004	02	25	21	41	55.15	35	12.21	-4	2.49	3.6
2004	02	25	22	9	38.19	35	4.56	-3	54.36	3.6
2004	02	25	22	14	41.16	35	7.31	-3	56.95	3.7
2004	02	26	6	8	34.07	35	13.50	-4	5.54	4.2
2004	02	26	12	7	5.06	35	12.20	-3	55.76	5.4
2004	02	27	0	59	1.02	35	6.53	-3	55.61	4.6
2004	02	27	3	12	36.64	35	5.34	-3	55.88	5.1
2004	02	27	8	39	13.23	35	5.73	-3	57.45	3.8
2004	02	27	9	36	33.31	35	7.38	-3	55.24	3.9
2004	02	27	14	35	13.83	35	1.08	-3	59.04	3.6
2004	02	27	16	50	42.13	35	8.59	-3	54.68	4.8
2004	02	28	5	43	38.81	35	8.69	-3	58.38	3.4
2004	02	28	5	49	6.08	35	6.45	-3	57.46	3.8
2004	02	28	7	39	14.70	35	7.38	-3	57.25	3.5
2004	02	28	16	29	24.90	35	11.45	-4	1.35	5.0
2004	02	28	21	3	52.52	35	6.87	-3	57.39	3.2
2004	02	29	2	56	55.23	35	10.15	-3	53.26	4.1
2004	02	29	10	14	7.02	35	4.68	-3	55.95	4.0
2004	02	29	10	40	01.10	35	6.76	-3	55.03	3.5
2004	02	29	11	5	44.24	35	4.00	-3	56.99	3.7
2004	02	29	11	46	25.69	35	11.62	-3	58.85	3.5
2004	02	29	22	8	40.37	35	0.14	-3	57.74	3.6
2004	03	01	1	1	43.73	35	2.80	-3	43.87	3.2
2004	03	01	1	20	52.15	35	9.11	-3	55.42	3.6
2004	03	01	2	18	10.32	35	11.34	-3	56.43	4.0
2004	03	01	4	59	24.85	35	8.79	-3	57.89	4.0
2004	03	01	8	16	51.46	35	1.72	-3	55.61	3.4
2004	03	02	14	56	20.05	35	12.46	-3	56.77	4.2
2004	03	02	20	36	27.59	35	11.52	-3	54.38	4.9
2004	03	02	22	28	5.69	35	8.33	-3	56.80	4.2
2004	03	03	1	45	23.73	35	16.04	-4	3.65	4.5
2004	03	03	4	29	2.64	35	13.06	-3	55.97	3.6
2004	03	03	6	36	50.14	35	8.73	-3	48.78	3.9
2004	03	04	5	46	51.26	35	9.38	-3	59.49	3.5
2004	03	05	15	52	50.62	35	13.11	-3	54.46	4.0
2004	03	05	23	50	28.87	35	10.31	-3	50.84	3.5
2004	03	06	1	20	3.97	35	2.12	-3	59.89	3.3
2004	03	06	3	53	16.55	35	16.16	-3	52.51	3.4
2004	03	06	9	11	2.15	35	12.35	-3	52.59	4.0
2004	03	06	22	30	17.35	35	13.49	-3	55.95	3.4
2004	03	06	23	35	7.50	35	7.35	-3	56.04	3.2
2004	03	07	4	29	21.26	35	5.70	-3	54.51	2.0
2004	03	07	5	56	9.56	35	16.70	-4	3.87	3.6
2004	03	07	6	45	59.74	35	4.36	-3	55.66	3.9
2004	03	07	7	54	33.01	35	2.10	-3	58.78	3.2
2004	03	07	8	6	30.26	35	7.50	-3	59.14	3.4
2004	03	07	11	14	37.95	35	5.36	-3	56.55	3.5
2004	03	07	13	4	10.25	35	4.98	-3	55.16	3.6
2004	03	07	15	38	59.21	35	3.83	-3	55.15	4.1
2004	03	08	1	31	54.89	35	7.06	-3	55.44	3.8
2004	03	08	11	47	11.94	35	7.52	-3	53.49	3.6
2004	03	09	0	15	20.10	35	5.42	-3	52.07	3.5
2004	03	09	11	12	22.08	35	6.91	-3	57.63	3.9
2004	03	10	2	28	12.56	35	9.39	-3	53.60	3.4
2004	03	10	3	48	49.32	35	5.05	-3	57.59	4.3
2004	03	10	11	58	33.43	35	4.15	-3	44.83	3.7
2004	03	12	18	11	56.57	35	4.53	-3	54.07	3.6

2004	03	12	19	27	16.83	35	4.83	-3	54.20	3.5
2004	03	12	20	20	45.92	35	4.94	-3	58.25	3.6
2004	03	12	23	35	31.20	35	18.99	-4	7.65	3.9
2004	03	13	21	41	27.80	35	7.57	-3	51.16	3.8
2004	03	15	19	55	19.96	35	5.60	-3	55.40	3.5
2004	03	15	22	18	32.02	35	5.78	-3	56.94	4.5
2004	03	16	2	58	18.22	35	1.08	-4	0.18	4.0
2004	03	17	18	12	0.30	35	11.44	-4	2.78	3.4
2004	03	18	11	45	34.15	35	15.00	-4	5.23	4.1
2004	03	18	22	19	41.05	35	12.74	-4	1.14	3.5
2004	03	18	22	58	28.77	35	9.52	-3	59.22	3.7
2004	03	19	3	12	45.74	35	7.18	-3	49.61	3.5
2004	03	19	6	2	48.33	35	7.01	-3	55.61	3.9
2004	03	19	7	2	28.21	35	5.14	-3	53.35	3.3
2004	03	20	9	37	29.60	35	7.92	-3	59.08	5.2
2004	03	20	16	18	1.38	35	3.78	-3	48.78	3.6
2004	03	20	20	24	2.93	35	10.77	-3	58.21	3.8
2004	03	21	8	18	46.56	35	16.16	-4	0.81	3.8
2004	03	22	2	28	49.89	35	5.23	-3	55.53	4.0
2004	03	22	5	18	2.95	35	2.27	-3	57.85	4.1
2004	03	22	5	25	15.00	35	6.05	-3	56.24	3.3
2004	03	24	1	16	25.31	35	9.70	-3	58.49	3.1
2004	03	24	6	26	11.02	35	4.07	-3	57.51	3.5
2004	03	25	7	20	59.76	35	5.56	-3	56.17	3.8
2004	03	25	22	38	39.71	35	1.76	-4	0.70	4.2
2004	03	26	10	22	4.57	35	12.29	-3	55.89	3.5
2004	03	26	16	34	10.17	35	5.03	-3	56.48	3.7
2004	03	27	19	15	69.53	35	4.20	-3	58.23	3.8
2004	03	27	22	32	27.56	35	15.42	-4	5.96	3.4
2004	03	29	13	54	25.02	35	6.41	-3	57.07	3.4